Office of Legacy Management

Natural and Enhanced Attenuation of Soil and Groundwater at Monument Valley, Arizona, and Shiprock, New Mexico, DOE Legacy Waste Sites

2007 Pilot Study Status Report

June 2008

U.S. Department of Energy

Office of Legacy Management

This page intentionally left blank

Natural and Enhanced Attenuation of Soil and Groundwater at Monument Valley, Arizona, and Shiprock, New Mexico, DOE Legacy Waste Sites

2007 Pilot Study Status Report

June 2008

This page intentionally left blank

Contents

Figures

Tables

Appendixes

Acronyms and Abbreviations

ATCA	*Atriplex canescens*
cm	centimeter
cm^3	cubic centimeters
DOE	U.S. Department of Energy
ET	evapotranspiration
EVI	enhanced vegetation index
ft	foot
g/g	gram per gram
ha	hectare
kg	kilogram
L	liter
LAI	leaf area index
LM	Office of Legacy Management
m	meter
M	mole
m/year	meter per year
m^2	square meters
m^3	cubic meters
MG	Miracle-Gro
mg/g	milligram per gram
mg/kg	milligram per kilogram
mg/L	milligram per liter
mm	millimeter
mm/yr	millimeter per year
MWL	meteoric water line
MV	Monument Valley
p	probability
ppm	parts per million
RPM	revolutions per minute
SAVE	*Sarcobatis vermiculatus*
Stdev	standard deviation
TARA	*Tamarix ramosissima*
t/ha	tons/hectare
TOC	total organic carbon
UA	University of Arizona
UMTRA	Uranium Mill Tailings Remedial Action
WCR	water content reflectometers
WFM	water flux meters
‰	per mil

End of current text

Executive Summary

The U.S. Department of Energy (DOE) Office of Legacy Management (LM), the Navajo Uranium Mill Tailings Remedial Action program, the University of Arizona (UA), and Diné College are exploring remedies that include natural and enhanced attenuation processes for groundwater contamination at DOE's LM sites at Monument Valley, Arizona, and Shiprock, New Mexico.

Monument Valley

DOE removed radioactive tailings from Monument Valley, a former uranium millsite, in 1994. Nitrate and ammonium, waste products of the milling process, remain in a shallow groundwater plume spreading from a millsite source. A conventional cleanup strategy might involve drilling wells and pumping groundwater to a treatment facility on the surface. Pilot studies jointly funded by LM and UA are answering two questions: (1) what is the capacity of natural processes to remove nitrate and slow plume dispersion, and (2) can we efficiently enhance natural attenuation if necessary? Below are highlights of 2007 pilot study results that help answer these questions.

Source Containment and Removal

One objective of planting phreatophytes in the source area is to control the soil–water balance and limit percolation and leaching of nitrate, much like an evapotranspiration (ET) disposal cell cover. Plantings are purposefully under-irrigated to prevent recharge. However, in 2007, we increased irrigation rates to enhance denitrification. Soil moisture profiles are monitored with neutron hydroprobes and time-domain reflectometry; percolation flux is monitored with water flux meters. Although monitoring data show that percolation is not occurring, we may decrease irrigation rates in 2008 because monitoring data show wetting trends at depth (see Section 2.5).

About 1.7 hectares (ha) of the source area was planted in 1999 and the remaining 1.6 ha was planted in 2006, primarily with the native desert shrub *Atriplex canescens* (four-wing saltbush). We monitor plant canopy growth and nitrate concentrations in plant tissues annually to evaluate growth and nitrate extraction rates (see Section 2.1.1). Plant canopy volume and growth rates varied across the plantings, probably in response to the age of the planting, irrigation rates, and soil fertility (see Section 2.1.2). Total nitrogen uptake estimates were 204 kilograms (kg) in the 1999 planting (since 2000) and 42 kg in the 2006 planting.

An area of poor plant growth exists in the western third of the 1999 planting. Previous analysis suggested that the discolored soils in this area had both an excess and a deficiency of several ions. Follow-up investigations in 2007 included (1) a greenhouse study, conducted by students at Diné College (Tsaile campus), of effects of high salt content on uptake of certain micronutrients, and (2) a laboratory analysis of the discolored soils in areas with stunted plant growth. Micronutrient amendments in the greenhouse study greatly improved both biomass production and survival of plants grown in discolored soil. Laboratory analyses suggested that nodules in the discolored soil likely formed from the co-precipitation of iron and manganese during the milling process. Changes in the redox state induced by irrigation water and increased soil biological activity may have caused colored bands observed near irrigation emitters. We now need to determine if excessive bioaccumulation of manganese is occurring in saltbush.

Planting and irrigating the source area has been exceptionally effective in removing nitrate from the soil by microbial denitrification, the conversion of nitrate to nitrogen gas. Denitrification rates rose when soils were wettest and dropped when plantings matured and dried the soil. Batch and column studies have shown that ethanol, a carbon source, can also greatly enhance denitrification. However, a 2007 field study that supplied ethanol though the irrigation system did not enhance denitrification rates. Denitrification rates are usually highest in wet, anaerobic soils. Average soil moisture content remained well below field capacity, suggesting that in the source area, soil moisture (not carbon) is the limiting factor for dentrification.

Groundwater Phytoremediation

The pilot studies are evaluating natural and enhanced attenuation remedies for groundwater contamination in the alluvial aquifer at Monument Valley with a focus on two attenuation processes: phytoremediation to remove nitrate and sulfate and to slow plume dispersion, and microbial denitrification.

Our preliminary studies found that protecting existing native phreatophytic shrubs (*Atriplex canescens* and *Sarcobatus vermiculatus*) from grazing could double biomass production, transpiration rates (water extraction from the aquifer by plants), and nitrogen uptake rates. We also demonstrated how, on a small scale, greenhouse-grown transplants of native shrubs could be established in denuded areas of the plume, and with managed irrigation, send roots 30 feet and deeper into the alluvial aquifer. In fall 2005, we fenced four large plots (grazing exclosure and revegetation plots) to see if the preliminary studies could be repeated on a large scale. After two growing seasons, canopy cover of phreatophytic shrubs was more than 2 times greater inside than outside the grazing exclosures. However, growth of shrub transplants remained low in the revegetation plots because of herbivory by small mammals.

Phreatophytic shrubs growing over the nitrate plume may extract enough water to slow the spread of the plume during the time it takes for denitrification to reduce nitrate to safe levels. In 2006 and 2007, we measured transpiration rates of individual *A. canescens* and *S. vermiculatus* plants both inside and outside the grazing exclosure plots using sap-flow instrumentation. We then extrapolated these data to a landscape scale using Quickbird and MODIS satellite estimates of shrub cover. The results show that even under current conditions (heavy grazing), ET is already removing large quantities of water from the plume; ET rates are almost double precipitation. In contrast, annual ET rates were about 8 times greater for volunteer phreatophytes protected from grazing for several years inside the source area fence. Using a conservative estimate, managing (but not eliminating) grazing could more than double the amount of water extracted by phreatophytes growing over the plume.

Groundwater Denitrification: Monitoring and Modeling

The pilot studies have shown that natural attenuation is occurring in the plume. In 2007 we began evaluating the feasibility of relying on or enhancing natural attenuation processes as part of the final remedy. We (1) characterized the occurrence and rates of natural attenuation processes (denitrification, sorption, and dispersion), (2) completed laboratory microcosm experiments for injecting carbon sources to enhance denitrification, (3) conducted a temporal and special analysis of plume well data, and (4) calibrated a nitrate transport model to predict and compare natural and enhanced attenuation scenarios.

Results of these studies confirm that the natural attenuation of nitrate is occurring at the site. Dispersion and sorption, estimated from the laboratory microcosm experiments, had minor effects on nitrate transport. Denitrification appears to be the dominant process as determined by microcosm decay and isotopic fractionation experiments, field-scale isotopic fractionation analyses, and numerical modeling. The modeling exercise suggested that although natural attenuation is occurring, it may take more than 150 years to achieve cleanup standards without enhancements. However, the modeling exercise also suggested that the injection of ethanol as a substrate for denitrification could substantially increase denitrification rates and shorten the cleanup time by more than 100 years.

Land Farming

We are considering land farming an active phytoremediation alternative only if more passive alternatives (natural and enhanced attenuation) are found to be inadequate. Land farming would involve pumping plume water from the aquifer to irrigate fields of native plants. This would remove nitrate and sulfate from the aquifer, convert nitrate into healthy plant tissue, and—mimicking natural gypsic soil horizons in the area—store sulfate as gypsum in the farm soil. Irrigation would be managed to prevent contaminants from leaching back into the aquifer. As with other phytoremediation alternatives, land farming would improve the rangeland ecological condition and could produce a crop such as native plant seed that could be marketed for mine-land reclamation for the Navajo Nation.

The land-farm pilot study was designed and constructed in 2005 to compare different crops and different nitrate concentrations in irrigation water. Although a drop in well-pumping rates caused nonuniform irrigation rates among treatments, and required us to alter the original experimental design, results show that plants receiving the highest nitrate concentration—750 milligrams per liter of nitrate—grew the largest, and *A. cansecens* grew significantly larger than *S. vericulatus*. In 2008, we plan to conduct a pump test on the plume extraction well and sample nitrate and sulfate accumulation in land-farm soils and plants.

Shiprock

Groundwater at the Shiprock sites became contaminated by uranium, nitrate, and sulfate during milling operations. In 2003, DOE began pump-and-treat remediation. Phytoremediation was later advocated in addition to active remediation, primarily to help control hydraulic gradients and limit the spread of plumes. Phytoremediation test plots were set up in 2006, with assistance from Diné College student interns, to evaluate the feasibility of planting and irrigating native phreatophytes until their roots access groundwater. Test plots were set up southwest of the Shiprock disposal cell in a large soil borrow pit overlying a mill-related nitrate plume, and on a terrace northeast of the disposal cell overlying a uranium plume that flows into the San Juan River floodplain. The feasibility study also measured oxygen and deuterium isotope signatures for evidence that volunteer phreatophytes have accessed groundwater.

Diné College interns measured plant growth in the test plots in fall 2007. Overall, transplants had grown larger in the terrace plots than in the borrow pit plots and, as at Monument Valley, *A. cansecens* grew significantly larger than *S. vericulatus*.

Analysis of oxygen and deuterium isotope signatures for different water sources led to the following inferences:

- San Juan River water consists of a mixture of summer and winter precipitation, as would be expected as water is released from the Navajo Dam upstream.

- Water from tailings in the Shiprock disposal cell appears to be local summer and winter precipitation that has percolated through the disposal cell cover.

- Water from wells in the San Juan River floodplain are similar to river water, indicating that the wells intercept the floodplain aquifer. Water in the tissue of *Tamarix* plants growing adjacent to the floodplain wells are rooted into and extracting water from the aquifer.

- Mature *S. vermiculatus* plants growing on the terrace may be extracting water from the capillary fringe above the alluvial aquifer that passes between the disposal cell and the floodplain.

- Water from wells near the northeast end of the terrace had signatures that plotted close to water from tailings in the disposal cell, indicating possible movement of water from the disposal cell to the terrace at that location.

- Water in tissue of mature phreatophytic shrubs growing in the borrow pit appears to be primarily from the vadose zone water and possibly a mixture of vadose zone and shallow groundwater.

1.0   Introduction

The U.S. Department of Energy (DOE) is conducting pilot studies of enhanced attenuation remedies for contaminated groundwater at former uranium mill tailings sites near Monument Valley, Arizona, and Shiprock, New Mexico. At Monument Valley, nitrate, ammonium, and sulfate levels are elevated in an alluvial aquifer spreading away from a source area where tailings have been removed. At Shiprock, nitrate, sulfate, and uranium concentrations are elevated in groundwater near a disposal cell constructed to contain uranium mill tailings.

The pilot studies at Monument Valley were mandated by a DOE environmental assessment. They help us evaluate and demonstrate alternative remedies before a final strategy is selected (DOE 2004a). Preliminary studies suggested that natural and enhanced phytoremediation may be a viable option for reducing nitrate and sulfate levels in the alluvial aquifer and at the plume source, and are consistent with revegetation and land management goals for the site (DOE 2002, 2004b).

In May 2005, DOE and the Navajo Nation jointly approved a second (and final) phase of pilot studies as proposed in a work plan published by DOE in 2004 (DOE 2004c). The purpose of the final phase is to evaluate the capacity of natural processes and methods to enhance natural processes that degrade and slow the migration of contaminants both in the alluvial aquifer and at its source. The pilot studies are focusing on phytoremediation and bioremediation processes. Phytoremediation relies on the roots of plants to remove, degrade, and slow the migration of contaminants. Bioremediation relies on microbial denitrification to reduce concentrations of nitrate in the source area and plume.

In 2006, DOE published first-year (2005) results of the pilot study, a synopsis of the enhanced natural attenuation approach, and a decision framework for using the results of the pilot studies to choose a final remedy for nitrate, ammonia, and sulfate at Monument Valley (DOE 2006). Summaries of the 2006 results of Monument Valley's pilot studies were subsequently published (DOE 2007). Summaries of the third-year (2007) results of Monument Valley's pilot studies are presented in Section 2.0 of this report.

Phytoremediation studies commenced in 2006 at the Shiprock site to evaluate the use of plants to remove groundwater through uptake and transpiration as a way to contain or hydraulically control the migration of groundwater contaminants. Summaries of the 2007 phytoremediation tasks at Shiprock are presented in Section 3.0 of this report.

End of current text

2.0   Monument Valley Pilot Studies

The Monument Valley pilot studies are answering two questions: (1) what are the capacities of natural attenuation processes to remove nitrate and slow plume dispersion, and (2) can we efficiently enhance natural attenuation? The pilot studies are evaluating the natural and enhanced attenuation of both the nitrate plume and its source. Details of the rationale for and descriptions of all Monument Valley pilot-study tasks are available elsewhere (DOE 2004c, DOE 2006, DOE 2007). Only summaries of tasks conducted during calendar year 2007 are presented in this section.

2.1   Source Containment and Removal

In 1994, DOE completed a mandated remediation of *radioactive* constituents in tailings and soils at the site. Materials with radium-226 concentrations exceeding 15 picocuries per gram were removed and hauled to a disposal cell near Mexican Hat, Utah. However, in 1997, sampling within the footprint of a former tailings pile (subpile soil) revealed elevated levels of ammonium and nitrate, ranging from 45 to 1,060 milligrams per kilogram (mg/kg) and 0 to 273 mg/kg, respectively. The subpile soil is assumed to be a continuing source of contamination for the alluvial aquifer extending to the north.

This section provides summaries of work conducted in 2007 on the following tasks (task numbers are from the 2004 work plan [DOE 2004c]):

- Phreatophyte Growth and Total Nitrogen (N) (Task 5.4.6)

- Causes and Recourses for Stunted Plant Growth (Task 5.4.3)

- Soil Water and Recharge Monitoring (Task 5.4.5)

- Enhanced Microbial Denitrification in the Source Area (this is a follow-up activity of Evaluate Natural Denitrification Processes) (Task 5.4.7)

- Nitrate and Ammonium in Source Area Soils (Task 5.4.1)

2.1.1   Phreatophyte Growth and Total Nitrogen

About 1.7 hectares (ha) of the subpile source area was planted in 1999, mainly with the native desert shrub, *Atriplex canescens* (four-wing saltbush), to function as a phytoremediation cover. The purposes were (1) to create a water balance cover, limiting deep percolation and seepage of nitrate, and (2) to extract nitrate converting it into plant tissue. The rectangular irrigated plot was planted with approximately 4,000 *A. canescens* seedlings grown from seed collected on Navajo Nation land and raised in a greenhouse at the University of Arizona (UA) (Figure 2–1). In March 2006, the remaining 1.6 ha of the source area (subpile soil and evaporation pond soil) was planted and irrigated. A total of 3.3 ha of the source has now been planted with a phytoremediation cover, and over 7,300 plants are now growing in the irrigated planting. *A. canescens* shrub growth and nitrogen uptake have been monitored since 2000. A relatively small number of dead or missing plants were replaced throughout the 2007 growing season.

Figure 2–1. 2007 Quickbird satellite photograph of the original 1999 source area planting.

Table 2–1 presents 2007 growth results for the established plants in the 1.7 ha planting that took place in 1999. For this more mature planting, plants could not be counted or measured because the rows have become overgrown, making access impractical. However, given observations of the mature size and dense growth of the plants, the abundant annual seed production, and the occasional volunteer seedlings, and the fact that plants were killed by burrowing animals or herbivory, survival was estimated to be well in excess of 90 percent.

Table 2–1. Plant cover in the 1999 planting estimated using an October 2007 Quickbird image.

1999 Planting Sections	Total Area (m^2)	Plant Cover (%)	Plant Cover (m^2)
West	3,729	34.7	1,294
West Middle	4,807	26.6	1,279
East Middle	4,541	47.6	2,162
East	4,255	70.6	3,004
Total	17,332	44.7	7,739

Plant cover, estimated using an October 2007 QuickBird satellite image, ranged from 27 percent in areas where growth has been stunted since early in the study (see Section 2.2.2) to 71 percent in areas of greatest growth. At the end of the 2007 growing season, mean plant cover for the 1999 planting was 45 percent, up slightly from 43 percent at the end of the 2006 growing season.

In October 2007, the height and width of every 50th plant in each irrigated row of the 2006 planting (subpile soil and evaporation pond soil) was measured in the field. Plant biomass was estimated using a regression with plant canopy volume; a double sampling relationship established previously (Figure 2–2). Subsamples of leaves and stems from 12 plant samples (six from the 1999 planting and six from the 2006 planting) were analyzed to estimate nitrogen content.
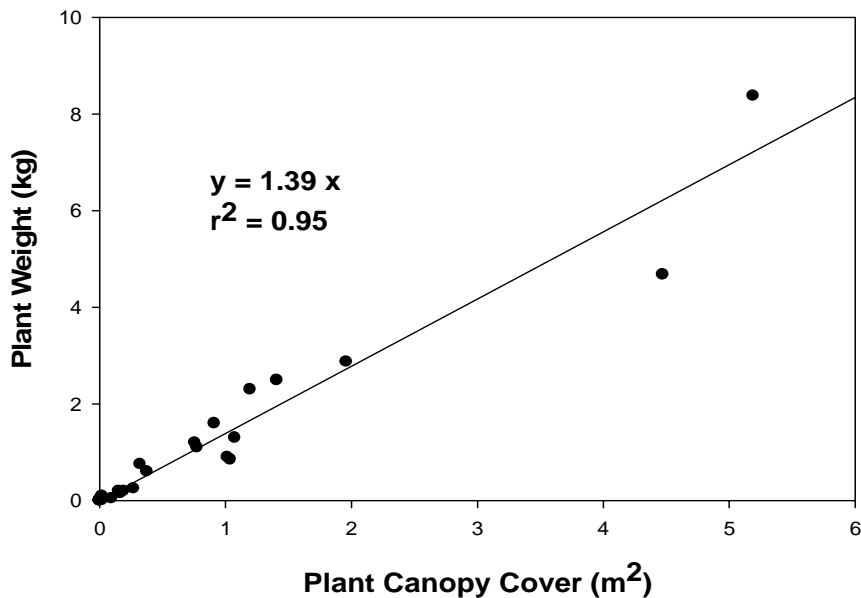
Figure 2–2. Linear regression relationship of plant dry-weight biomass as a function of plant canopy cover.

Plant growth in the 2006 planting (in the subpile Extended Field sections and in the evaporation pond) is shown in Table 2–2. Canopy cover in the Extended Field sections was still relatively low; however, marked differences in growth were observed by section. Sections adjacent to the area of stunted growth in the 1999 planting (see Section 2.1.2) had the lowest plant cover, 0.9 percent (Extended Field West) and 3.3 percent (Extended Field South). Plants in Extended Field North tended to be smaller on the west side and larger on the east side. This corresponds to growth trends in the adjacent areas of the more mature 1999 planting. Average plant cover was highest in Extended Field North (41 percent). At the end of the 2007 growing season, mean plant cover of all three Extended Field sections was 16 percent, up from 1.2 percent at the end of the 2006 growing season. Mean survival for all three Extended Field sections was 97.5 percent. Canopy cover in the evaporation pond remained low at 2.5 percent, but up from 0.3 percent at the end of the 2006 growing season.

Table 2–2. Survival and plant cover in Extended Field by ground measurements.

2006 Planting Sections	Total Area (m^2)	Plant Cover (%)	Plant Cover (m^2)	Live Plants	Survival (%)
Extended Field West	3,016	0.9	28	528	98.3
Extended Field North	4,374	40.8	1,785	1,605	98.3
Extended Field South	5,427	3.3	180	1,241	96.3
Extended Field Total	12,817	15.5	1,993	3,374	97.5
Evaporation Pond	2,859	2.5	70	568	97.9

Table 2–3 is a summary of canopy volume, dry-weight biomass, and plant tissue nitrogen and sulfur results for the 1.7 ha planting in 1999. The mean nitrogen content was 1.9 percent, not significantly different from the mean of 2.2 percent in 2006 ($p < 0.05$). Total nitrogen uptake for the 2000–2007 period was 204 kilograms (kg) compared to 189 kg at end of the 2006 growing season. Mean standing biomass was estimated at 6.2 t/ha, up from 5.2 t/ha in 2006.

Table 2–3. Estimated canopy volume, dry-weight biomass, nitrogen and sulfur uptake in the 1999 planting.

1999 Planting Sections	Dry Biomass (kg)	Dry Biomass (kg/ha)	Nitrogen Uptake (kg)	Nitrogen Uptake (kg/ha)	Sulfur Uptake (kg)	Sulfur Uptake (kg/ha)
West	1,799	4,824	34.2	92	3.4	9.2
West Middle	1,777	3,697	33.8	70	3.4	7.0
East Middle	3,005	6,617	57.1	126	5.7	12.6
East	4,176	9,814	79.3	186	7.9	18.6
Total	10,757	24,952	204	474	20	47

Table 2–4 is a summary of canopy volume, dry-weight biomass, and plant tissue nitrogen and sulfur results for plants in the 2006 plantings. Mean nitrogen content in the Extended Fields was 1.5 percent (not significantly different from 2006; $p < 0.05$). Total nitrogen uptake for the 2006–2007 period was 42 kg, up from 2.5 kg at the end of the 2006 growing season. The canopy volume in the evaporation pond was 19.4 cubic meters (m^3), up from 1.2 m^3 in 2006, and dry-weight biomass in the evaporation pond was 98 kg, up from 22 kg in 2006. Plants in the evaporation pond were not sampled for nitrogen and sulfur in 2007.

Table 2–4. Measured canopy volume, dry-weight biomass, nitrogen and sulfur uptake in 2006 plantings.

Area	Canopy Volume (m^3)	Dry Biomass (kg)	Dry Biomass (kg/ha)	Nitrogen Uptake (kg)	Nitrogen Uptake (kg/ha)	Sulfur Uptake (kg)	Sulfur Uptake (kg/ha)
Extended Field West	4.7	38	126	0.6	2	0.1	0.3
Extended Field North	1,200.4	2,481	5,672	37.2	85	5.2	11.9
Extended Field South	56.8	251	463	3.8	7	0.5	1.0
Extended Field Total	1,261.9	2,770	6,261	42	94	6	13
Evaporation Pond	19.4	98	343				

Figure 2–3 shows *Atriplex* and *Sarcobatus* recruitment in 2007 in areas that were denuded in 1999. The text in Figure 2–3 documents observations of plant stands. Plants in these areas are contributing to phytoremediation, including preventing recharge, extracting nitrate, and providing hydraulic control.

Check instance of ATCA and SAVE in "heel print" image.

Walked on road along fence line from gate near shed to corner.

Identified plant nearest to each fence post. There were 100 plants. All were ATCA.

Walking back towards gate, counted any SAVE visible across the width of the field. This was done to verify presence of SAVE. Counted 24 SAVE.

Looking at this stand from various other view points and from within the stand, almost all were ATCA with a small number of SAVE.

Looking at the stand north of the road, there was an approximately equal mix of ATCA and SAVE mearest to the fence line, transitioning fairly quickly to mostly SAVE.

17-Oct-07

Figure 2–3. Observations of plant stand in northeast corner of fenced site, and across the road from this site, to determine predominate plant types (ATCA, SAVE).

2.1.2 Causes and Recourses for Stunted Plant Growth

There is an area of poorer plant growth in the western third of the 1999 subpile soil planting. Previous analyses of soil samples from areas with both poor and good growth suggested that nitrate, sulfate, calcium, magnesium, strontium, and vanadium were higher in the poor-growth areas. Conversely, concentrations of iron, manganese, phosphate, potassium, sodium, and uranium were significantly lower in the poor-growth areas. The stunted growth of *Atriplex* shrubs may be due to the combined effects of both an excess and a deficiency of several ions. In a previous greenhouse study, growth of Sudan grass in soil obtained from a poor-growth area was significantly less than growth in a soil sample taken from a good-growth area. Chemical analysis of Sudan grass tissue samples was inconclusive as to the causative agents of poor growth. Tests also found that soil bulk densities, another suspected cause of poor plant growth, were not significantly different in poor-growth and good-growth areas.

Greenhouse Study

We hypothesized that the high salt content may be preventing adequate uptake of essential elements or micronutrients, especially iron and copper, needed to support plant health. To test this hypothesis, students at the Diné College in Tsaile, Arizona, conducted a greenhouse study to evaluate whether amendments with adequate micronutrients increased or suppressed the phytotoxic effects. The study consisted of the following treatment structure:

- Soils

    — Poor-growth soil (stained MV [Monument Valley])

    — Good-growth soil (good MV collected outside of the stained area)

    — Mixture of 2 parts stained soil to 1 part Miracle-Gro (MG) All-Purpose Potting Mix (stained + MG)

    — Mixture of 2 parts good-growth soil to 1 part MG All-Purpose Potting Mix (good + MG) Fertilizer solutions

- Water only (negative control)

    — Iron: 10 parts per million (ppm) (low iron content), 20 ppm (medium iron content), and 40 ppm (high iron content) iron chelate

    — Copper: 10 ppm (low copper content), 20 ppm (medium copper content), and 40 ppm (high copper content) cupric chloride

    — Iron and copper mixture: 10 ppm (low iron and copper content), 20 ppm (medium iron and copper content), and 40 ppm (high iron and copper content) iron chelate and cupric chloride

- Plant species

    — *Atriplex canescens*

Eight-week-old seedlings of *Atriplex canescens* were transplanted into 1.0 liter (L) pots. Initial biomass measurements were obtained for a random subsample of the seedling as they were potted. Plants were irrigated according to the treatment schedule listed in Table 2–5. Mortality, plant-height, and plant-width measurements were taken weekly. Biomass was measured after 43 days of growth.

Results (Table 2–5 and Table 2–6; Figure 2–4) indicate that the plants sown in the stained soil did not respond well to the micronutrient amendment with the exception of plants receiving the iron-and-copper treatments. Plant survival rate improved dramatically; in fact, plant survival was 100 percent for treatment I compared to the other treatments in the stained soil. Additionally, we recovered significantly ($p < 0.05$) more plant biomass for treatment I compared to the negative control and any of the treatments that involved copper alone.

Plant growth (survival, biomass recovered, and change in plant size over time) improved significantly upon amendment of the stained MV with 1 part MG All-Purpose Potting Mix. The addition of micronutrients, however, was not beneficial to the plants when compared to the control.

Table 2–5. Percent survival, growth as a change in volume, and the total dry biomass harvested (± standard error of the mean) from Atriplex seedlings sown in the different soil and fertilizer treatment combinations (n = 4 plant replicates per treatment). Low Fe = low iron content; Med Fe = medium iron content; Hi Fe = high iron content; Low Cu = low iron content; Med Cu = medium copper content; Hi Cu = high copper content; Low Fe + Cu = low iron and copper content; Med Fe + Cu = medium iron and copper content; Hi Fe + Cu = high iron and copper content.

Treatment	Soil	Fertilizer	% survival	ΔV (cm^3)	Dry Biomass
A	Stained MV	Negative Control	20	129	1.4 (0.1)
B	Stained MV	Low Fe	20	253	1.6 (0.2)
C	Stained MV	Med Fe	0	51.7	1.1 (0.1)
D	Stained MV	Hi Fe	0	10.4	0.9 (0.2)
E	Stained MV	Low Cu	0	-61.4	0.6 (0.1)
F	Stained MV	Med Cu	0	-45.5	0.5 (0.1)
G	Stained MV	Hi Cu	40	-5.1	1.6 (0.6)
H	Stained MV	Low Fe + Cu	80	5.3	1.9 (0.5)
I	Stained MV	Med Fe + Cu	100	12.3	2.5 (0.2)*
J	Stained MV	Hi Fe + Cu	60	31.4	1.9 (0.4)
K	Stained MV + MG	SR fertilizer	100	663	3.8 (0.6)
L	Stained MV + MG	Low Fe	80	420	1.9 (0.4)
M	Stained MV + MG	Med Fe	100	544	4.2 (0.8)
N	Stained MV + MG	Hi Fe	80	167	2.4 (0.6)
O	Stained MV + MG	Low Cu	80	742	2.0 (0.2)
P	Stained MV + MG	Med Cu	100	707	2.5 (0.2)
Q	Stained MV + MG	Hi Cu	60	551	1.9 (0.2)
R	Stained MV + MG	Low Fe + Cu	100	661	3.1 (0.5)
S	Stained MV + MG	Med Fe + Cu	80	962	3.5 (0.6)
T	Stained MV + MG	Hi Fe + Cu	80	632	2.1 (0.3)
U	Good MV	Positive Control		24.5	1.6 (0.4)
V	Good MV + MG	Positive w/ Fertilizer		301	1.1 (0.2)

Table 2–6. Macro- and micronutrients in pooled plant tissue samples analyzed after the harvest.

Treatment	N (%)	P (%)	K (%)	Ca (%)	Mg (%)	Fe (ppm)	Zn (ppm)	Mn (ppm)	Cu (ppm)
A	1.3	.10	1.6	2.20	0.65	180	22	85	5
B	1.2	.09	1.0	1.30	0.38	140	18	33	6
C	1.2	.09	1.5	2.10	0.60	260	22	59	6
D	1.1	.15	1.4	1.80	0.48	510	30	66	10
E	1.7	.18	1.2	1.40	0.27	200	24	42	7
F	1.7	.16	1.8	2.40	0.55	210	29	57	9
G	1.3	.14	1.5	2.00	0.54	550	27	100	12
H	1.0	.17	1.7	2.20	0.57	2000	26	160	38
I	1.0	.11	1.3	2.10	0.40	610	25	86	46
J	0.9	.13	1.6	2.60	0.56	550	28	78	65
K	1.3	.18	2.6	2.20	0.57	190	32	110	6
L	1.4	.29	3.3	1.90	0.46	390	50	130	8
M	1.7	.24	2.7	1.90	0.58	640	42	94	8
N	1.9	.37	4.7	2.20	0.60	350	51	120	11
O	1.9	.30	4.3	2.80	0.64	250	51	170	8
P	1.6	.38	4.0	2.20	0.69	70	50	130	14
Q	1.8	.29	4.2	2.40	0.78	260	63	160	22
R	1.5	.23	3.3	2.10	0.55	600	42	130	21
S	1.6	.27	3.8	1.80	0.53	230	45	96	33
T	1.8	.17	2.9	2.10	0.66	220	24	66	25
U	1.5	.12	2.7	2.30	0.63	260	38	47	9
V	1.7	.24	4.4	2.00	0.64	82	49	50	9

N = nitrogen; P = phosphorous; K = potassium; Ca = calcium; Mg = magnesium; Fe = iron; Zn = zinc;
Mn = manganese; Cu = copper

Figure 2–4. A photograph of the Atriplex plants taken 4 weeks after the start of the greenhouse experiment. Plants were sown in the stained MV soil (treatments A through J), and stained MV soil was supplemented with potting mix (treatments K through T) and amended with micronutrients as described in Table 2–5 above.

Laboratory Analyses of Field Samples

In light of the Diné College studies, we revisited the issue of what caused the chemical staining and dark mottling in the subpile soil. We conducted further analyses of the discolored soils at the Monument Valley site to attempt to understand the nature of the contaminants affecting plant growth. We focused on the shallow soils in the stained area of the fields that showed black or gray mottling. We measured carbon species to determine if the black and gray material was charcoal. However, Table 2–7 shows that soils were low in organic carbon, and that calcium carbonate could account for the inorganic carbon in soils that were high in total carbon.

Table 2–7. Location and characteristics of soil samples from the stained area at the Monument Valley Uranium Mill Tailings Remedial Action (UMTRA) site. The color of the soil and degree of mottling is given. VLBM = very light black mottling; LBM = light black mottling; MBM = medium black mottling; HBM = heavy black mottling; LGM = light gray mottling. TOC = total organic carbon; TC = total carbon; CaCO$_3$ = calcium carbonate. CaCO$_3$ was determined by titration. See Section 2.5 for location maps.

Color	Mottling	Location	TOC	TC	CaCO$_3$
Dark red	MBM	MV E 4-15	0.03	0.03	<0.1
Dark red		MV E 1-3	0.05	0.43	0.44
Dark red		MV E 5-1	0.10	0.39	0.37
Dark red	LBM	MV EM 2-1	0.10	0.44	0.39
Medium red		MV EM 3-12	0.03	0.02	0.02
Medium red	LBM	MV EM 4-6	0.05	0.13	0.13
Dark red		MV E 1-12	0.03	0.05	0.02
Light red		MV E 2-6	0.08	1.43	1.47
Dark red	LBM	MV E 4-1	0.09	0.15	0.08
Medium red	MBM	MV EFW 2-1	0.11	0.43	0.36
Medium red	MBM	MV EFW 3-1	0.05	0.59	0.54
Light red	MBM	MV WM 2-1	0.12	1.8	1.74
Medium red	LBM	MV W 3-6	0.02	0.02	<0.1
Medium red	VLBM	MV W 1-3	0.03	0.04	<0.1
Dark red	HBM	MV EM 4-9	0.03	0.07	<0.1

An inspection of the soil samples showed the presence of numerous soft manganese nodules, which could have formed from the co-precipitation of iron and manganese during the leach of materials from the ore into the shallow soil. Analyses of soils containing nodules showed they contained 2.81 milligrams per gram (mg/g) of manganese and 3.08 mg/g of iron, confirming that they were manganese nodules. The different oxidation states of manganese and iron can account for the different stain colors seen in the subpile soils. An explanation of their presence in the subpile soil follows (explanation by Dr. Janick Artiola, Soil, Water, and Environmental Science Analytical Lab, UA):

> Manganese (Mn) is relatively abundant in soils—900 mg/kg—ranging from 20 to 3,000 mg/kg. The chemistry of Mn in soils is very complex because it can have three possible oxidation states (II, III, IV) within the pH-redox range of most soil systems (Lindsay 1979). Many Mn complexes are colored. The most-reduced forms (MnII) are more soluble and can form oxides, hydroxides, and carbonates in the soil, such as pyrolusite, pyrochroite, and manganese sulfates (e.g., MnSO$_4$, which is reddish-pink). More-oxidized forms of Mn can also react with sulfates, producing green colors (e.g., Mn$_2$(SO$_4$)$_3$). The

most-stable forms (least soluble) of Mn are Mn(IV)—like pyrolusite (beta-MnO_2)—and Manganite (MnOOH).

The formation or dissolution of Mn nodules is typically associated with, and has been mostly studied in, marine environments, but soils with past or present significant redox fluctuations, as occurs in leach ponds for ore extraction, can also have Mn nodules. Manganese nodules (a few millimeters in diameter) have been shown to be present in the soils of the Monument Valley subpile soil area, especially in the stained areas and where the former evaporation ponds are located.

This site is under irrigation and revegetation, and these recent events may be altering the redox reactions (usually enhanced via wet/dry cycles) of Mn significantly. Although it has not been proven, the colored bands near irrigation emitters may indicate the presence of soluble and redox active Mn species that could either co-precipitate or dissolve in response to soil–water redox changes. One possible scenario is the recent induced change from less oxidized and more-mobile forms of Mn to more-oxidized Mn species and less soluble Mn species due to increased biological activity (irrigation, plant rhizoidal-microbial activity). Further studies would be needed to determine the origin of the Mn nodules and their relationship to soluble forms of Mn present in the soil-pore water. Additional studies would also be needed to determine whether this element is bioaccumulating in plants, at what rates it is bioaccumulating, and how Mn uptake may affect plants in the ecology of that environment.

2.1.3 Enhanced Microbial Denitrification in the Source Area

Planting and irrigating the source area has been exceptionally effective in removing nitrate from the soil by the microbial process know as denitrification, the conversion of nitrate to nitrogen gas. Nitrification is the conversion or oxidation of ammonium to nitrate, which can be brought about by nitrifying bacteria. Denitrification rates in the Monument Valley soil are likely limited by low levels of total organic carbon (TOC). Previous batch and column studies showed that ethanol greatly enhances denitrification; hence, the possibility of stimulating denitrification by supplying ethanol through the irrigation system was evaluated in 2006 and 2007.

A pilot study initiated in 2006 evaluated the addition of ethanol as a carbon source to enhance or speed up denitrification in the source area. Ethanol was distributed through a few of the subpile irrigation lines using venturi injection systems. A 15 percent ethanol solution was injected into drip lines to deliver a final ethanol concentration of 0.15 percent. The ethanol solution was replenished every month from May until September 2007. Three venturi systems were installed starting at the southeast end of the 1999 planting and distributed through irrigation tubing into the 2006 planting to the south. Three lines were set in place in such a way that they fed ethanol to three irrigation lines in the 2006 planting (five plants per line) and three irrigation lines (five plants per line) in the new planting area. Three control lines in the 1999 and 2006 planting areas directly adjacent to the venturi lines were monitored for comparison.

Soil samples were collected in May, July, and October 2007 to monitor for nitrate, ammonia, TOC, nitrous oxide production, and moisture at three soil depths (0.3, 1.3, and 2.7 meters [m]). Denitrification was measured in laboratory microcosms in soil samples collected near randomly selected plants in each treatment. Denitrification was assayed by the production of nitrous oxide

in incubation vessels containing acetylene, which blocks the conversion of nitrous oxide to dinitrogen gas.

Results for 2007 were generally similar to those reported in 2006, except that ethanol had a slightly stimulatory effect on denitrification in 2006, but no significant ($p > 0.05$) effect in 2007. Significance levels of treatments are shown in Table 2–8, and mean and standard errors of dependent variables for each treatment are shown in Table 2–9.

Table 2–8. Effect of soil depth, planting age (old vs. new plantings), ethanol injection, and sampling month on soil variables measured in the Subpile Soil Enhanced Denitrification Pilot Study (2007). The table gives "p" values or "ns" (not significant at $p < 0.05$) for each variable, and if a variable is significant, it indicates the direction of the treatment effect.

Variable	Soil Depth	Planting Age	Ethanol	Month
Nitrate	ns	0.013 (Old > New)	ns	0.003 (May > July, Oct.)
Ammonium	ns	ns	ns	ns
TOC	ns	ns	ns	0.003 (Oct. < May, July)
Moisture	< 0.001 (0.3 m > 1.3 m > 2.7 m)	< 0.001 (Old < New)	ns	ns
Denitrification	ns	ns	ns	0.028 (May < July, Oct.)

Table 2–9. Means and standard errors of soil variables measured in the Subpile Soil Enhanced Denitrification Pilot Study (2007), reported by soil depth, planting type, month, and ethanol treatment. NO_3^- = nitrate; NH_4^+ = ammonium; g/g = grams per gram; ng/kg/hr =nanograms per kilogram per hour.

Variable	NO_3^- (mg/kg)	NH_4^+ (mg/kg)	TOC (%)	Moisture (g/g)	Denitrification ng/kg/hr
Soil Depth					
0.3 m	14.9 (3.8)	4.41 (2.28)	0.417 (0.021)	0.028 (0.003)	14.3 (4.1)
1.3 m	12.8 (2.1)	1.18 (0.36)	0.346 (0.013)	0.059 (0.002)	9.7 (3.3)
2.7 m	21.6 (4.07)	4.15 (1.93)	0.362 (0.049)	0.052 (0.002)	14.2 (7.8)
Planting					
New	11.6 (1.48)	4.90 (1.94)	0.396 (0.040)	0.069 (0.002)	8.33 (2.3)
Old	20.8 (3.5)	1.67 (0.057)	0.356 (0.013)	0.057 (0.003)	17.1 (5.7)
Month					
May	24.9 (4.9)	3.80 (1.71)	0.449 (0.044)	0.062 (0.003)	18.2 (3.1)
July	13.4 (1.68)	4.72 (2.40)	0.406 (0.014)	0.065 (0.008)	16.6 (8.2)
October	10.1 (2.09)	1.13 (0.24)	0.263 (0.011)	0.062 (0.004)	21.0 (3.3)
Ethanol					
Yes	13.9 (1.93)	2.11 (0.92)	0.392 (0.013)	0.061 (0.003)	8.69 (2.6)
No	18.7 (3.40)	4.36 (1/76)	0.359 (0.013)	0.065 (0.002)	16.7 (5.6)

Ethanol injection did not result in decreased soil nitrate or ammonium, increased TOC, or enhanced rates of denitrification in either the new or old plantings. The stimulatory effect of ethanol observed in the laboratory was not observed in the field due to the low levels of soil moisture in the field. Therefore, the injection of ethanol as a method to increase the rate of denitrification in the subpile soil was not supported. In general, and despite daily irrigation at twice the rate that was applied in 2007, the gravimetric water content of the soil was less than 0.07 grams per gram (g/g) and was significantly drier for the established plants and with depth.

The plants were growing vigorously and were using all the water applied; hence, soil moisture, rather than carbon, appeared to be the limiting factor for denitrification. Denitrification proceeds most rapidly in saturated, anaerobic soils, whereas these soils were well below field capacity (approximately 0.14 g/g).

Although ethanol injection did not enhance the rate of denitrification, the rates reported in Table 2–9 are substantial, and as mentioned, they resulted in a further decrease in soil nitrate levels in 2007. Hence, continued irrigation of the 1999 and 2006 plantings will result in further nitrate removal from the soil and will continue to control the water balance to minimize discharge from the subpile soil to the aquifer, through enhanced evapotranspiration (ET).

2.1.4 Nitrate and Ammonium in Source Area Soils

Nitrate and ammonium in source area soils have been monitored since 2000. An initial characterization of the source area in 1997 discovered elevated soil ammonium in the area of the former New Tailings Pile (subpile soils). A more detailed survey conducted in June 1997 included analysis of both nitrate and ammonium levels from subpile soils sampled in a radial pattern away from location 866 (DOE 2002). The original phytoremediation planting area was delineated, irrigation lines were installed, and more than 4,000 *Atriplex* plants were sown based on these initial results. The location and layout of the 1999 planting were based on the distribution of ammonium in subpile soils. Ammonium is more toxic and was of greater concern, so the planting was designed to contain and remove it. However, subsequent sampling indicated that nitrate is more widespread. Because nitrate is also more mobile than ammonium, it represents a more immediate source of nitrogen in the alluvial aquifer. An intensive sampling program conducted in 2005 determined the full extent of nitrate and ammonium in the source area (subpile soils and evaporation pond soils). These "extended fields" were planted with more than 4,000 additional *Atriplex* plants in spring of 2006.

In 2007, 40 random points within the source areas (subpile evaporation pond soils) were sampled for nitrate and ammonium using neutron hydroprobe ports as starting points (see Section 2.5). Samples were extracted at depths of 1 foot (ft), 3 ft, 6 ft, 9 ft, 12 ft, and 15 ft at each point unless bedrock was encountered at a shallower depth. All samples were analyzed in the DOE Environmental Sciences Laboratory using a variation of the "Standard Batch Leaching" procedure (Stoller 2006). Samples were air-dried and sieved through a #10 mesh (< 2 millimeters [mm]). Twenty-gram samples of < 2 mm material were mixed with 50 mL 1 mole (M) potassium chloride in 125 mL Nalgene bottles, stirred at 8 revolutions per minute (RPM) for 2 hours, and centrifuged for 20 minutes at 3,500 RPM. The potassium chloride solutions were decanted, and the centrifuge bottles were again filled with 50 mL 1M potassium chloride, stirred for 30 minutes, and decanted. Samples were again centrifuged for 20 minutes at 3,500 RPM and decanted. Decanted potassium chloride solutions were then filtered (0.45 υm [micrometer] paper). Potassium chloride extractions were analyzed by ion chromatography for nitrate, and with Hach spectrophotometry for ammonia. All analyses were performed the same day that extraction took place.

Figure 2–5 and Figure 2–6 show time series of source area soil monitoring results for the 1999 and 2006 planting areas. The results show that the loss of nitrate (denitrification) in the original planting was greatest at times of peak soil moisture. By 2005, the initial rapid rate of denitrification subsided due to a decrease in soil moisture, likely caused by greater transpiration

from the maturing plant community. However, with increased irrigation in 2006, nitrate levels in the original planting declined again, from 95 mg/kg in 2005 to 73 mg/kg in March 2007. This represents a 65 percent decrease since 2000, when irrigation commenced. Water content in the 2006 Extended Field plantings were greater than in the 1999 planting area where plants are larger and transpire more water, apparently stimulating denitrification and causing the substantial drop in soil nitrate (Figure 2–6).

Nitrate and Ammonium in Subpile Soil
(Original Field)
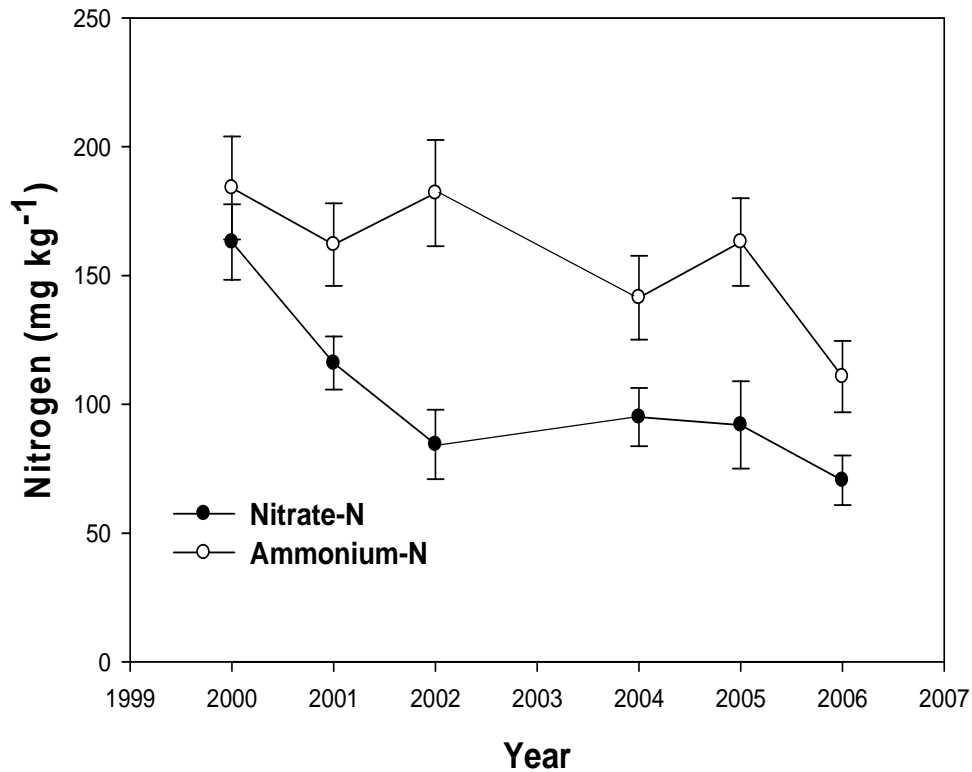
Figure 2–5. Nitrate and ammonium concentrations in the subpile soil phytoremediation plot. The field was not sampled in 2003, and irrigation was interrupted from 2003 to 2004.
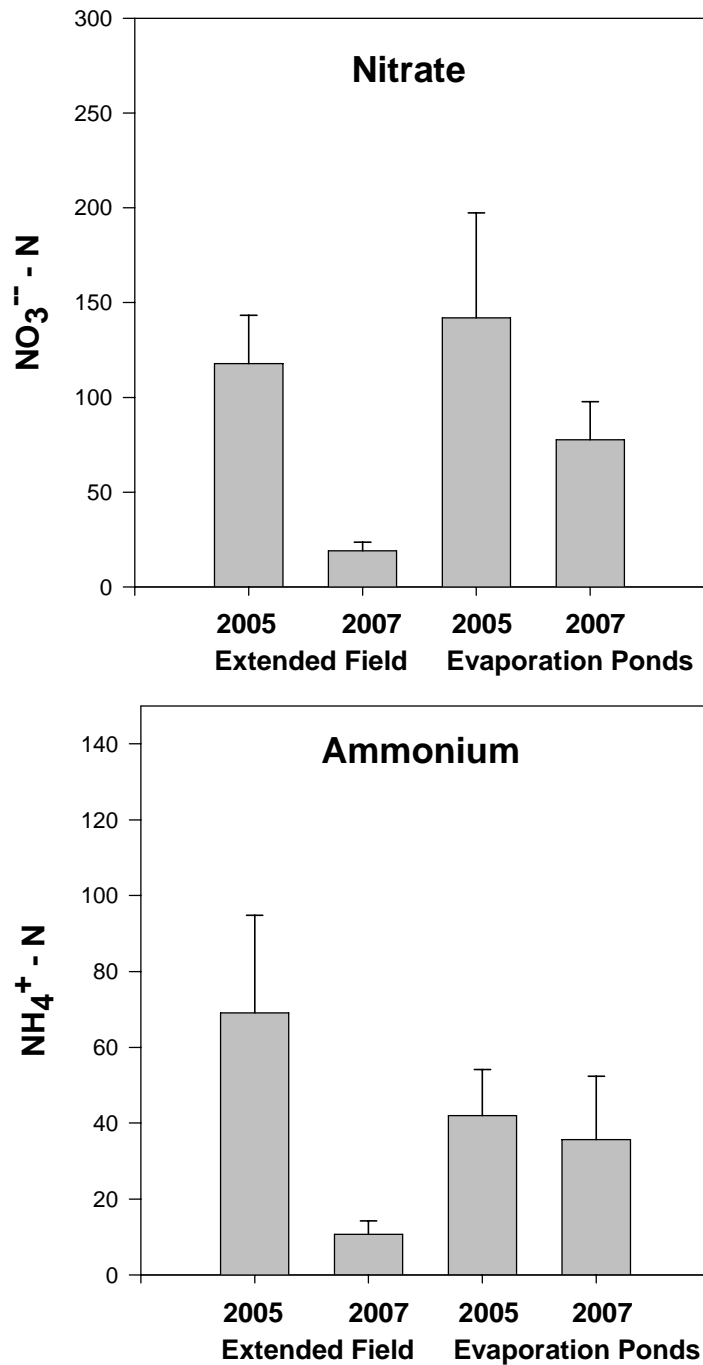
Figure 2–6. Nitrate-N and ammonium-N in Extended Fields and evaporation pond areas in 2005 (initial survey) and 2007 after 1 year of irrigation.

2.2 Natural and Enhanced Attenuation of Groundwater

The pilot studies are evaluating natural and enhanced attenuation as the primary remedies for groundwater contamination at Monument Valley. Several natural processes may be acting to decrease nitrate and sulfate levels in the alluvial aquifer. Enhanced attenuation can be described as initiating or augmenting natural and sustainable attenuation processes in an effort to increase

the magnitude of natural processes beyond that which occurs without intervention. Enhanced attenuation approaches may be implemented if there is insufficient evidence to show, with a high level of certainty, that the total capacity of natural attenuation processes are capable of attaining groundwater remediation objectives.

The pilot studies are designed to acquire field data needed to estimate the capacity of natural and enhanced attenuation processes. The objectives of natural attenuation pilot studies are to determine if the capacity of all natural processes acting to lower nitrate and sulfate levels in the alluvial aquifer (1) exceed rates of contaminant loading from sources and (2) will achieve remediation requirements in a reasonable timeframe. The enhanced attenuation pilot studies are focusing on enhancements that are sustainable—that do not require long-term, continuous intervention. The goals are to slow plume movement, extract nitrate and sulfate, and increase microbial denitrification.

Preliminary studies found that protecting native *A. canescens* and *S. vermiculatus* plants from grazing can double biomass productivity, transpiration rates (water extraction from the aquifer), and nitrogen uptake rates. Preliminary studies also found that transplants could be successfully established, grow vigorously for several years in small exclosure plots, and with managed irrigation, send roots 30 ft into the nitrate and sulfate plume (DOE 2004c).

2.2.1 Grazing Exclosures

In 2005, two grazing exclosure plots were constructed at the site. Previous studies in these and earlier exclosures demonstrated that grazing protection may have positive effects on biomass productivity, ground cover, and rates of phreatophyte transpiration and nitrogen uptake. An additional study was initiated in 2007 to investigate shrub density and vegetation cover in the two exclosure plots and adjacent control plots not protected from grazing. The purpose of the study is to better understand how grazing protection may change plant community composition and phreatophyte shrub density over several years' time.

A relevé was performed within each exclosure plot and within each control area in early November 2007. No significant differences in species composition were noted between the inside and outside of the exclosure plots, but some differences were noted between the north and south areas, probably the result of differences in groundwater depths. The most common species in all areas were four-wing saltbush, tansy mustard (*Descurainia sophia*), and Russian thistle (*Salsola tragus*). More plant species were found in the north than the south (18 and 12, respectively). Greasewood (*Sarcobatus vermiculatus*) and shadscale (*Atriplex confertifolia*) were found both inside and outside the south plot but not the north. Resinbush (*Vanclevea stylosa*) and purple sage (*Poliomintha incana*) were found both inside and outside the north plot, but not the south. Because of the late season, this relevé does not represent year-round differences in species composition, as many early-season species were not visible or lacked structures for positive identification. Also, at the time of sampling, a damaged fence was repaired in the native north exclosure plot, where extensive livestock trampling was observed within the exclosure.

Line transects were used to quantify differences in plant cover. Twenty 5-m transects were randomly placed within each native grazing exclosure and equal-sized control area. Teams recorded the cover types directly under points at 1-dm intervals on each transect tape. T-tests were used to compare means and identify statistically significant differences. Results of the transect samples are summarized in Table 2–10.

Table 2–10. Vegetation cover inside and outside grazing exclosure plots.

Cover Type	Native South Inside	Native North Inside	Native South Outside	Native North Outside
Atriplex canescens	16.3	10.6	1.6	8.9
Atriplex confertifolia	0.6	-	0.8	-
Sarcobatus vermiculatus	10.4	-	4.1	-
Total phreatophyte shrubs	27.3	10.6	6.5	8.9
Ephedra torreyana	-	1.3	-	-
Ephedra viridis	-	0.2	-	-
Gutierrezia sarothrae	0.3	-	0.9	-
Poliomintha incana	-	0.7	-	0.4
Vanclevea stylosa	-	0.3	-	2.1
Yucca angustifolia	-	-	-	0.6
Total non-phreatophyte shrubs	0.3	2.5	0.9	3.1
Ambrosia acanthicarpa	-	0.9	-	-
Chamaesyce maculate	-	0.5	-	-
Descurainia sophia	1.6	3.4	2.8	2.2
Machaeranthera sp.	-	0.1	-	-
Mentzelia multiflora	0.1	0.2	0.1	0.2
Salsola tragus	9.2	3.6	6.6	5.7
Suaeda torreyana	-	-	2.3	-
Total forbs	10.9	8.7	11.8	8.1
Plant litter	15.6	15.2	12.1	12.8
Bare ground	45.9	63.1	68.7	67.0
Total vegetative cover	38.5	21.7	19.2	20.2

Species composition data from the transects generally support the relevé data. Phreatophyte shrub cover is significantly higher inside the grazing exclosures than outside (19.0 percent and 7.7 percent, respectively; $p = 0.005$). Total vegetative cover is also significantly higher (30.1 percent inside and 19.7 percent outside; $p = 0.025$). Because the north plot experienced grazing pressure in 2007, means were analyzed for phreatophyte shrub and total cover inside and outside the north plot alone. No significant differences were found. Therefore, differences in the south plot (27.3 percent inside and 6.5 percent outside for phreatophytes and 38.5 percent inside and 19.2 percent outside for total cover) are probably more representative of the effect of grazing exclosures than the combined data after two growing seasons. No significant differences exist between plots with respect to non-phreatophyte shrubs or forbs.

To estimate shrub density, the distance from each sampling point to the nearest phreatophyte shrub of a given species was recorded (point-to-plant distance) as well as the distance between that shrub and its nearest conspecific neighbor (plant-to-plant distance). Density was calculated for each species using (1) closest-individual method, (2) nearest-neighbor method, and (3) a combined method, summarized below. The results of the density calculations are presented in Table 2–11.

(1) Closest-individual method (as presented in Bonham 1989):

$$D = \frac{1}{(2d)^2}$$

where d is the mean point-to-plant distance of the sampled shrubs

(2) Nearest-neighbor method (Cottam and Curtis 1956):

$$D = \frac{1}{(1.67d)^2}$$

where d is the mean plant-to-plant distance of the sampled shrubs

(3) Combined method (Waugh 2002):

$$D = \left[\frac{3.717^A}{3.473} \right] d$$

$$A = (1.9131) \left[\sqrt{s^2 / (y)(r_n)} \right]$$

$$d = \frac{n}{\pi \sum_{i=1}^{n} y}$$

where n is the number of samples,

y is the mean point-to-plant distance,

r_n is the mean plant-to-plant distance, and

s^2_y is the sample variance of all distances

Table 2–11. Shrub density inside and outside grazing exclosure plots.

Area	Closest Individual	Nearest Neighbor	Combined Method
Native South Inside	250.1	227.0	312.9
Native South Outside	442.8	501.7	459.9
Native North Inside	839.2	719.7	729.8
Native North Outside	2,463.5	1,781.6	1,873.6

Each shrub included in the density measurements was assessed for size/age class. Three size classes were recorded for each species of shrub: small, medium, and large. The results of the size/age class assessment are summarized in Table 2–12.

Table 2–12. Shrub size/age classes inside and outside grazing exclosure plots.

Area	Shrub Size Class		
	Large	**Medium**	**Small**
Native South Inside	47.7	35.5	16.9
Native South Outside	21.0	21.9	57.1
Native North Inside	12.8	10.3	77.0
Native North Outside	5.1	10.3	84.6
Average Inside	30.3	24.2	47.0
Average Outside	13.1	16.1	70.9

Although the phreatophyte shrub cover is lower outside the grazing exclosures than inside, average shrub density outside is estimated to be more than twice the density inside (1,167 vs. 521.4 shrubs per acre). This may be, in part, because the outside areas generally contain more small shrubs than the inside areas, but the relationship between cover and density is unclear. These data are most useful as a baseline to compare potential changes in future years.

2.2.2 Revegetation Plots

In 2006, two fence plots, which measure 50 m by 50 m, were installed for a large-scale transplanting demonstration (Revegetation Plots). The goal was to promote an increase in the extraction of nitrate and plume water. The two fenced plots are located in a denuded area overlying the proximal region of the plume with the highest nitrate concentrations. The plots also span a range of depths to groundwater. Depths to groundwater are about 30 ft for Revegetation Plot 1 and 40 ft for Revegetation Plot 2. The Revegetation Plots were planted, and irrigation began in spring 2006.

Plant growth in the Revegetation Plots is shown in Table 2–13. Canopy cover was 16.0 percent in Revegetation Plot 1 and 5.9 percent in Plot 2. Field observations indicate that the smaller cover in Plot 2 was probably due to increased grazing by small animals living within the fenced area. Average canopy volume per plant in Plot 1 was 0.02 m^3 while the volume for plants in Plot 2 averaged 0.01 m^3. Plastic screens were placed over the plants in 2006 to protect them from grazing. Figure 2–7 compares plant canopy area of the Revegetation Plots with other 2006 plantings. The mean plant cover for both Revegetation Plots was 11 percent (up from 3.3 percent at the end of 2006). Mean survival was 96.9 percent.

Table 2–13. Evaluation of annual growth and survival of plants in the revegetation plots. The plots are located in the region designated as Plume Area 1 representing the hotspot of nitrate contamination.

Area name	Total Area (m^2)	Plant Cover (%)	Plant Cover (m^2)	Live Plants	Survival (%)
Revegetation Plot 1	2,921	16.0	466.9	614	96.8
Revegetation Plot 2	2,919	5.9	172.8	630	96.9
Total	5,840	11.0	639.7	1,244	96.9
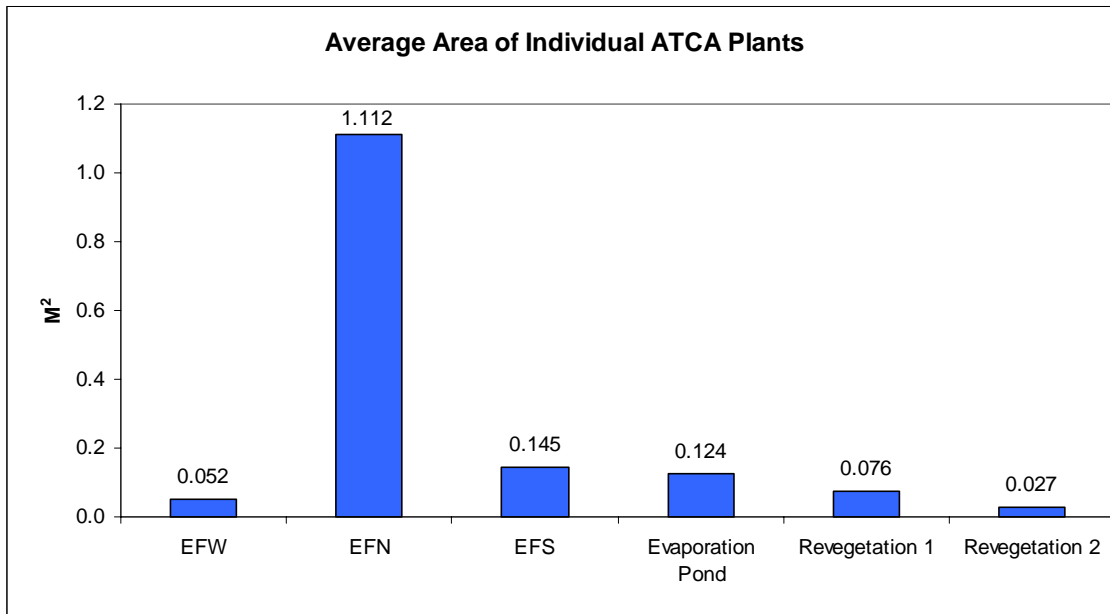
Figure 2–7. Average area of individual Atriplex *planted in 2006.*

Table 2–14 is a summary of canopy volume, dry-weight biomass, and plant tissue nitrogen and sulfur results for plants in the Revegetation Plots. Leaf and stem biomass and nitrogen and sulfur contents of six saltbush plants were measured. Mean nitrogen content of leaves and stems was 1.5 percent, compared to 3.14 percent in 2006. Total nitrogen uptake was 13.3 kg, compared to 4.0 kg at the end of 2006. Mean sulfur content of leaves and stems was 0.24 percent, compared to 0.66 percent in 2006. Total sulfur uptake was 2.2 kg, compared to 0.85 kg at the end of 2006.

Table 2–14. Measured canopy volume, dry-weight biomass, nitrogen and sulfur uptake.

Area	Canopy Volume (m³)	Dry Biomass (kg)	Dry Biomass (kg/ha)	Nitrogen Uptake (kg)	Nitrogen Uptake (kg/ha)	Sulfur Uptake (kg)	Sulfur Uptake (kg/ha)
Revegetation Plot 1	12.1	649.0	2,222	9.7	33.3	1.6	5.3
Revegetation Plot 2	6.3	240.2	823	3.6	12.3	0.6	2.0
Total	18.4	889.2	3,045	13.3	45.6	2.2	7.3

2.2.3 Phreatophyte Transpiration

The plant community growing over the plume could play an important attenuation role by controlling, through ET, the spread of the plume away from the site during the time it takes for natural denitrification to reduce nitrate to safe levels. Unfortunately, the plume area has been heavily grazed, and plant cover is currently low. However, dense plant communities can develop when grazing is controlled (Section 2.2.1).

The purpose of this task was to estimate plant ET for Grazing Exclosure Plots 1 and 2 and in control areas surrounding the plots. We then extended the findings to the whole site and to areas of interest within the site using Quickbird and MODIS satellite imagery calibrated by ground

measurements. Exclosure Plot 1 is dominated by greasewood but contains saltbush plants, whereas Exclosure Plot 2 is mainly saltbush. Sap flow measurements were used to estimate ET for greasewood and saltbush plants growing in Grazing Exclosure Plot 1 in 2006 and in both plots in 2007, and in surrounding control plots both years. A draft manuscript with methods and analyses has been submitted for publication in a journal (Appendix A). The main findings are summarized below.

An analysis of 2006 and 2007 data showed that plant transpiration was significantly higher in 2007 compared to 2006, but that plant type and whether the plants were inside or outside exclosures were not significant factors. Leaf area index (LAI) and ET were high in both years (Table 2–15). The combined 2006 and 2007 data were adequately modeled by a sigmoidal response to maximum daily air temperature (Figure 2–8). This allowed us to project the results over an annual cycle to estimate total ET over different areas of the site for 2007 based on shrub cover (Figure 2–9, Table 2–16). Over the whole site, annual ET was estimated to be 0.203 m, compared to only 0.117 m of rainfall. On the other hand, the area of volunteer plants inside the source area fence had 1.69 m of estimated ET.

Table 2–15. Summary of LAI and sap flow data. Mean values were pooled across species and grazing treatment but separated by year based on the ANOVA results. SE = standard error of the mean. 2006 values were significantly lower than 2007 values for each variable (p < 0.05).

	LAI 2006	LAI 2007	ET Leaf 2006 (mm/m^2/day)	ET Leaf 2007 (mm/m^2/day)	ET Canopy 2006 (mm/m^2/day)	ET Canopy 2007 (mm/m^2/day)
ATCA						
In	2.96	3.78	1.66	2.95	4.91	11.15
Out	3.19	4.47	2.81	4.38	8.96	19.58
SAVE						
In	3.71	3.98	3.06	6.72	11.35	26.75
Out	2.05	4.45	3.07	4.42	6.29	19.67
Mean	**2.96**	**3.85**	**2.66**	**4.74**	**7.97**	**16.79**
SE	**0.22**	**0.27**	**0.27**	**0.69**	**1.16**	**2.59**
n	**31**	**32**	**13**	**17**	**13**	**17**

Transpiration by Sap Flow Measurements at the Monument Valley UMTRA Site

$$T = 5.58/(1+ e^{-(T_a-29.0)/3.50})$$
$$r^2 = 0.76$$
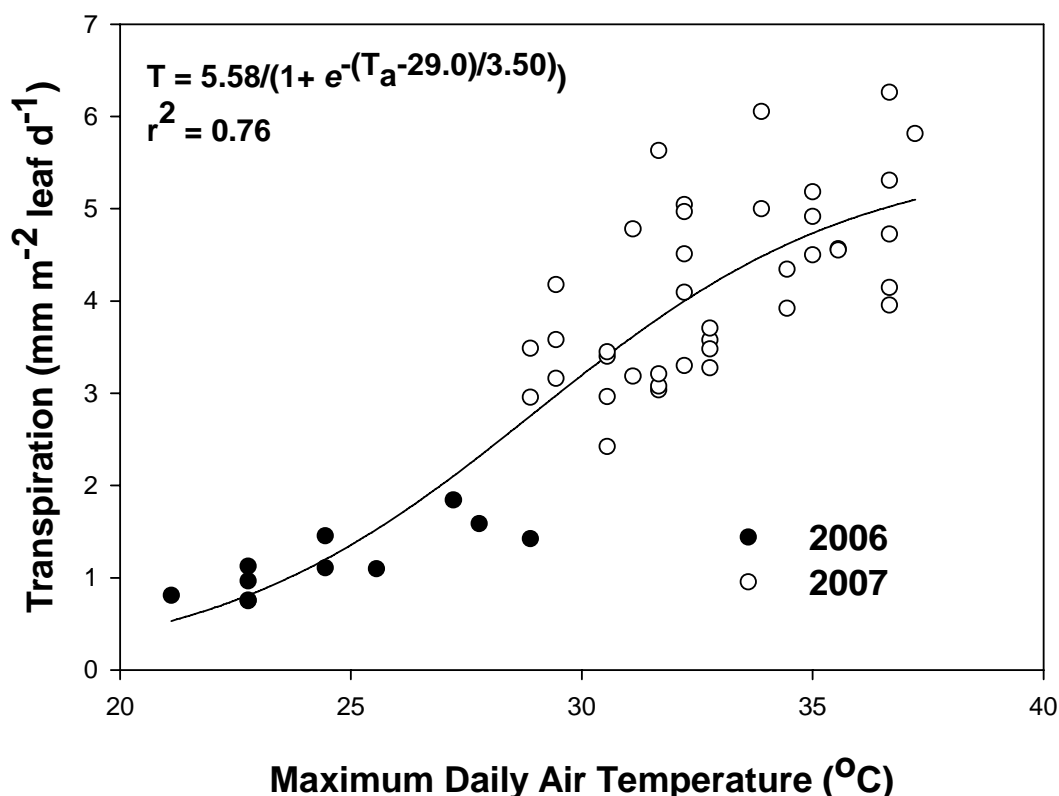
Figure 2–8. Relationship between plant transpiration and maximum daily air temperature at the Monument Valley UMTRA site. Results for greasewood and saltbush were not significantly different and were combined for this analysis.

Table 2–16. Shrub cover and ET at the Monument Valley UMTRA site for 2007. ET was determined by sap flow sensors and projected over the site using fractional cover determined by Quickbird imagery, by ground estimates of LAI, and by the relationship between sap flow and air temperature (Figure 2–8).

Site	Area (ha)	2007 Cover (%)	2007 Biomass (kg ha^{-1})	2007 ET (m yr^{-1})[a]
Volunteer Plants Inside Fence (Site 1)	1.15	77.1	10,717	1.690
SAVE Stand Just Outside Fence (Site 2)	1.57	14.9	2,017	0.334
Entire SAVE Stand Outside Fence (Site 3)	21.45	13.3	1,849	0.290
Sparse ATCA (Site 4)	182.4	9.25	1,286	0.202
SAVE Exclosure (Site 5)	0.26	32.9	4,573	0.724
ATCA Exclosure (Site 6)	0.18	9.30	1,293	0.203
Irrigated Planting	1.64	48.0	6,672	0.555*
Whole Site	**318**	**9.48**	**1,317**	**0.20**

[a]Corrected for lower LAI of irrigated planting (2.14) compared to natural stands (3.85).
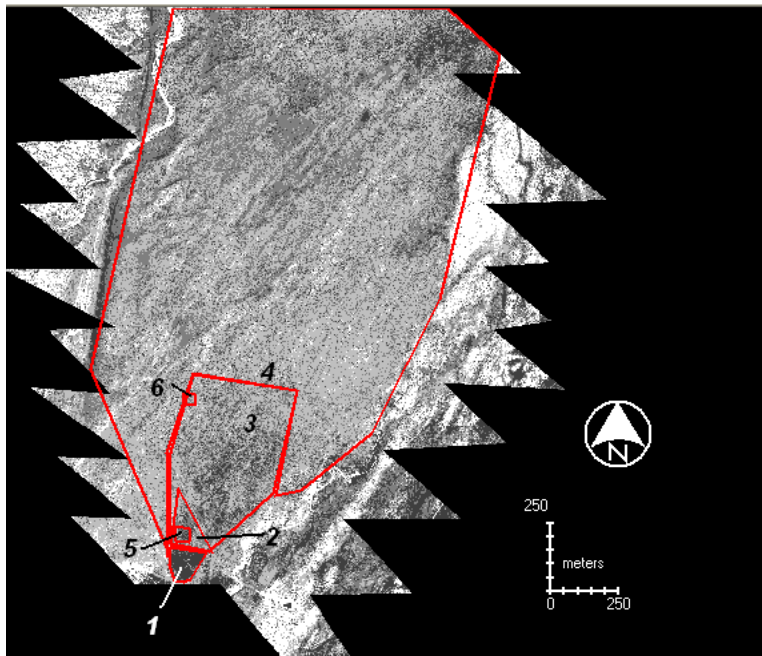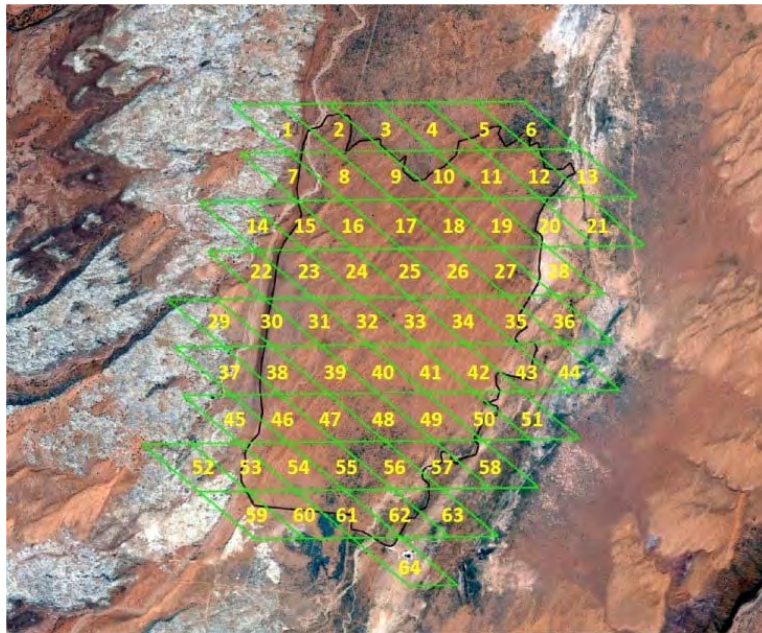
Figure 2–9. Satellite images used in determining ET and fractional cover. Top: Location of MODIS pixels superimposed on a Quickbird image. Bottom: Quickbird image classified to show shrub cover as black pixels. Areas of interest were: (1) the volunteer (unirrigated) ATCA and SAVE stand inside the site fence; (2) a portion of the natural SAVE and ATCA stand just outside the fence (to compare with [1]); (3) the full extent of the natural SAVE and ATCA stand north of the fenced area; (4) the area of sparse ACTA over the whole plume; (5) the SAVE exclusion plot; (6) the ATCA exclusion plot.

These results show that the plant community is already discharging large volumes of water from the plume, and that restricting grazing may greatly enhance hydraulic control of the plume by increasing the transpiration rates of native plants growing over the plume. A conservative estimate is that restricting (but not eliminating) grazing could double the discharge of water from

the plume. Although the exact rate of inflow into the plume is not known, it is likely that doubling the rate of discharge would stop the plume from migrating farther from the site (see Section 2.3).

Projecting the sap flow results over larger areas and longer time spans introduces some error and uncertainty into the estimates. We used our scaling method to estimate plant transpiration in the established source area plantings, where we add a known amount of water in irrigation. We have established that these plants use all the water presented to them in ET, as no discharge of water past the root zone has been detected by water flux meters (WFMs) or neutron probe readings of moisture content (see Section 2.5). Our estimate of 2007 ET, by extrapolation of sap flow results, was 0.555 m for the source area planting. We added an estimated 0.452 m in the irrigation system and an additional 0.117 arrived as precipitation, for a total application of 0.569 m, very close to the estimate by sap flow results.

The sap flow results are only valid for 2006 and 2007, when data were collected. Monitoring the site over time will require a remote-sensing method to assess vegetation status and ET. We previously developed a remote-sensing method based on the MODIS enhanced vegetation index (EVI) and maximum daily air temperature. MODIS EVI data is available in 250-m-resolution imagery in 16-day intervals, with each interval containing a composite of daily, or near-daily, cloud-free images.

The EVI was very sensitive to changes in vegetation at the site despite the low plant cover (Figure 2–10). Note the general upward trend in vegetation density since 2003, consistent with informal observations that grazing pressure was relaxed since 2003. Note also that the protected area has had a sharp increase in vegetation density since 2003.

When the ET method was applied to the Monument Valley site, the results (Figure 2-11) plotted closely to the sap flow results and the extrapolated results based on the equation in Figure 2–8. Therefore, the water balance and vegetation status at this site can be monitored non-intrusively in the future.

Vegetation Trends at the Monument Valley UMTRA Site
2000-2007
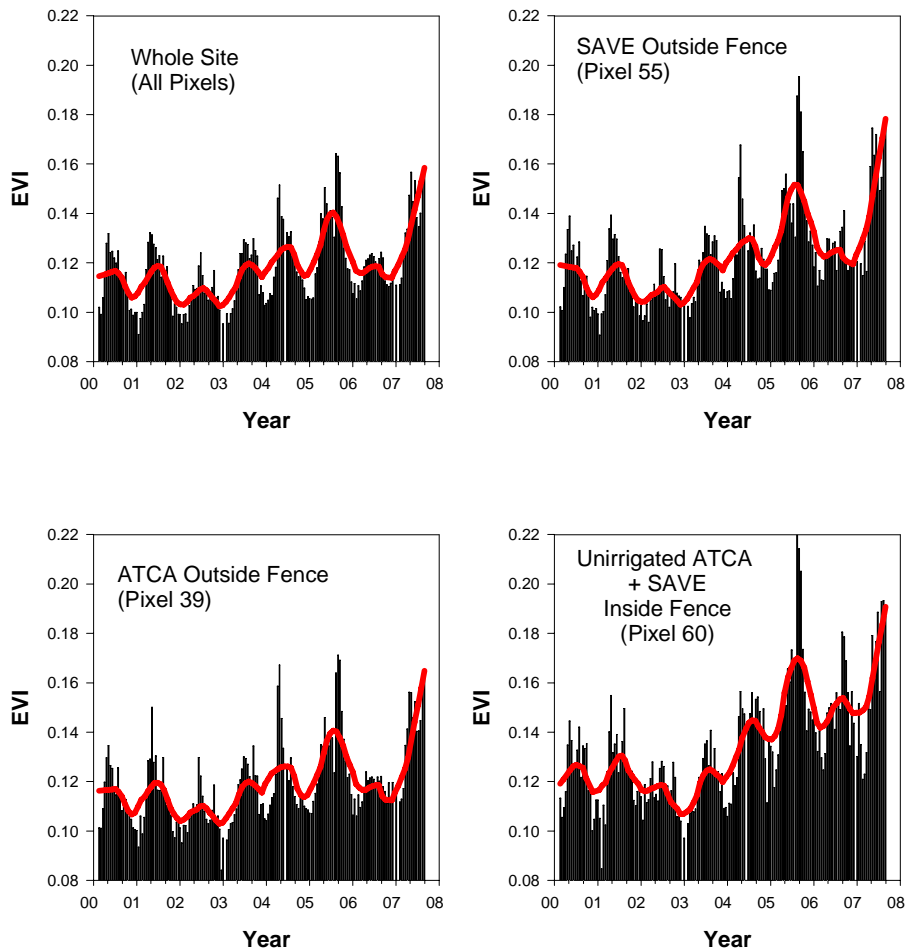
Figure 2–10. EVI values for selected area at the Monument Valley UMTRA site from 2000 to 2007, showing 16-day composite values of EVI and smoothed trend lines over time (red line). See Figure 2–7 for pixel locations.
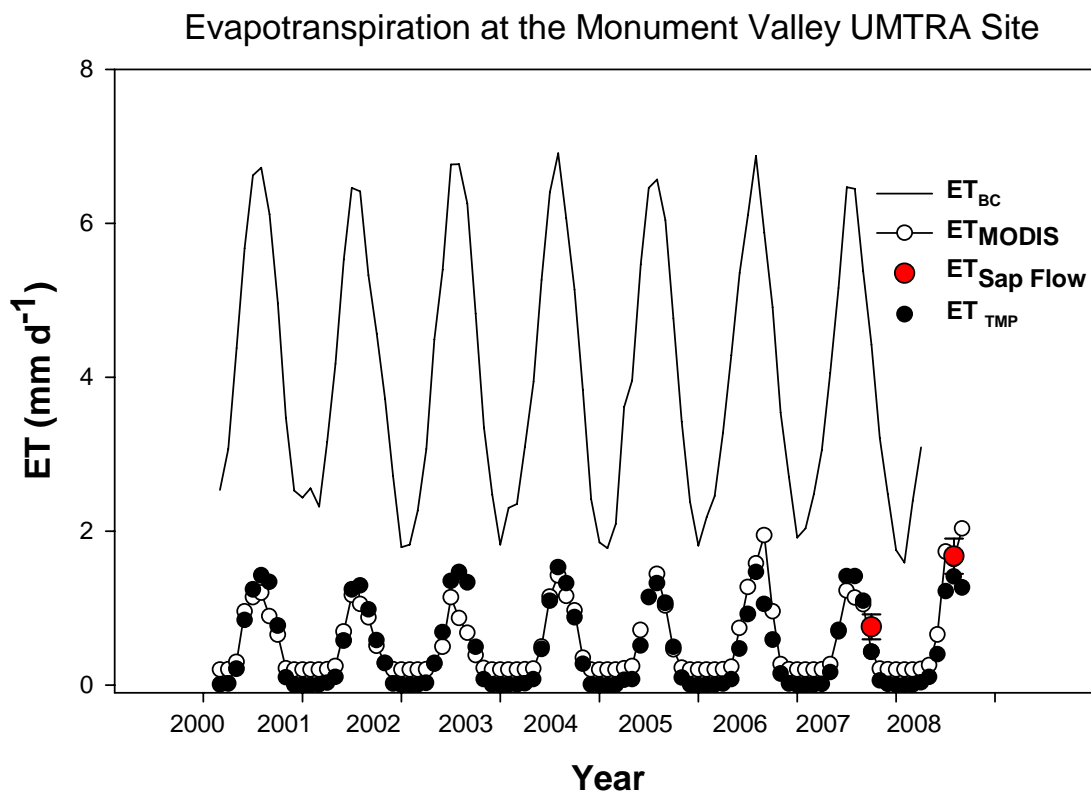
Figure 2–11. ET over the whole Monument Valley UMTRA site (2000–2007). The solid line shows potential ET determined by the Blaney-Criddle method, the open circles show ET projected from the MODIS EVI and maximum daily temperature, the red circles show the sap flow results in 2006 and 2007, and the closed circles show ET projected from sap flow results and the temperature response modeled in Figure 2–6.

2.3 Natural and Enhanced Attenuation Analysis

Groundwater in the alluvial aquifer at the Monument Valley site is contaminated by ammonium and nitrate. There is evidence that natural attenuation is occurring at the site, but the feasibility of using natural attenuation as a remediation strategy remains uncertain. The purpose of this investigation was to characterize the occurrence and rate of natural attenuation at the site. Because the contamination occurred over a relatively brief period (1964–1968) and entered the aquifer from a well-defined source area (the tailings subpile soil), the dispersion and decay of nitrate and ammonium in the plume lends itself to solute transport modeling. These models can serve as a check on conclusions based on stable isotope and denitrification studies in earlier status reports (DOE 2006, DOE 2007), and they provide estimates of the time required for attenuation of the plume under different treatment options.

We were able to use multiple independent methods to develop rate coefficients for nitrate attenuation, providing a robust model of natural attenuation of nitrate in the plume. In addition, this task modeled enhanced attenuation that could be achieved by injecting ethanol or methanol into the plume as a carbon source to stimulate natural rates of denitrification. The results of this task are summarized below; Appendix B contains the complete report.

Natural attenuation is the combined effect of several naturally occurring processes, such as biodegradation, sorption, and dispersion that decrease the concentrations of chemicals in the aquifer over time. Sorption was determined for nitrate in column studies at UA, and for nitrate in the plume by mobility relative to chloride. Spatial and temporal nitrate concentration data was collected from a transect of monitoring wells located along the plume centerline and was used to model dispersion and sorption processes, while ^{15}N and denitrification assays were used to model biodegradation, the conversion of nitrate to ammonium to N_2 and N_2O gasses. From these data, we developed a model (the MT3DMS Model) of first-order rate coefficients for natural attenuation and denitrification. The model was then compared to measurements of nitrate, ammonium, and oxygen in the observations wells from 1985 to 2007, producing calibrated estimates of rates of natural attenuation and of enhanced attenuation. We then projected the time required to reduce nitrate levels to 10 milligrams per liter (mg/L) (as N) based on the calibrated model.

2.3.1 Laboratory Microcosm Experiment

The results of microcosm experiments are presented in Figure 2–12, showing nitrate decay kinetics. Natural denitrification (without amendment) was relatively slow compared to the decay observed with both ethanol and methanol amendments. These data, as well as the enrichment factor derived for a previous ethanol study, are presented in Table 2–17.
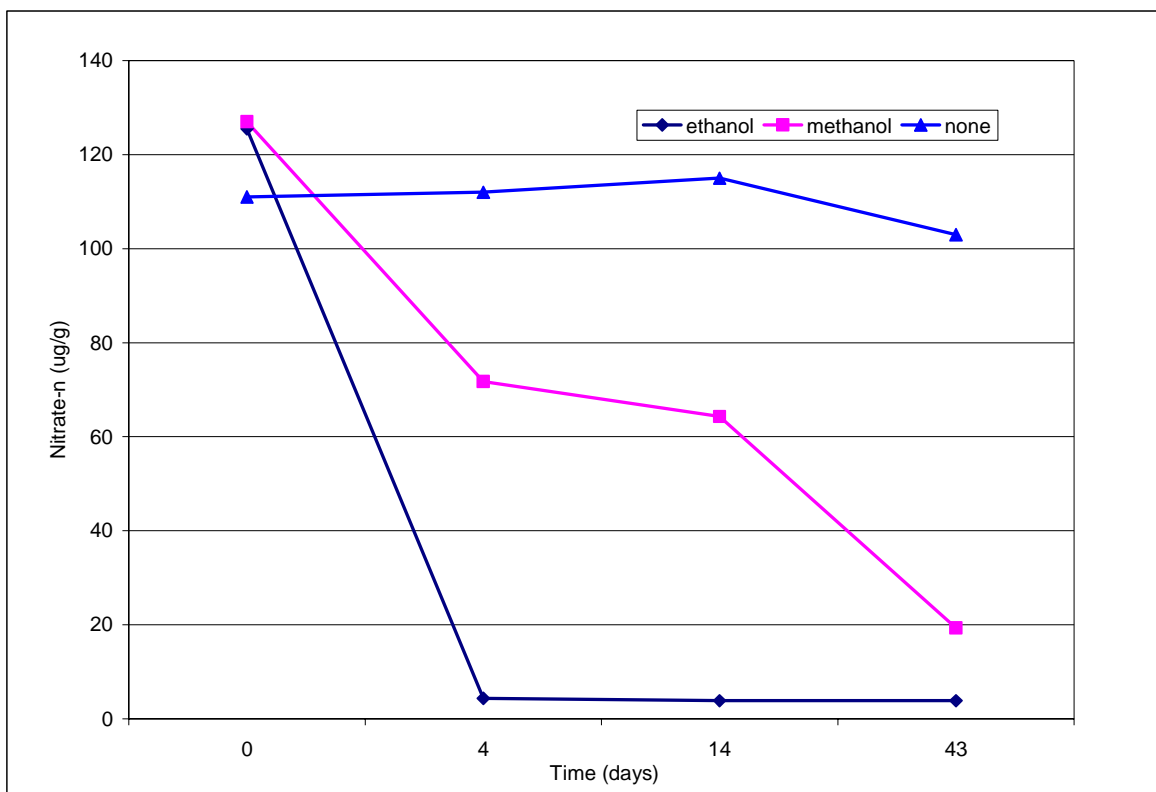
Figure 2–12. Microcosm nitrate depletion in soil slurries with or without methanol or ethanol amendment.

Table 2–17. Natural, ethanol-, and methanol-enhanced denitrification first-order rate coefficients obtained from laboratory microcosm concentration data.

First-order rate description	k (hr^{-1})	k (yr^{-1})	Half-life (yr)
2006-natural	2.00E-05	0.2	3.96
2007-natural	8.33E-05	0.7	0.95
2006-with ethanol	3.30E-03	28.9	0.02
2007-with ethanol	2.00E-03	17.5	0.04
2007-with methanol	1.95E-03	17.1	0.04

The natural denitrification rates (expressed as half-lives of nitrate), 3.5 and 1.0 years, and the ethanol-enhanced rate coefficients varied from 0.04 to 0.02 years, which represent an increase of approximately two orders of magnitude. Table 2–18 gives the rate coefficients and half-lives for the laboratory microcosm based on ^{15}N enrichment relative to ^{14}N. The denitrification rates estimated from isotopic fractionation were 2.0 and 0.03 years for natural attenuation and ethanol-enhanced decay, respectively, very similar to the results obtained by N_2O assays.

Table 2–18. Natural, ethanol-, and methanol-enhanced denitrification first-order rate coefficients obtained from laboratory microcosm ^{15}N isotopic-enrichment data.

Substrate Description	E	Δs(t)[a]	δs(o)[b]	α	1- α	time (yr)	k (yr^{-1})	Half Life (yr)
natural	-0.91	0.3	-7	0.999	0.001	21.5	0.3407	2.03
methanol	-18.1	0.3	-7	0.982	0.018	0.12[#]	3.4541	0.20
ethanol	-9.45[c]	0.3	-7	0.991	0.009	0.03[#]	29.705	0.02

[a]δs(t) = average plume δ 15N
[b]δs(o) = most enriched plume δ 15N
[c]enrichment value previously reported for ethanol (Jordan et al. 2007).

2.3.2 Temporal and Spatial Analysis of Field Data

Figure 2–13 shows the dissolved oxygen transient concentrations, Figure 2–14 shows the NH_4 data, and Figure 2–15 presents the NO_3 concentration data as a function of time. The oxygen content in the aquifer decreased from 1992 to 1994 to the range required to initiate denitrification; hence, this is the likely start time for loss of nitrate from the plume. NH_4 concentrations showed a decreasing trend over time. The groundwater near the source area had a decreasing trend for NO_3 concentrations, but groundwater at distances down-gradient from the source area had an increasing trend for NO_3 concentrations (wells 653 and 650). The increasing concentration trends at the edge of the plume suggest that the plume is moving or expanding.
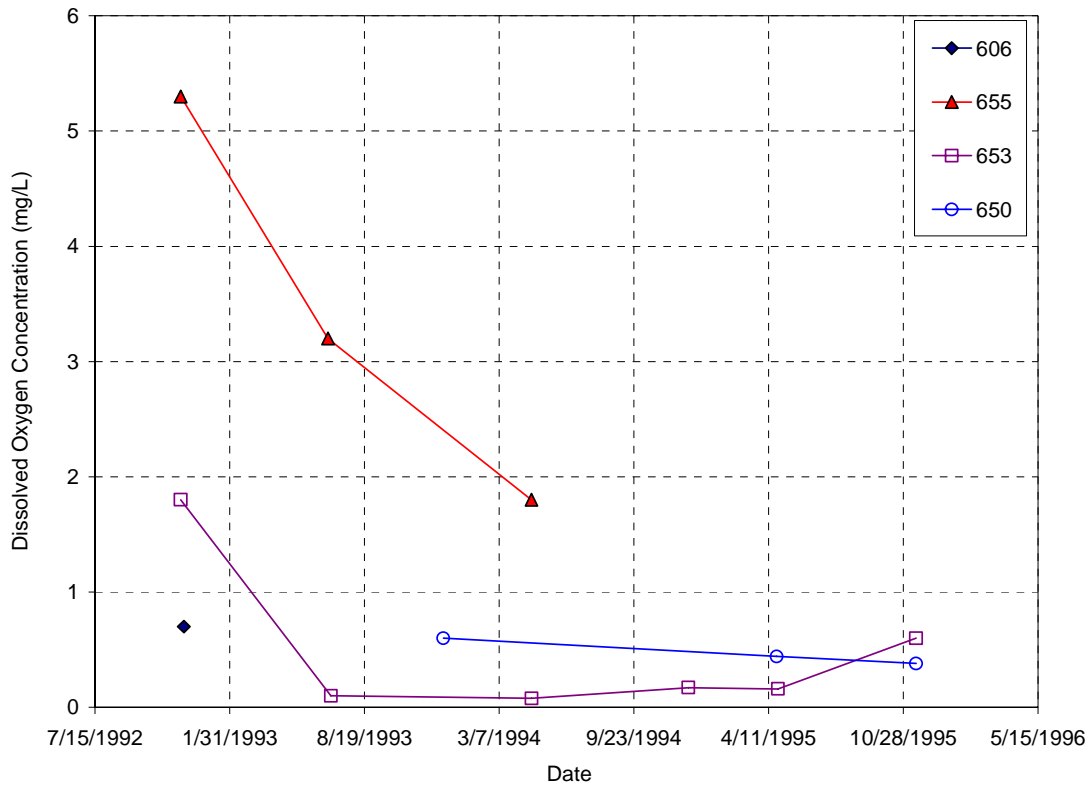
Figure 2−13. Dissolved oxygen concentration as a function of time.
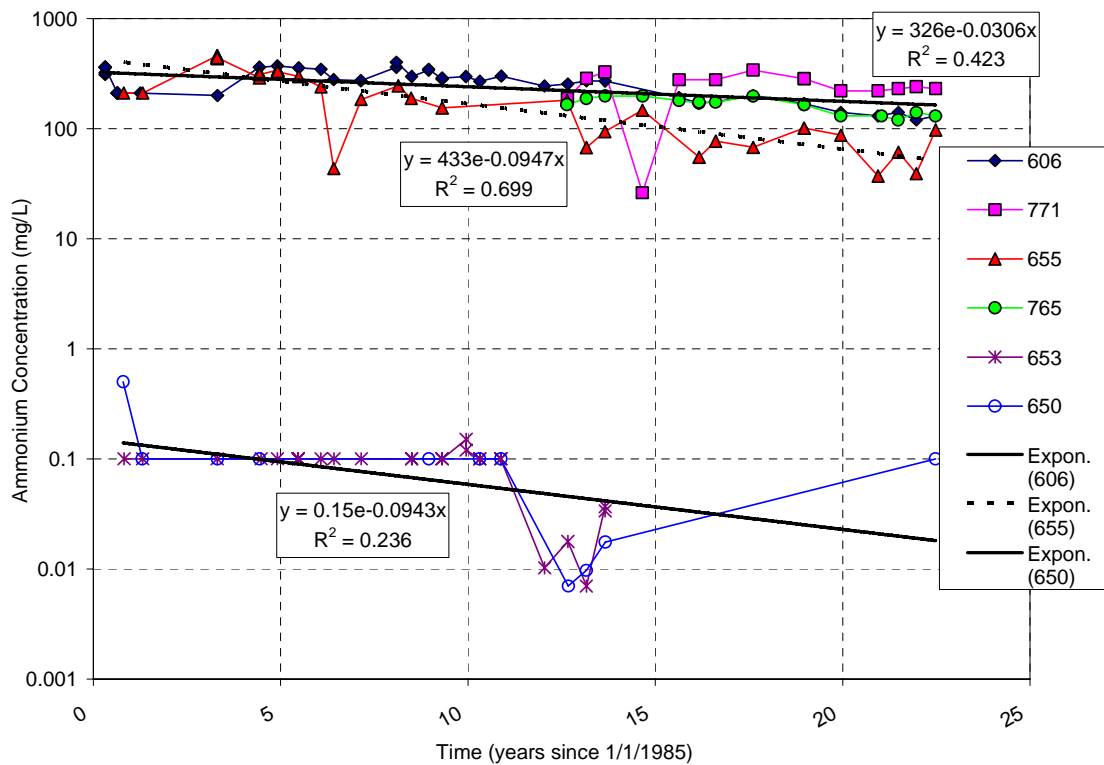
Figure 2−14. Ammonium concentration as a function of time.
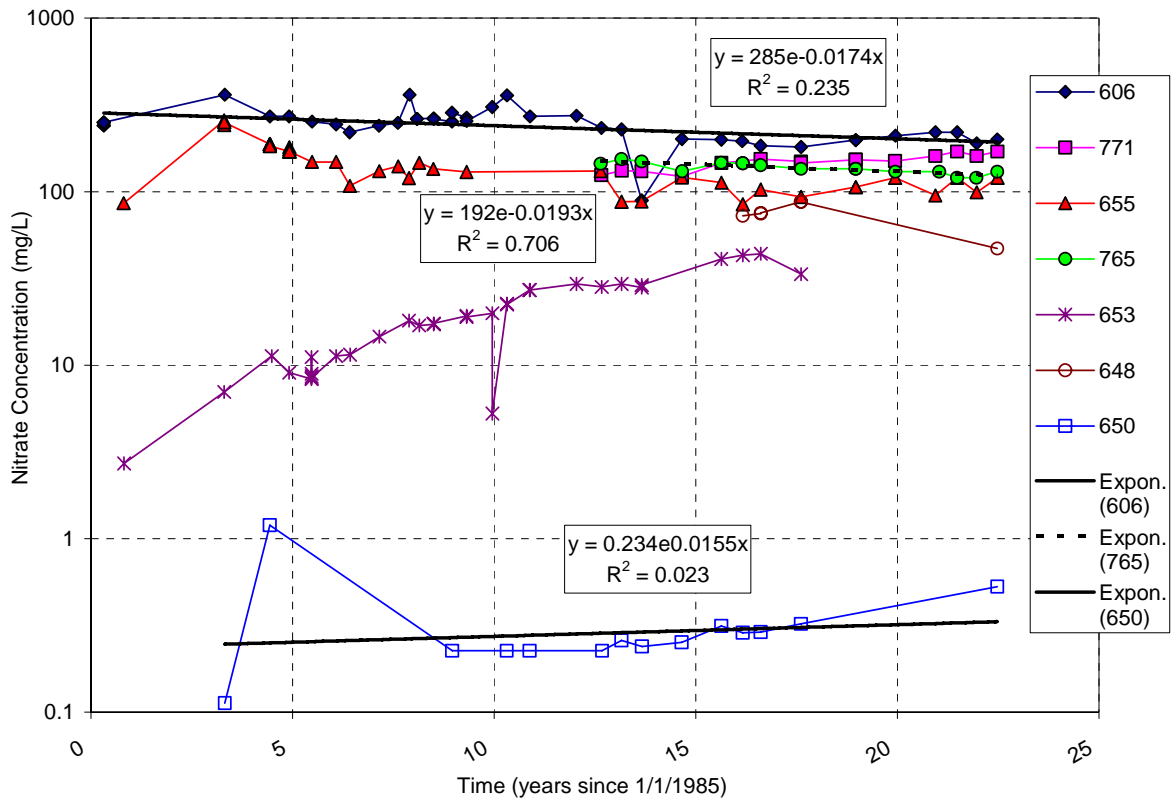
Figure 2–15. Nitrate concentration as a function of time.

2.3.3 Spatial Data

The spatial behavior of the groundwater contamination plume was evaluated by plotting the transect NO_3 concentrations versus distance from the source area, which is approximately the center-line of the major axis of the plume. Both NH_4 (Figure 2–16) and NO_3 (Figure 2–17) decrease with distance from the source, but the NO_3 extends further from the source. This is expected because nitrate is more mobile in soils and aquifers than ammonium. The composite rate coefficient for the whole plume was estimated for NO_3 from the regression exponent multiplied by the nitrate transport velocity. The nitrate decay rate expressed as half-life was 1.9 years for the 1993 data and 2.0 years for 2007 data, similar to coefficients determined in denitrification and ^{15}N assays. The composite rate includes dispersal as well as denitrification, but nearly all of the nitrate attenuation was due to denitrification in this model.

2.3.4 Model Predictions of Natural and Enhanced Attenuation

The calibrated MT3DMS nitrate transport model was then used for predicting natural attenuation. Figure 2–18 presents the results of the prediction for natural and ethanol-enhanced attenuation conditions. This simulation was extended through time until the concentrations in the entire model domain reached the 10 mg/L standard, which occurred in approximately 160 years for the natural attenuation case, whereas the enhanced denitrification prediction shows nitrate concentrations lowered to the regulatory standard throughout the model domain approximately 50 years after the start time of the prediction, which is 110 years earlier than the natural attenuation prediction.
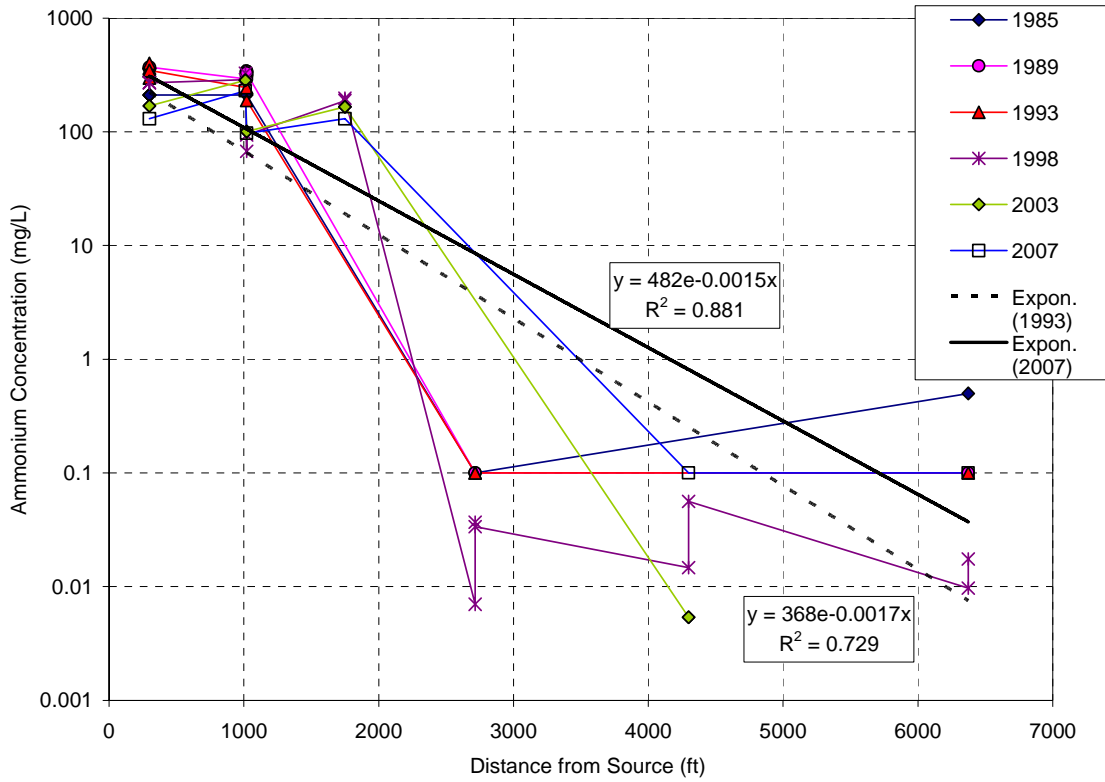
Figure 2–16. Ammonium concentration as a function of distance along transect A-A'.
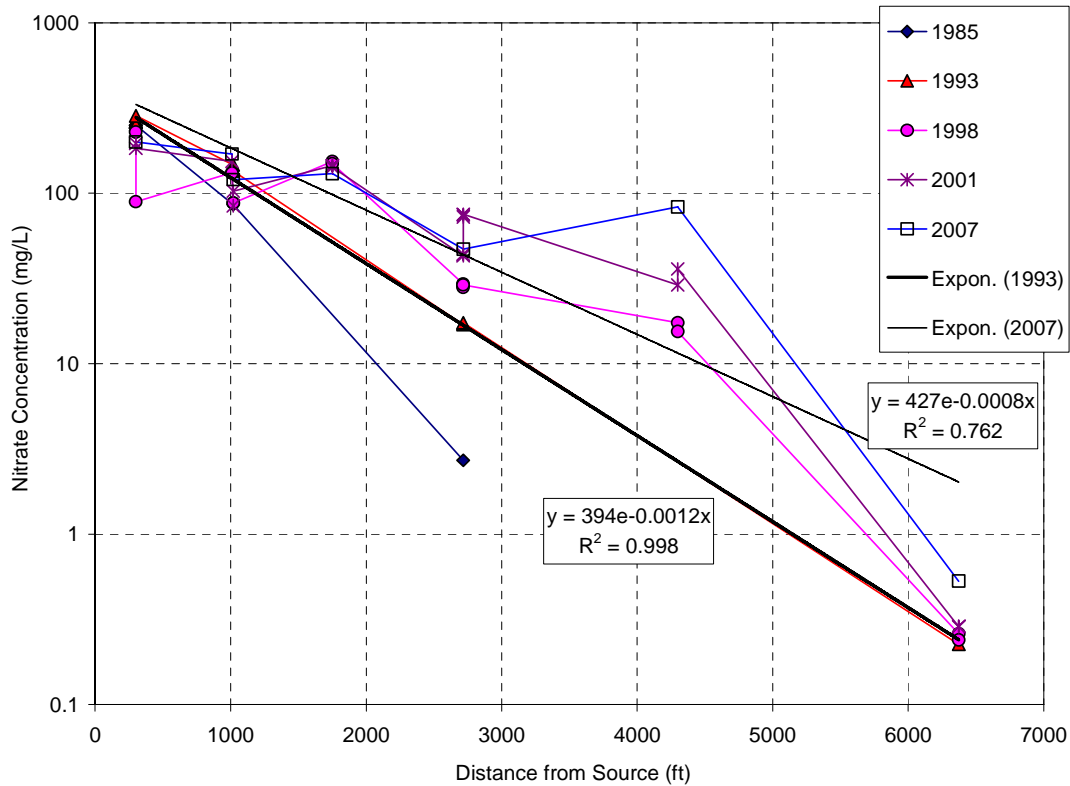
Figure 2–17. Nitrate concentration as a function of distance along transect A-A'.
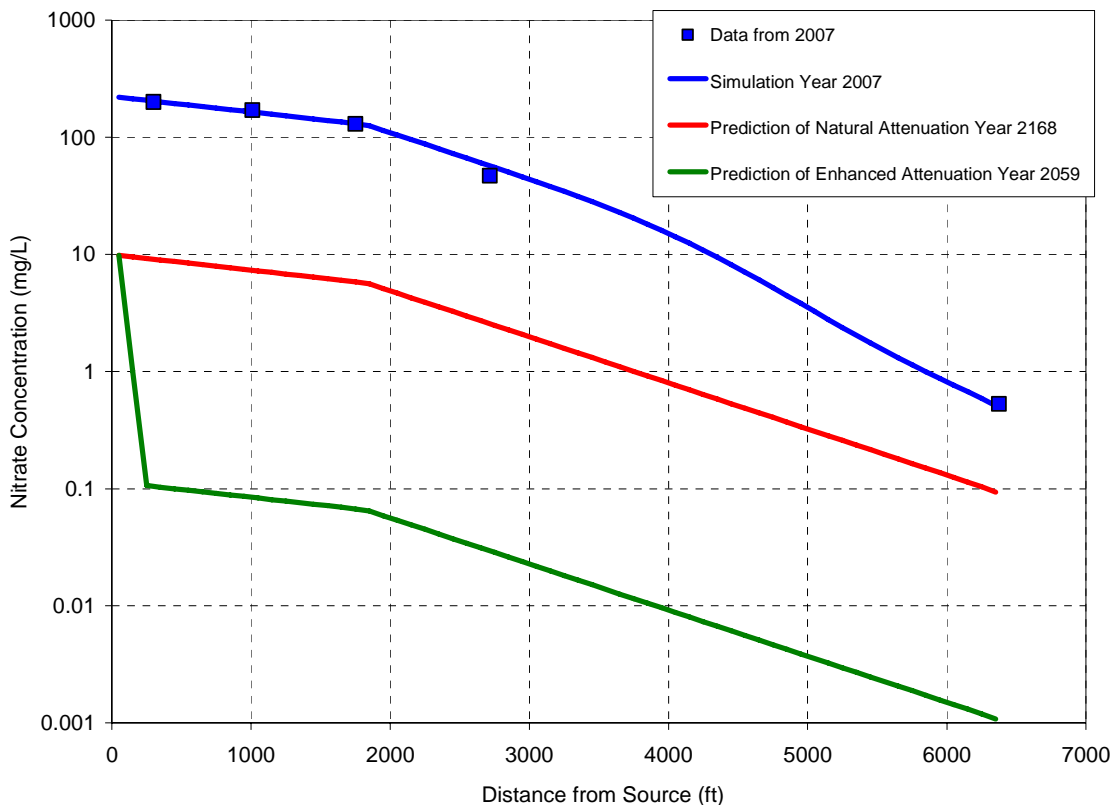
Figure 2–18. MT3DMS transport model transient calibration to nitrate concentrations versus distance along transect A-A'.

2.3.5 Conclusions

Natural attenuation of nitrate has been observed at the site by the decreases in concentrations over space and time. The feasibility of using natural attenuation for a remediation strategy for groundwater requires that attenuation occurs at a rate that will achieve cleanup within a reasonable timeframe. The rates of composite attenuation were estimated from groundwater concentration data, which combine the effects of dispersion, diffusion, sorption, and denitrification. Dispersion and sorption were estimated from laboratory experiments, but had minor effects on NO_3 transport. The rate of microbial biodegradation through denitrification, which was the dominant attenuation process, was also quantified through a variety of methods, including microcosm decay and isotopic fractionation, field-scale isotopic fractionation, and numerical modeling.

2.3.6 Recommendations

The results suggest that nitrate in the Monument Valley alluvial aquifer is naturally attenuating. However, the rate of natural attenuation is such that it may take more than 100 years to complete cleanup. The model predictions of enhanced denitrification with the addition of ethanol as a substrate showed a substantial increase in the rate of nitrate attenuation. This work suggests that the use of enhanced denitrification may significantly reduce the time required for the attenuation of the NO_3 plume.

2.4 Active Groundwater Remediation: Land Farming

Land farming was selected as the most feasible and efficient *active* remedy for the nitrate and sulfate plumes. Land farming will be considered only if the more passive alternatives are found to be inadequate. The farm would serve several functions: (1) extract nitrates in irrigation water pumped from the plume; (2) convert nitrates into useful plant biomass; (3) reduce sulfate levels in the alluvial aquifer; (4) minimize water infiltration and the leaching of contaminants back into the aquifer; and (5) enhance the restoration of the disturbed ecosystem. Land farming consists of pumping the contaminated alluvial aquifer to irrigate and fertilize a farming operation on areas disturbed during the surface remediation. The land farm would produce a crop such as native plant seed for mine-land reclamation. Pumping would continue until nitrate concentrations in the alluvial aquifer drop below the 44 mg/L maximum concentration limit for nitrate.

2.4.1 Experimental Design and Operation

The treatment structure for the land-farm pilot study consisted of two main factors: (1) nitrate concentration in irrigation water supply and (2) crop species. There were four nitrate levels; no nitrate, 250 mg/L nitrate (a level not likely toxic to crop plants or to livestock feeding on the crop), 500 mg/L nitrate (a level not likely toxic to crops but possibly toxic to livestock), and 750 mg/L nitrate (a level possibly toxic to crops and livestock). The two crops in the cropping system are *Atriplex canescens* and *Sarcobatus vermiculatus*.

Water was delivered to the land farm via two wells: a clean water well pumped from the DeChelley aquifer and a well contaminated with nitrate (approximately 750 mg/L nitrate), well 649. Plants in the control (or "no nitrate") plots received 2 gallons of clean water per day. Plants in the 250 ppm nitrate plots were irrigated for 60 minutes with water from well 649 and for 180 minutes with water from the DeChelley aquifer to total 2 gallons per day. Plants in the 500 mg/L nitrate plots were irrigated for 180 minutes with contaminated water and for 60 minutes with clean water. Plants in the 750 ppm plots received 2 gallons of contaminated water per day from well 649.

In May 2007, a new solenoid was put in to adjust the irrigation timing from 2 to 4 hr per day per plant, however, this inadvertently resulted in shutting off the water entirely to the 0 ppm nitrate treatment for 2 months, and many of the plants within this treatment died. The problem was solved in July, and new seedlings were transplanted to replace those that had died. However, at this time, we found that the solar batteries that ran the pump for well 649 were not adequate, especially during the rainy season, to compensate for the increase in irrigation; hence, we had to eliminate two treatments (250 ppm and 500 ppm) from the treatment structure. Furthermore, the well was still drawing down, and the 750 ppm treatment was set to deliver only 2 hr of water per plant per day. The higher nitrate treatment plots received less irrigation water than the others. This was reflected in the soil moisture measurements (Figure 2–19); the overall soil profile is significantly ($p < 0.05$) drier for the 750 mg/L nitrate plot compared to the 0 and 250 ppm treatments.

One solution to poor production from well 649 is to find another high-nitrate well that is more productive than well 649. We also need to install more solar storage capacity on the pump house to make up for days when there is minimal sunlight. Another solution is to install an

aboveground storage tank adjacent to well 649, with sufficient capacity to supply high-nitrate irrigation requirement of 400 gallons per day to the land farm.
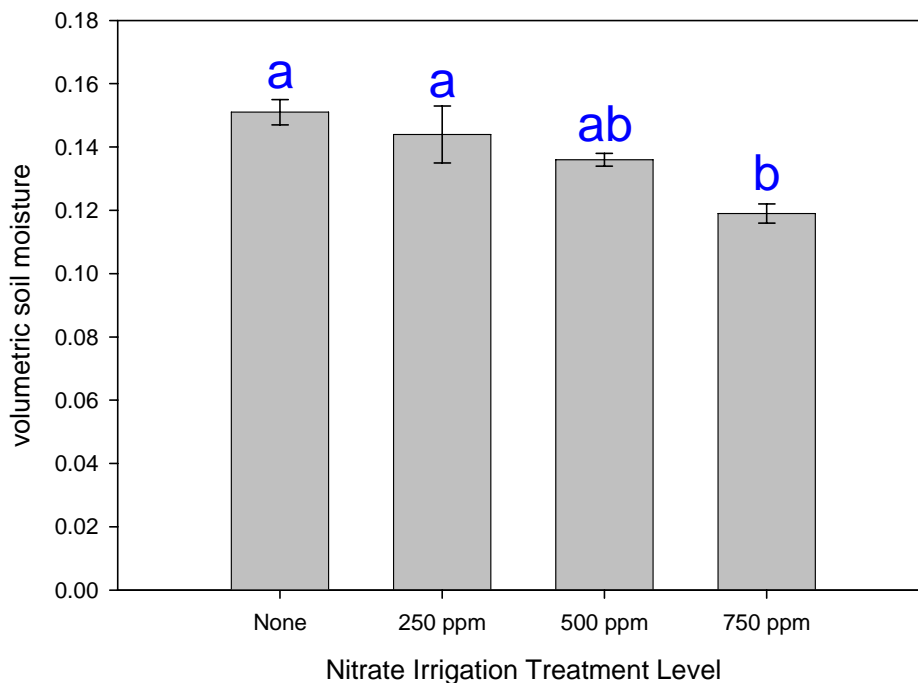
Figure 2–19. Average soil moisture across depth for each nitrate treatment level in the land-farm field. Soil moisture measurements were taken at 0.3 m intervals monthly in 16 ports randomly distributed throughout the land farm.

2.4.2 Crop Growth and Productivity

In October 2007, growth and productivity for the different combinations of crops and nitrate irrigation levels in the land farm were compared. A randomly distributed subset of plants (3 to 5 plants per plot) were measured in the land farm. Shrub canopy area was estimated from cross-sectional diameters using the formula for an ellipsoid. Plant volume was estimated using the formula for a hemispheroid, and these data were converted into aboveground biomass using a previous relationship found for the *Atriplex* shrubs.

Nitrogen uptake was slightly greater for plants harvested from the 750 mg/L nitrate plots compared to those receiving clean water (Figure 2–20). However, estimates of total biomass (Figure 2–21) were not significantly different between treatments, but on average, plants were larger for the 750 ppm treatment.
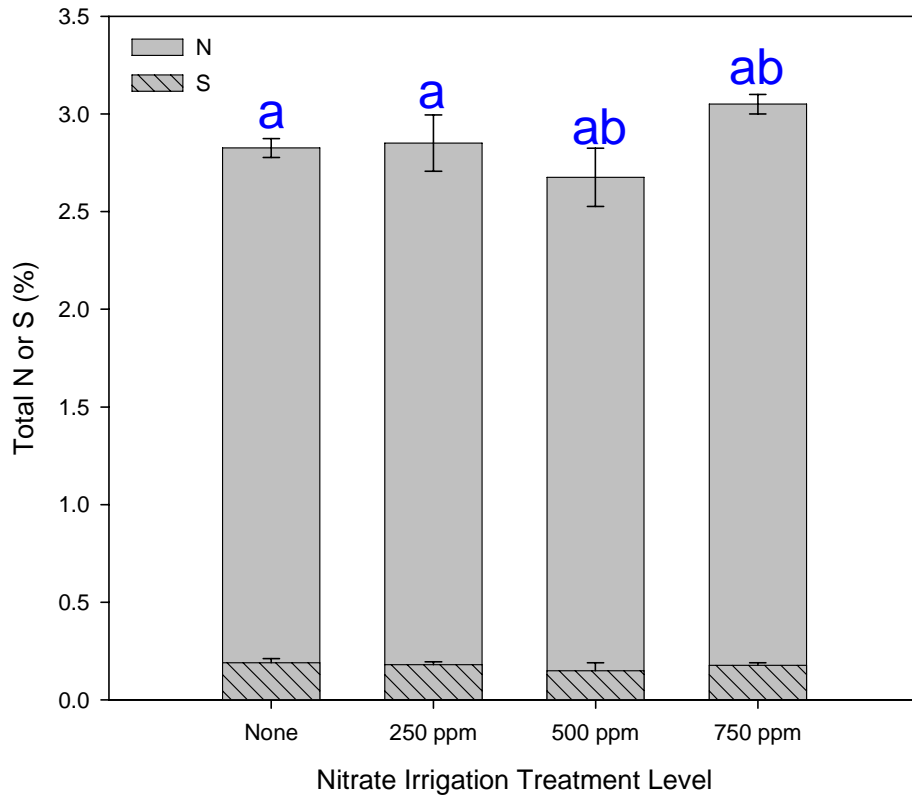
Figure 2–20. Average Total % N and S (a) for Atriplex shrubs harvested from the land-farm study. Error bars represent the standard error of the mean. Unlike letters indicate significant differences at alpha = 0.05.
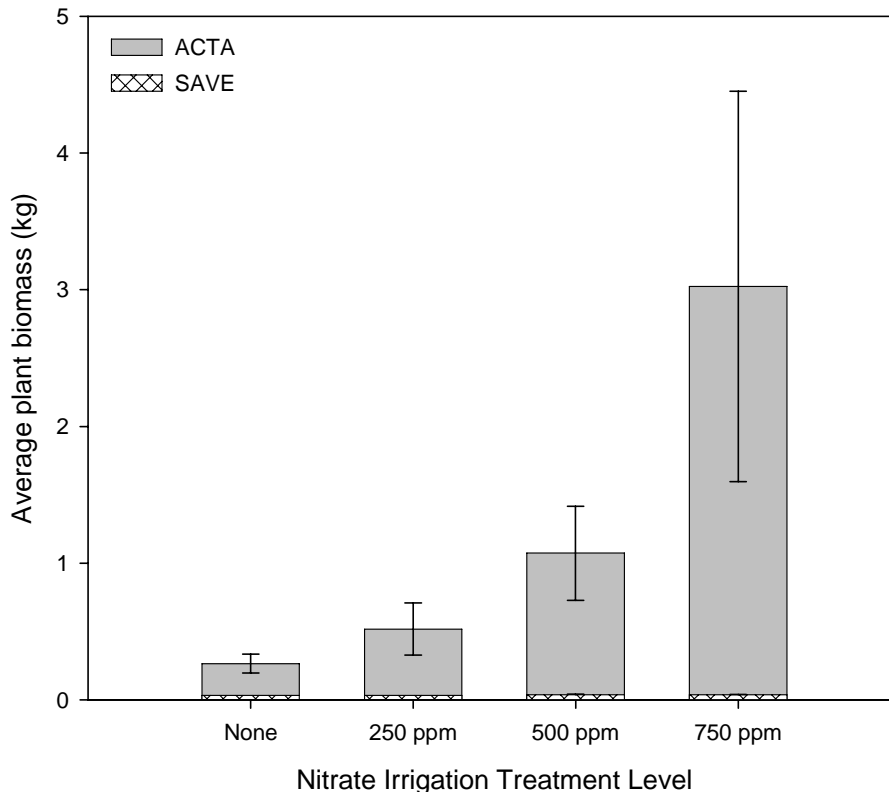
Figure 2–21. Average biomass for Atriplex (ACTA) and Sarcobatus (SAVE) extrapolated from volume:biomass relationship. Error bars represent the standard error of the mean. Unlike letters indicate significant differences at alpha = 0.05.

2.5   Soil Water and Recharge Monitoring

The original subpile (source area) phytoremediation plot has been irrigated each year since 2000, with the exception of 2003. The plants are purposely under-irrigated to prevent leaching of nitrate from the soil into the aquifer. Irrigation volumes have ranged from 0.16 m/yr to 0.36 m/yr during years, with water provided daily through drip emitters from March to October. In 2007, irrigation volumes were increased to encourage further denitrification in the subpile soil. Irrigation volumes were doubled in the new and established subpile soil plants, to receive 7.6 liters per day per plant (an annual application rate of 0.45 m of water. This same rate was provided to new plants in the land-farm experiment, in which plants were watered with high-nitrate well water (see Section 2.4).

2.5.1   Soil Water Content

Volumetric soil moisture was monitored with a neutron thermalization hydroprobe for all ports located within the source area (Figure 2–22) and for the irrigated land farm (Figure 2–23). The established plantings had soil moisture levels in the range of 0.10–0.13 cm^3 cm^{-3}, and they did not tend to increase with soil depth (Figure 2–22, top panel) or over months, except for a slight increase during the rainy season (Figure 2–22, bottom panel). This shows that the increased irrigation rate is suitable for the established plants. On the other hand, the moisture content was

higher in the new planting areas, with an accumulation of soil moisture up to 0.17 cm^3 cm^{-3} in the 2–3 m soil depth. The new plantings also had an accumulation of water at the 4–-5 m depth, but this was preexisting water, which was present before irrigation began. The highest levels of soil moisture were found at the 4–5 m depth in the unirrigated but vegetated control plot. The new plantings grew rapidly over the summer and there was only a slight increase in mean soil moisture over the irrigation season. Hence, by 2008 the new plantings should be able to utilize all the irrigation water provided and to lower soil moisture levels to those in the established planting areas.

In the land farm, soil moisture monitoring is needed to detect seasonal wetting fronts and to manage irrigation rates. Hydroprobe ports installed in 1999 were used to monitor volumetric moisture content for each experimental treatment. Readings were taken at 0.3 m depth increments to the bottom of the ports (about 5 m). Soil moisture monitoring began prior to irrigation in March 2007 and continued through September 2007. Soil moisture levels in the land-farm plots tended to be high in the 2–3 m depth (Figure 2–23 Top Panel) and to increase slightly over the growing season (Figure 2–23 Bottom Panel). Soil moisture was lowest in the 750 ppm nitrate treatment, which also had the greatest plant growth (see Section 2.4). These plantings contained a mix of greasewood and saltbush, and many of the greasewood plants grew slowly and had to be replaced; therefore, plant growth has not kept up with water application rates in the land farm. However, plants in all plots are now well established, and the plants should be able to keep up with water applications in 2008.

Average volumetric soil moisture readings in 2007 for all irrigation zones and for control (unirrigated) areas are summarized in Figure 2–24.

Hydroprobe port locations and depths are shown for control ports (Figure 2–25), subpile soil ports (Figure 2–26), Extended Field and evaporation pond ports (Figure 2–27), and land farm ports (Figure 2–28).
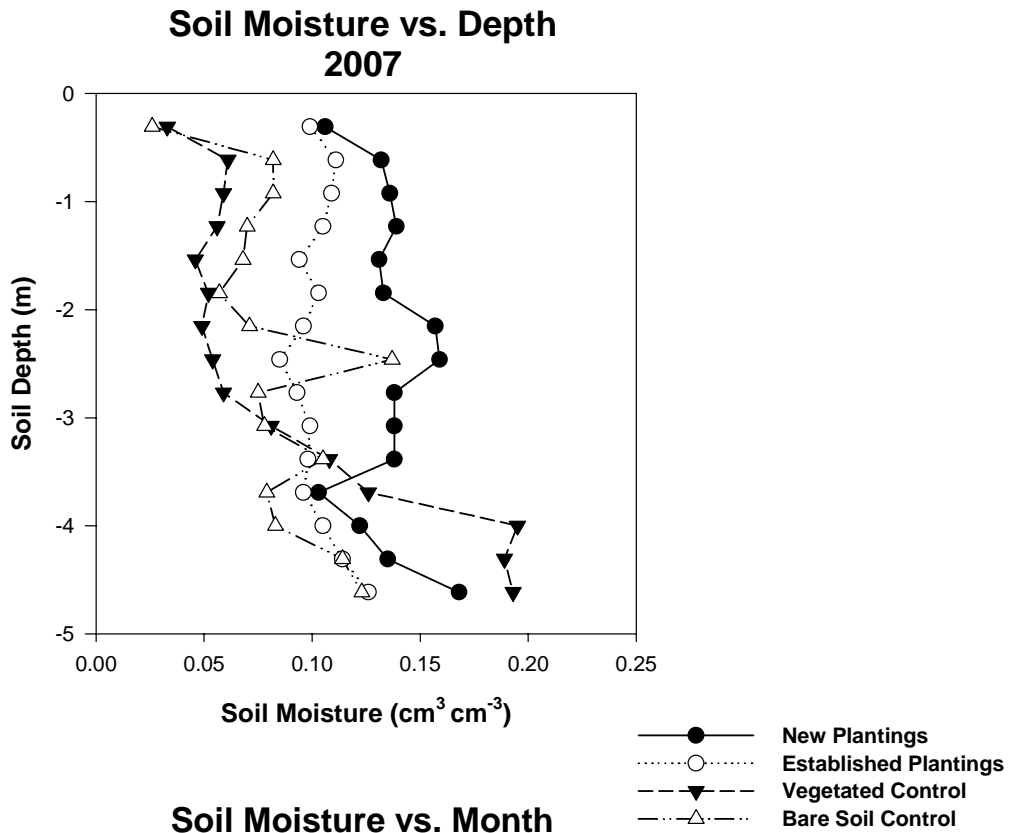
Figure 2–22. Soil moisture levels in subpile soil plantings and in vegetated and unvegetated control plots.
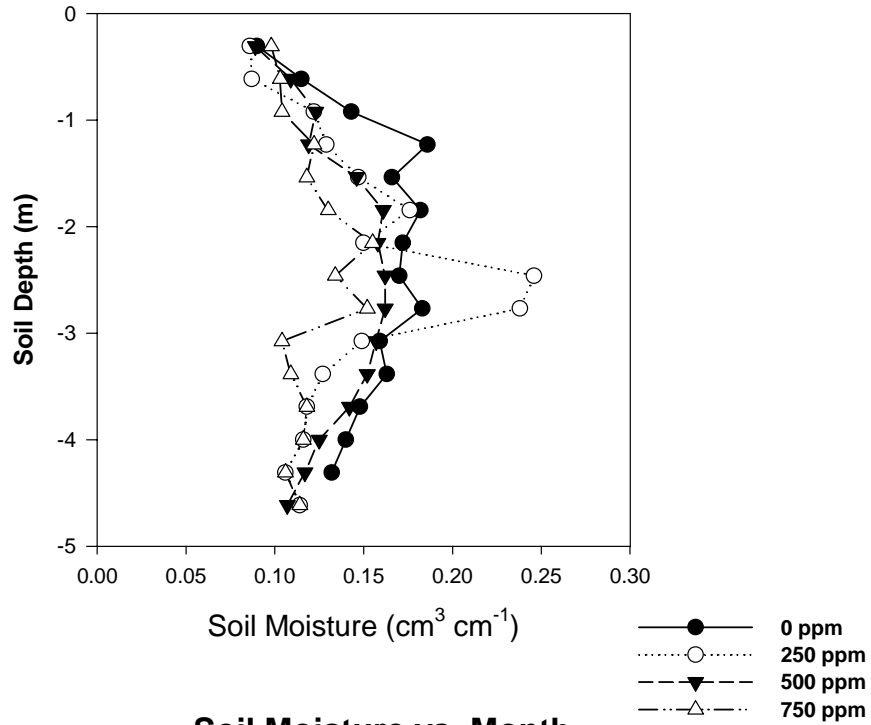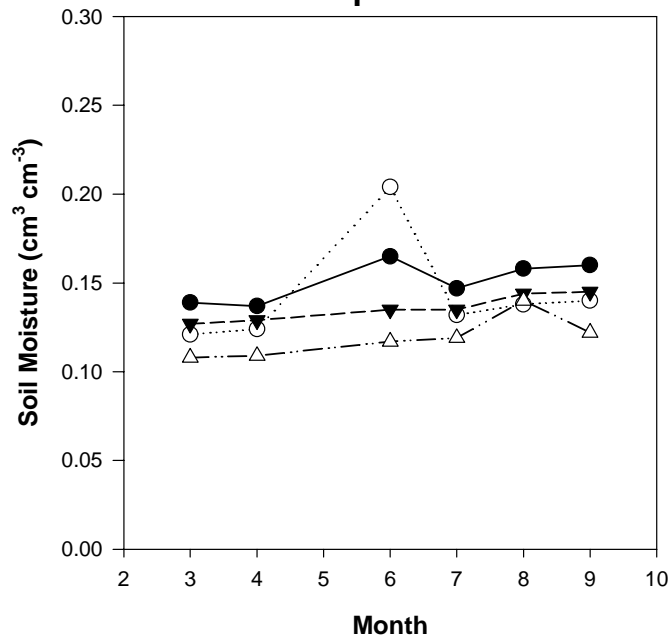
Figure 2–23. Soil moisture levels in the land-farm plots. Treatments indicated the level of nitrate in the irrigation water.
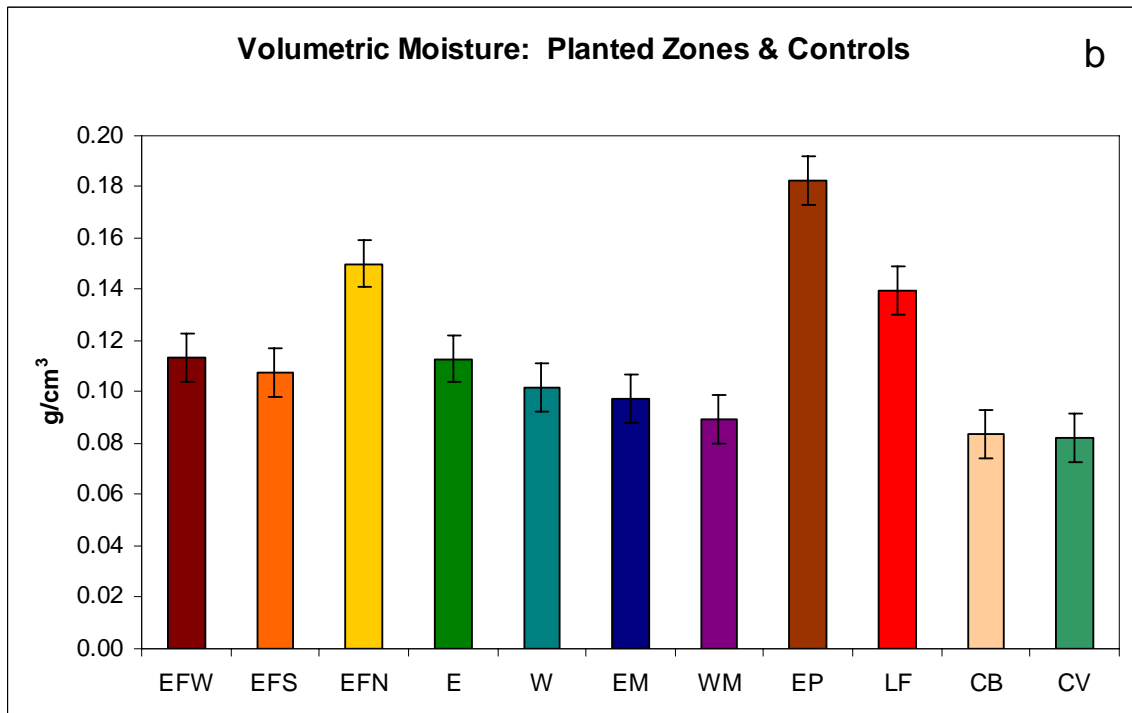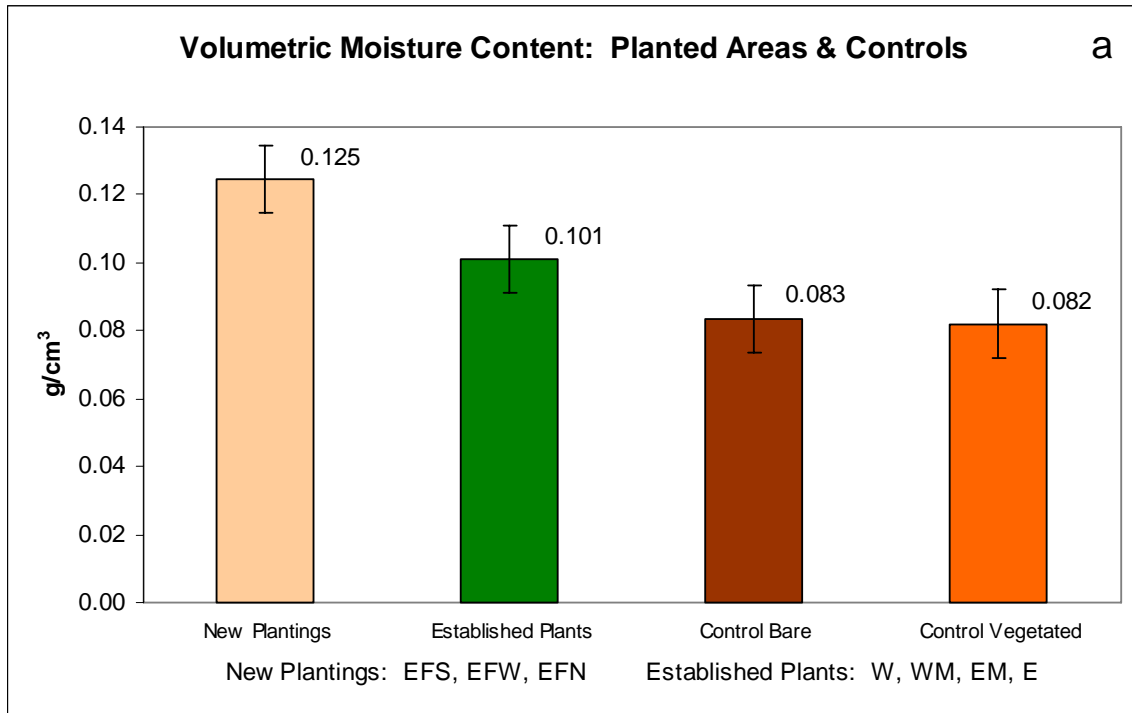
Figure 2–24. Volumetric soil moisture content averaged across depth and time for all zones within the established and new planting areas and controls (a) and for individual zones (b). Error bars represent standard error of the mean.
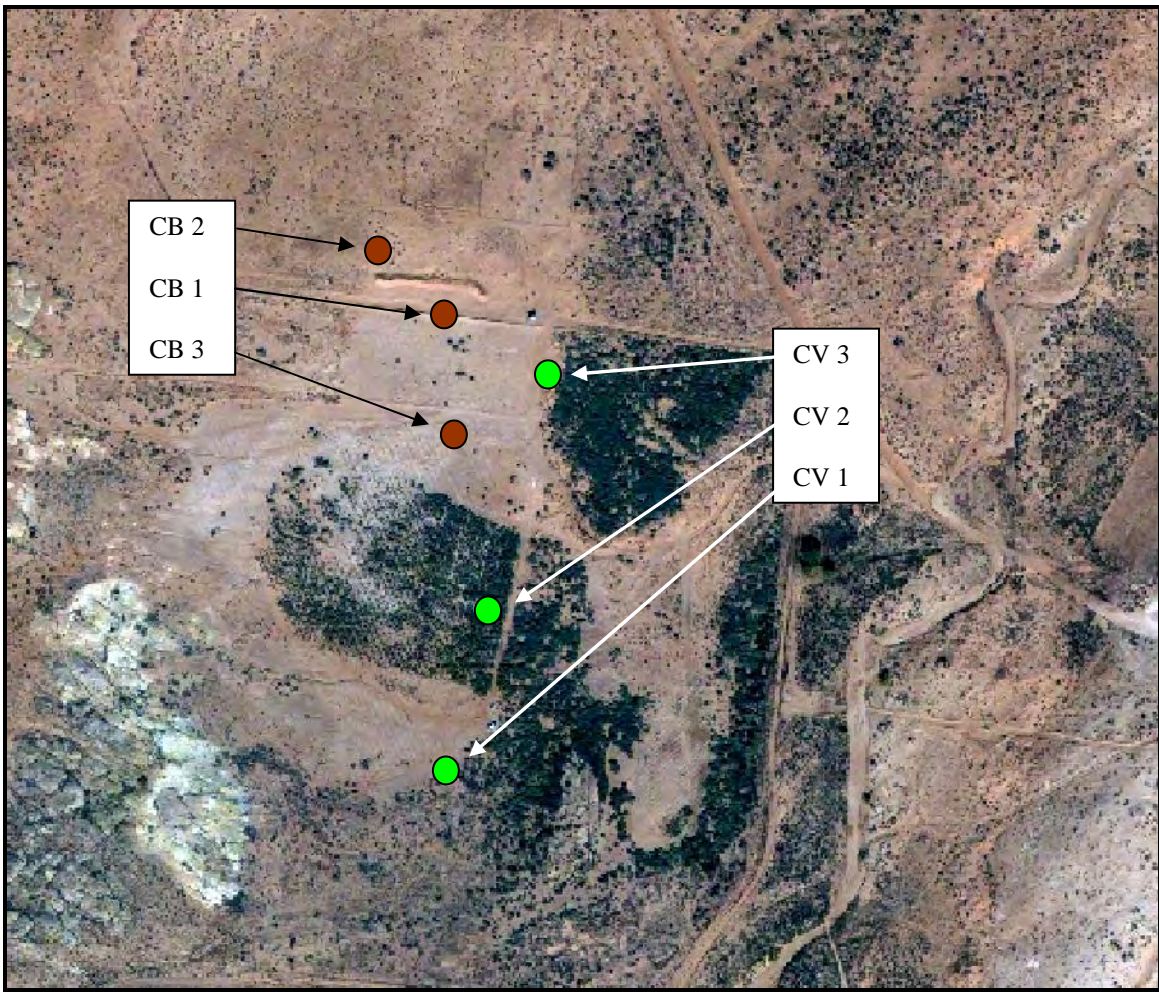
CB 1	CB 2	CB 3	Average
15'	15'	15'	15'
CV 1	CV 2	CV 3	Average
11'	13'	15'	14'

Figure 2–25. Control hydroprobe port locations and depths: Control Bare (CB) and Control Vegetated (CV). Target depth of all hydroprobe ports was 15'. CV 1 & 2: drilling stopped short of 15' by water table.
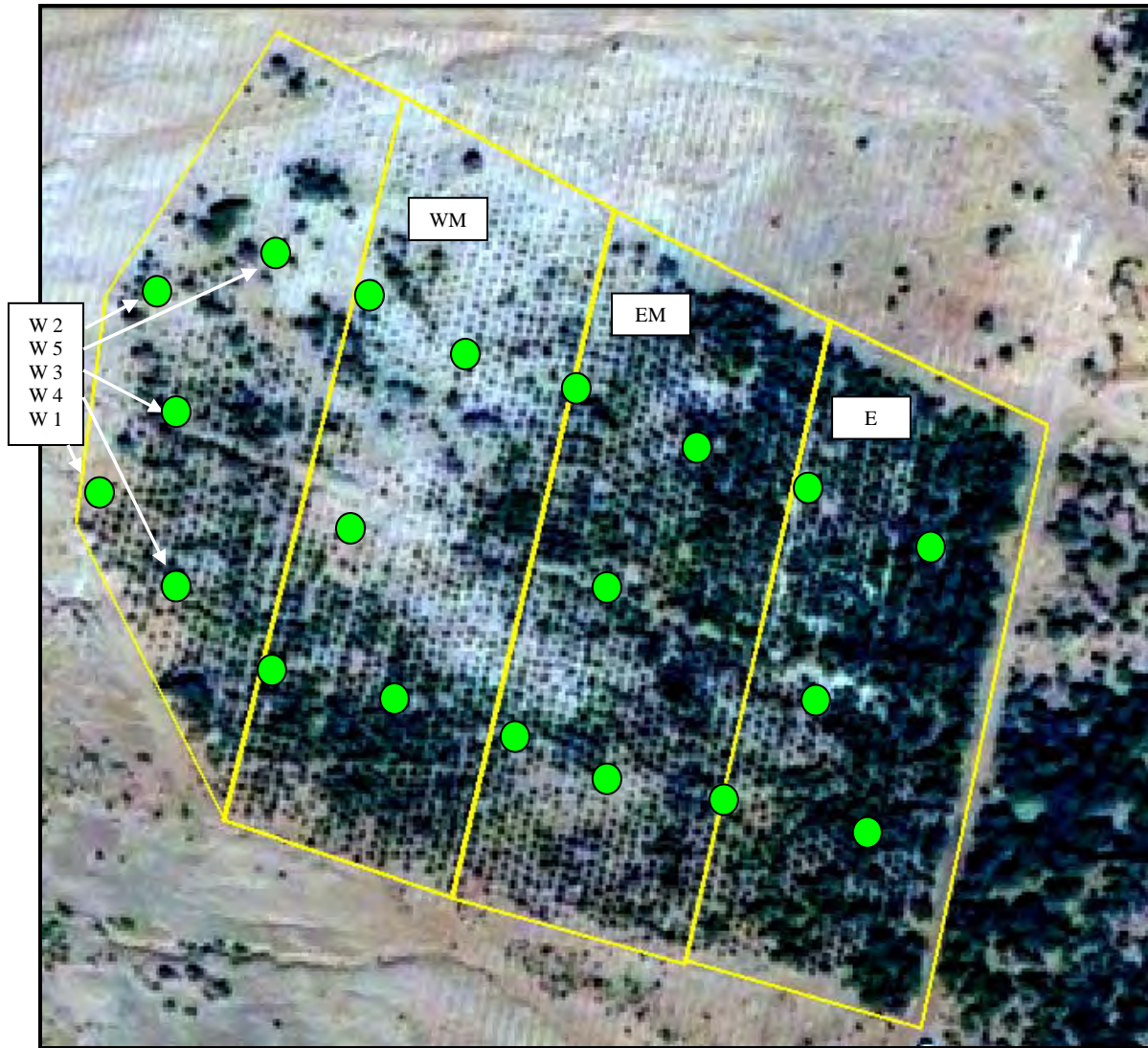
Number pattern repeats in all sections as shown in W section:

```
2 5
 3
1 4
```

W 1	W 2	W 3	W 4	W 5	Average
4'	10'	5'	2'	14'	7'
WM 1	WM 2	WM 3	WM 4	WM 5	Average
6'	14'	12'	7'	15'	10.8'
EM 1	EM 2	EM 3	EM 4	EM 5	Average
11'	15'	15'	15'	15'	11.2'
E 1	E 2	E 3	E 4	E 5	Average
13'	14'	15'	15'	15'	14.4'

Figure 2–26. Subpile soil hydroprobe port locations and depths: West (W), West Middle (WM), East Middle (EM), East (E). Ports short of 15' stopped by rock.
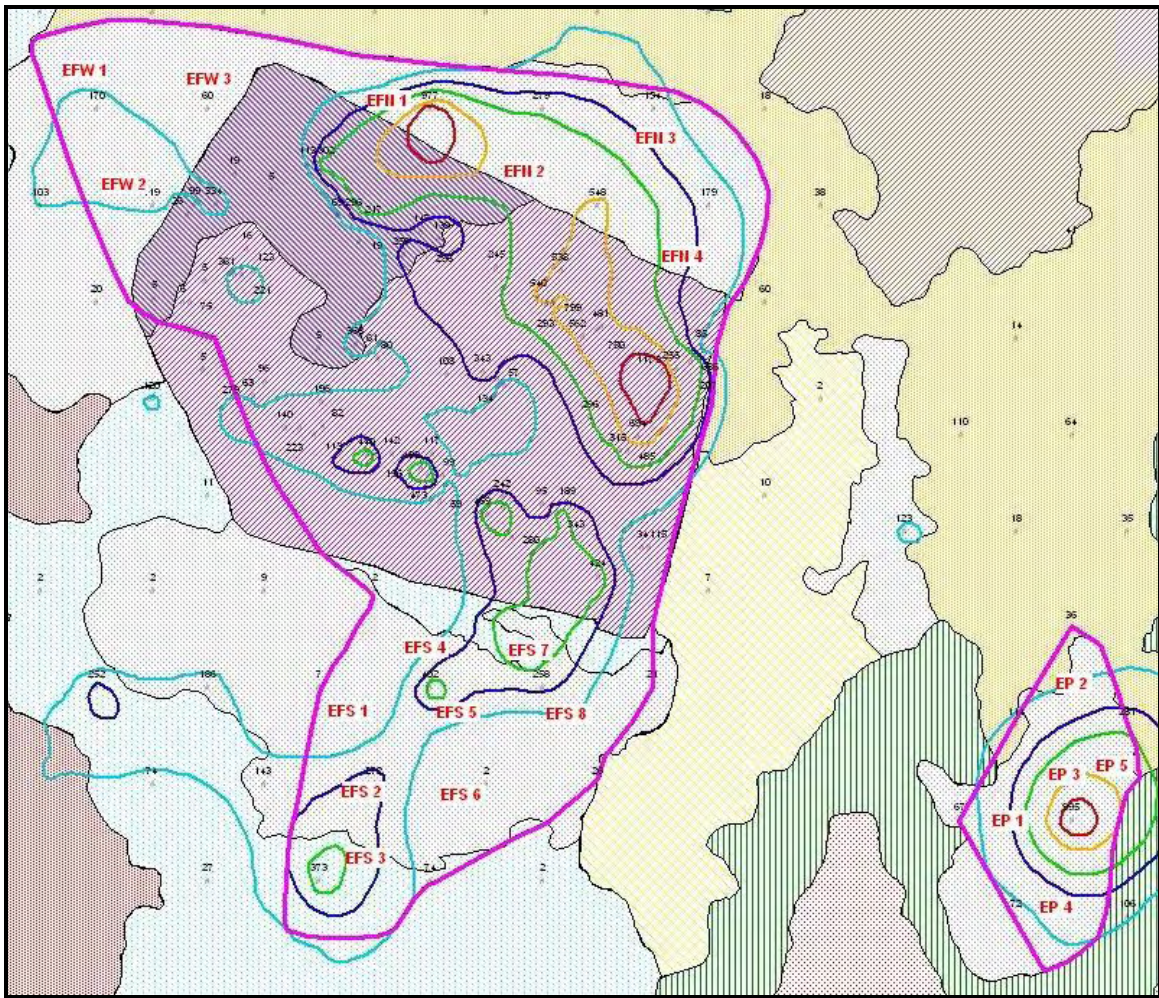
EFS 1	EFS 2	EFS 3	EFS 4	EFS 5	EFS 6	EFS 7	EFS 8	Average
10'	6'	7'	9'	10'	8'	11'	11'	9'

EFW 1	EFW 2	EFW 3	Average
8'	7'	10'	8.3'

EFN 1	EFN 2	EFN 3	EFN 4	Average
15'	15'	15'	15'	15'

EP 1	EP 2	EP 3	EP 4	EP 5	Average
8'	7'	7'	8'	7'	7.4'

Figure 2–27. Extended Field hydroprobe port locations and depths. In the Extended Field, ports short of 15' were stopped by rock layer, and in a few cases sand (hole caving in). In the evaporation pond, drilling stopped at the water table.
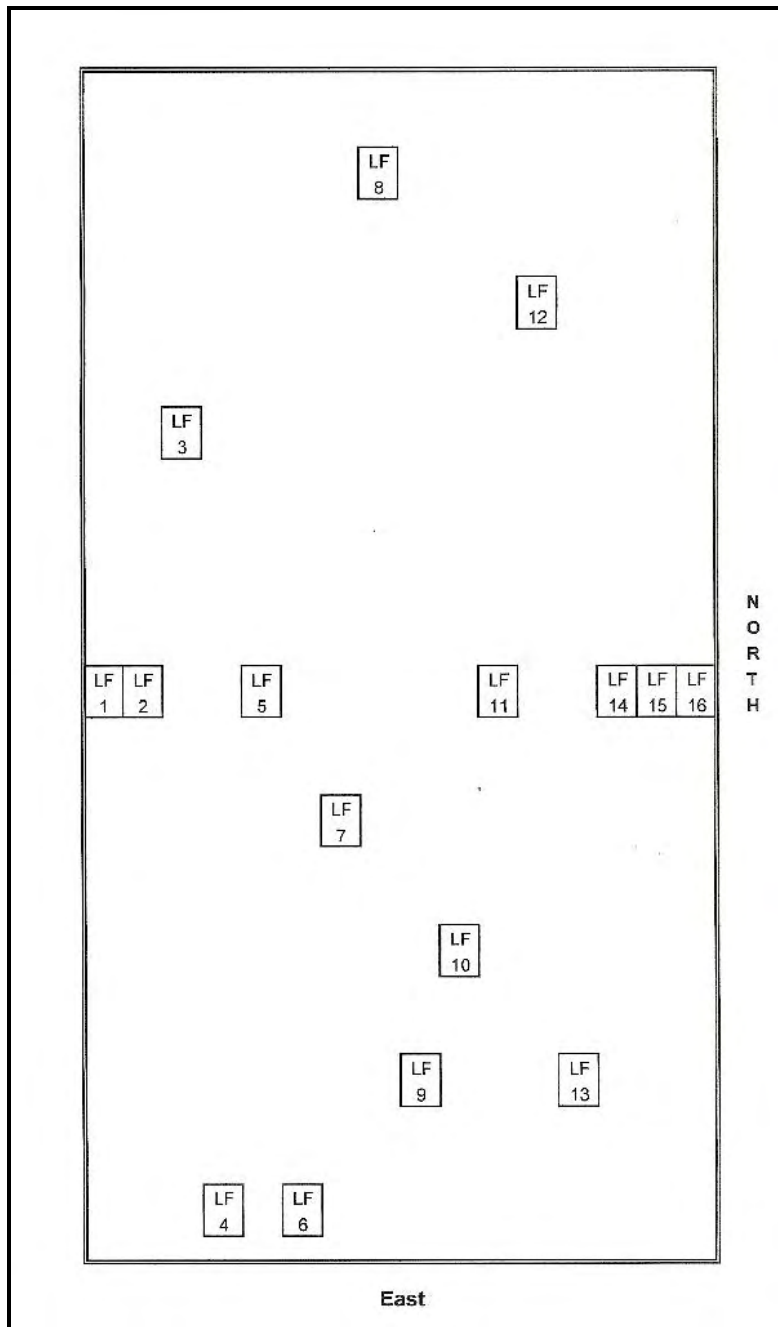
LF 1	2	3	4	5	6	7	8	9	10	11	12	13	14	15	16	Avg
14'	14'	14'	15'	15'	15'	15'	15'	15'	15'	15'	15'	15'	15'	15'	15'	14.8'

Figure 2–28. Land-farm hydroprobe port locations and depths. Ports short of 15' were stopped by bedrock or saturated soil (hole caved in).

2.5.2 Recharge Monitoring

Water content reflectometers (WCRs) and WFMs were installed in 2006 at four locations within the subpile plantings for real-time monitoring of soil moisture profiles and percolation flux. Monitoring is necessary to confirm that irrigation water is not moving below the root zone and

potentially leaching contaminants. Instrument clusters were installed in the south-central area of the 1999 planting (WFM1) and in the northeast (WFM2), northwest (WFM3), and southeast (WFM4) areas of the 2006 planting. Instrument clusters consisted of one WFM placed about 370 cm deep in the soil profile with four WCRs placed above the WFM at 30–60, 90–120, 180–210, and 270–300 cm depths.

WCRs were calibrated at the Environmental Sciences Laboratory following the methods of Kim and Benson (2002). The procedure involves (1) compacting a soil to a specified dry bulk density for three different moisture contents ranging from wetter than air-dry moisture content to slightly above the optimum moisture content as specified by the Standard Proctor Test, and (2) inserting a WCR into the soil to obtain a reading. The procedure was repeated three times. A linear calibration was used, so the products of the calibration were coefficients of a linear regression of the three sets of data.

The WFMs were installed near the bottom of the root zone and are capable of directly monitoring saturated and unsaturated water fluxes ranging from 0.02 millimeter per year (mm/yr) to more than 1,000 mm/yr (Gee et al. 2002). The WFMs, developed by Pacific Northwest National Laboratory, feature a funnel to direct water from the soil into a passive wick for moisture tension control, a miniature tipping bucket for real-time flux measurements that can be calibrated from the surface, and a pipe or chimney extending above the funnel to minimize divergent flow. Two WFMs were installed in March 2006; the other two were installed in July 2006.

The four WFMs have recorded 0 percolation since they were installed in March and July 2006. These results support the conclusion that infiltration from the combination of ambient precipitation and irrigation has been stored in the fine sand profile and is not percolating and leaching nitrate. In March 2007, water was injected in the WFM calibration tubes, and all instruments recorded tips showing that all were functioning correctly and capable of recording percolation events should they occur.

Results from WCRs placed above WFMs (Figure 2–29) show that soil water content (volumetric) is somewhat variable both spatially and temporally. The highest volumetric water content values (approximately 16 percent) occurred at the 180–210 cm depth in the mature 1999 planting (WFM1), while the lowest values occurred at the 30-60 cm depth, also in WMF1. Overall, water content was continuously higher in locations with more mature plants (WFM1 and WFM2) and lower at locations where plants remained small and immature (WFM3 and WFM4), the opposite of what would be expected. Water content deep in the profile (270–300 cm) was also greater and increasing in locations with larger, more mature plants—again, the opposite of what would be expected if irrigation rates were uniform across the plantings. By August 2007, water content at 270–300 cm in the WFM2 profile exceeded the estimated field capacity (13 percent volumetric moisture). Irrigation uniformity will be tested in 2008, and to prevent recharge from occurring, irrigation rates will be reduced until plant roots' access begins to dry the soil deep in the profile.
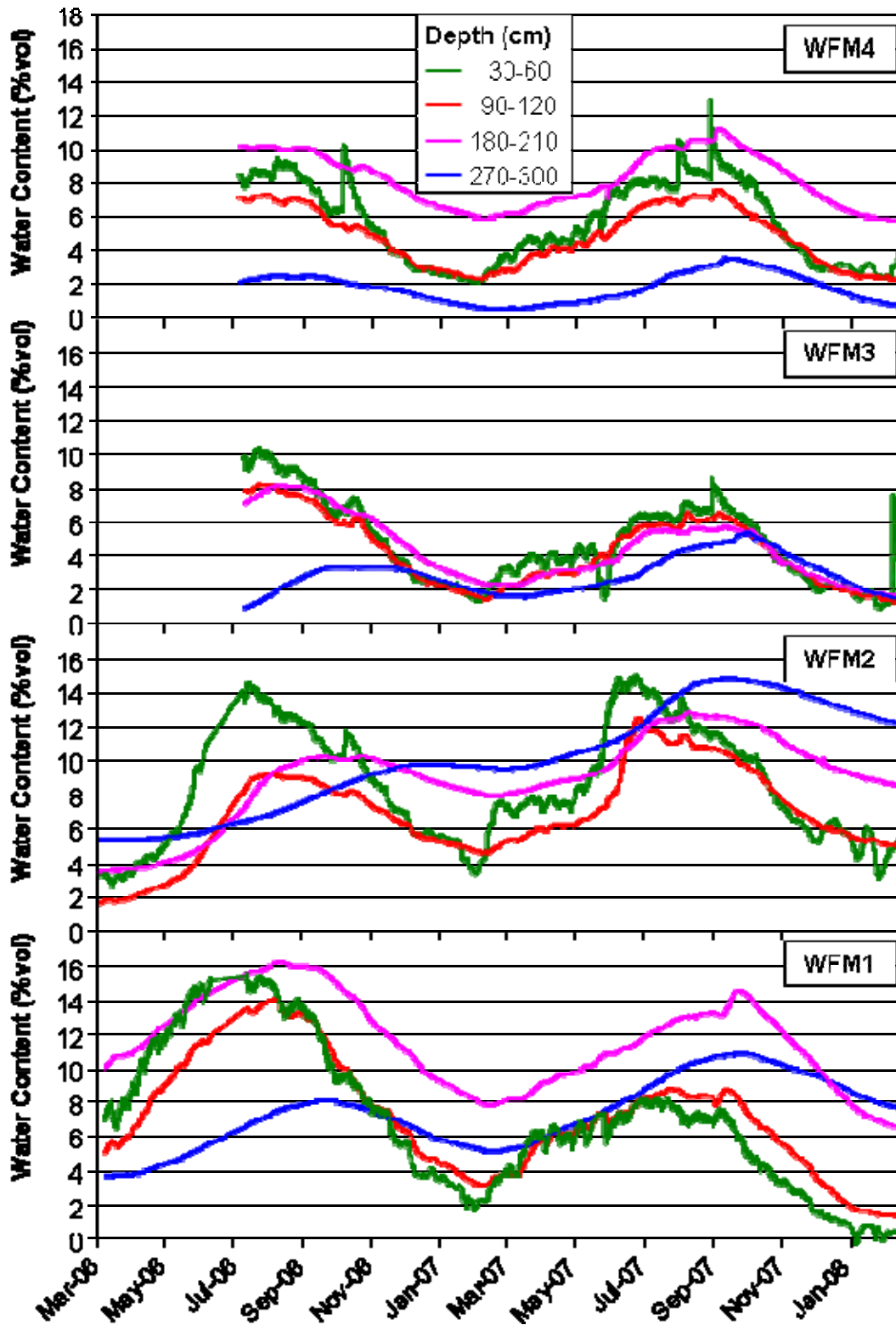
Figure 2–29. Hourly volumetric water content at four depths down to 300 cm monitored with WCRs at WFM Stations WFM1 (south-central), WFM2 (northeast), WFM3 (northwest), and WFM4 (southeast).

End of current text

3.0　Shiprock Pilot Studies

Shiprock was the site of a uranium-vanadium ore-processing mill that operated from 1954 to 1968. Mill tailings were contained in an engineered disposal cell in 1986. Groundwater in the millsite area was contaminated by uranium, nitrate, and sulfate as a result of milling operations. The groundwater system is divided hydrologically and physiographically into two regions. One plume, primarily nitrate, occurs south and then west of the disposal cell. Another plume with uranium occurs in the San Juan River floodplain below an escarpment north of the disposal cell.

In March 2003, DOE began pump-and-treat remediation of groundwater in a depression, a borrow pit for soil used to construct a compacted soil layer, or radon barrier, in the disposal cell cover (DOE 2002). Ten extraction wells and two interceptor drains were expected to produce about 20 gallons per minute, but as of March 2004, they were producing only about half of that amount. In 2004, DOE reevaluated the site conceptual model for the Shiprock site and provided recommendations for improving the groundwater treatment system (DOE 2004). One recommendation was to evaluate the feasibility of phytoremediation at the site, in this case the use of deep-rooted plants to enhance ET of water both in the borrow pit area south of the disposal cell, and on a terrace between the disposal cell and an escarpment above the San Juan River floodplain to the north. The goal of phytoremediation in these areas is hydraulic control, to limit the spread of contaminants.

Hydraulic control, in the context of phytoremediation, can be defined as the use of plants to remove groundwater through uptake and consumption in order to contain or control the migration of contaminants (EPA 2000). An increase in water extraction rates may occur naturally over time as the existing tamarisk stand matures. However, if feasible, manipulation of the plant ecology so as to accelerate water extraction by plants—enhanced phytoremediation—may be an economical addition to the current remedy.

Passive phytoremediation (no human intervention) and hydraulic control are already ongoing at Shiprock in the radon barrier borrow pit area and on the terrace between the disposal cell and the San Juan River floodplain. Volunteer tamarisk, black greasewood, and four-wing saltbush currently growing in the borrow pit area are likely extracting water, nitrate, and possibly other groundwater constituents. A few scattered black greasewood plants that have established on the terrace above the floodplain are also removing small amounts of water that might otherwise daylight in seeps at the base of the escarpment. Higher rates of water extraction by woody plants in both locations may improve hydraulic control.

Planting these areas—enhanced phytoremediation—may be an economical addition to the current groundwater compliance strategy. The success of enhanced phytoremediation would depend on several factors: depth to groundwater, phytotoxicity of groundwater constituents, site preparation methods, plant species selection, planting methods, soil amendments, and natural disturbances. The purpose of this pilot study is to begin evaluating the feasibility of phytoremediation at Shiprock.

3.1　Phytoremediation Test Plots

Test plots were set up in 2006 in the borrow pit area and on the terrace between the disposal cell and the escarpment above the San Juan River floodplain. At each location, two hand-irrigated

plots (measuring 15 m by 15 m) were created. In Figure 3–1, plots are labeled by their location relative to each other: SE Borrow Pit, SW Borrow Pit, NE Escarpment, and NW Escarpment. The SW Borrow Pit plot is approximately 1 m higher in elevation, and likely has a greater depth to groundwater, than the SE Borrow Pit plot. Depth to water is also greater at the SE Escarpment plot than at the SW Escarpment plot. Each plot has small planting basins for 42 plants (seven plants each in six rows on 7 ft spacing). Plants are irrigated from a large, elevated tank at each plot. A Navajo Nation employee keeps the tanks filled with water. Saltbush and greasewood transplants were grown in the greenhouses at UA from seed acquired on Navajo Nation land.
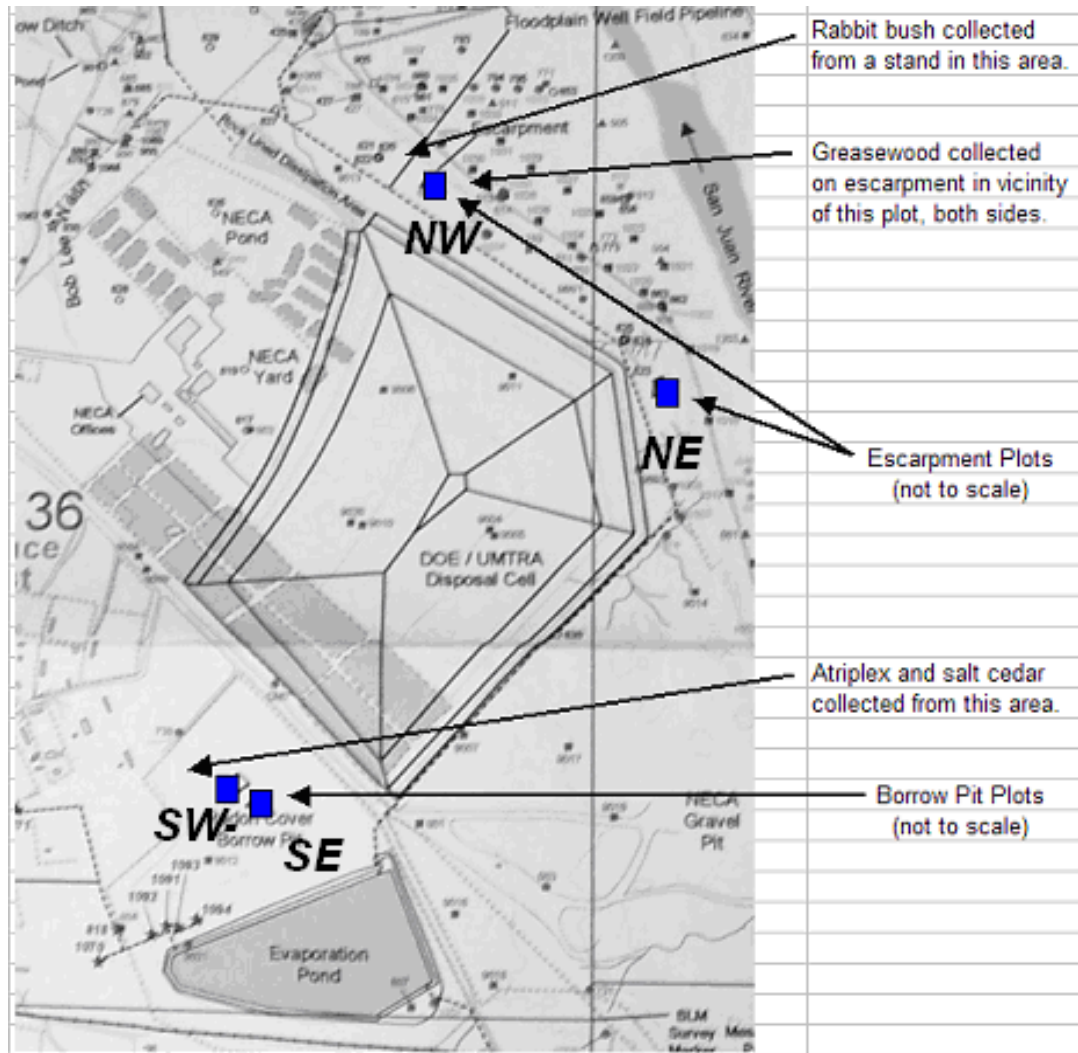
Figure 3–1. Map showing locations of phytoremediation test plots in the radon barrier borrow pit and on the terrace above the San Juan River escarpment.

Interns in the Environmental Sciences program at Diné College in Shiprock measured plant canopy dimensions in all plots in October 2007 (Figure 3–2). Overall, plants in the terrace plots have grown more than borrow pit plants ($p < 0.05$) even though the terrace plots were planted later. We have had problems keeping prairie dogs from chewing through irrigation lines and foraging on plants in the borrow pit plots. At both locations, differences between plots (SW and SE in the borrow pit and NE and NW on the terrace) are not significant. At this stage of the

study, soil type and depth to groundwater have not influenced canopy size. As we have observed in the Monument Valley plantings, in all plots, canopy cover and volume of *Atriplex* is significantly greater than *Sarcobatus* ($p < 0.05$).
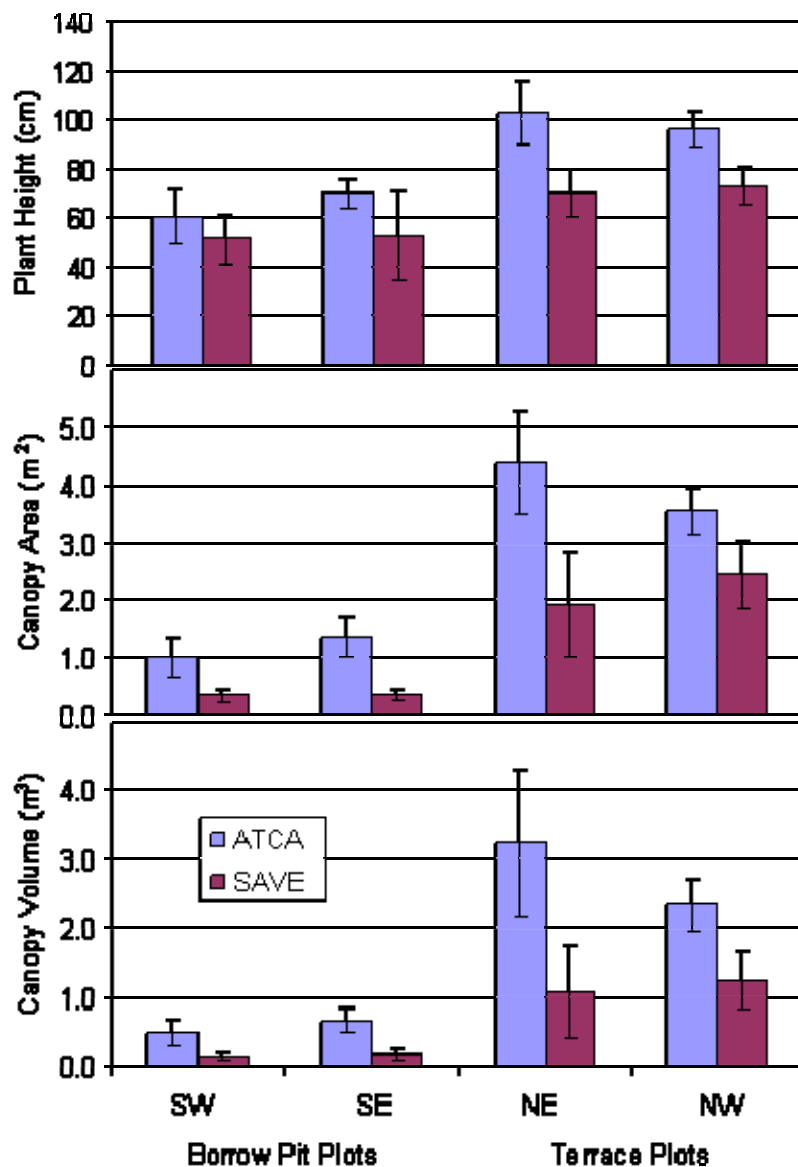
Figure 3–2. Plant height, canopy area, and canopy volume for Atriplex canescens *(ATCA or four-wing saltbush) and* Sarcobatus vermiculatus *(SAVE or black greasewood) in borrow pit and escarpment test plots. Error bars are 2(SEM).*

3.2 Transpiration Water Sources

Water isotope signatures can be used as evidence of whether volunteer phreatophytes have rooted into the shallow groundwater plumes and, hence, the feasibility of enhancing phytoremediation and hydraulic control. In 2006, oxygen and hydrogen isotope signatures were determined for plants growing naturally in the borrow pit and on the escarpment. Results were not conclusive. More extensive sampling was conducted in 2007, including water samples from

two hydroprobe ports in the Shiprock disposal cell. Saltcedar (*Tamarix ramosissima*, TARA) and four-wing saltbush (*Atriplex canescens*, ATCA) plants were sampled from the borrow pit area, saltcedar plants were sampled from the floodplain on the riverside of the extraction trench, and greasewood (*Sarcobatis vermiculatus*, SAVE) plants were sampled on the terrace above the escarpment (Figure 3–3). Isotope analyses were performed by the SIRFER Laboratory at the University of Utah.

Figure 3–3. Map of wells and approximate location of plant samples. Green squares show where Atriplex canescens *(ATCA) and* Tamarix ramosissima *(TARA) were sampled in the borrow pit area. Red squares show where* Sarcobatis vermiculatus *(SAVE) was sampled along the cell escarpment. Blue squares show where TARA plants were sampled in the floodplain below the cell.*

3.2.1 Explanation of Methodology

Enrichment of water in heavy isotopes is expressed as δD and $\delta^{18}O$, in units of per mil (‰) compared to a seawater standard, with positive numbers representing enrichment and negative numbers representing depletion of heavy isotopes relative to the standard (Coplen et al. 1999). Water samples extracted from stem sections of plants generally have isotope signatures similar to the source of water tapped by plant roots (but see Ellsworth and Williams 2007, discussed below). Hence, it is possible to infer the source of water used by a plant by comparing isotope

signatures in the plant to those of potential sources of water in the environment accessible to the roots.

As water evaporates, the residual unevaporated fraction becomes enriched in heavy isotopes (more positive δ values) due to gravity (Coplen et al. 1999). Water samples originating from a common source that have undergone different degrees of evaporation have δ values that fall along a common evaporation line when δD is plotted against $\delta^{18}O$. Atmospheric water generally has negative δ values because the light isotopes evaporate from seawater more readily than the heavy isotopes. On the other hand, rainwater becomes enriched in heavy isotopes relative to atmospheric water as water condenses into raindrops. In the southwestern United States, summer rains are typically more enriched in light isotopes than winter rains because summer rains originate from the nearby Gulf of Mexico whereas winter rains originate in the Pacific Northwest (which, by the time they reach the Southwest, have lost some of their heavy isotopes to rainfall along the way [e.g., Lin et al. 1996]). Groundwater and river water released from reservoirs have intermediate values, as they are a mixture of summer and winter rains (Lin et al. 1996). Plots of δD against $\delta^{18}O$ from rain samples fall along a meteoric water line (MWL) that has a steeper slope than an evaporation enrichment series. These principles were used to infer water sources of plants and well samples in this study. For this study, we used δD and $\delta^{18}O$ values reported for summer and winter rains at Page, Arizona, to plot the local meteoric water line (Lin et al. 1996).

3.2.2 Results and Interpretation of Isotope Signatures

Isotope data for all water and plant samples are presented in Table 3–1. Isotope signatures from plants and possible plant water sources are presented in Figure 3–4 (top panel). San Juan River water plotted along the MWL for nearby Page. The water is a mixture of winter and summer rains released into the river from the upstream Navajo Dam. Water from tailings in the Shiprock disposal cell, sampled in hydroprobe ports (plotted midway along the MWL), indicate that tailings water likely arises from local rainwater percolating through the disposal cell cover. The position along the MWL indicates that both summer and winter rains percolate through the cover, as expected, because the cover has a sand layer under a rock mulch, which would retard evaporation. However, more samples collected over a longer period, and moisture sensors would need to be installed in the cover and tailings to confirm this interpretation.

Table 3–1. Delta D and ^{18}O values for plant and well samples at Shiprock in 2007.

Sample Name	delta D	delta D stdev	delta ^{18}O	delta ^{18}O stdev	
Well 1089 Saltcedar 1	-104	0.7	-11.9	0.00	TARA growing on floodplain
Well 1089 Saltcedar 2	-109	2.0	-12.8	0.26	TARA growing on floodplain
Well 1089 Saltcedar 3	-101	1.3	-11.7	0.06	TARA growing on floodplain
Well 1109 Saltcedar 1	-99	0.1	-12.2	0.03	TARA growing near extraction trench
Well 1109 Saltcedar 2	-97	0.4	-10.7	0.05	TARA growing near extraction trench
Well 1109 Saltcedar 3	-96	1.1	-10.9	0.19	TARA growing near extraction trench
Well 1110 Saltcedar 1	-92	1.5	-9.9	0.13	TARA growing near extraction trench
Well 1110 Saltcedar 2	-99	0.7	-10.8	0.13	TARA growing near extraction trench
Well 1110 Saltcedar 3	-97	0.3	-10.9	0.16	TARA growing near extraction trench
Plot 3 SV 1	-70	3.3	-4.5	0.39	
Plot 3 SV 2	-71	1.2	-4.9	0.48	
Plot 3 SV 3	-73	0.1	-5.8	0.12	
Plot 3 SV 4	-68	0.2	-3.9	0.17	

Table 3–1 (continued). Delta D and ^{18}O values for plant and well samples at Shiprock in 2007.

Sample Name	delta D	delta D stdev	delta ^{18}O	delta ^{18}O stdev	
Borrow Pit SC 1	-65	1.5	-7.0	0.20	Up-gradient of cell—high contamination
Borrow Pit SC 2	-62	0.0	-6.2	0.03	Up-gradient of cell—high contamination
Borrow Pit SC 3	-64	0.7	-6.4	0.14	Up-gradient of cell—high contamination
Borrow Pit SB 1	-62	0.9	-4.8	0.01	Up-gradient of cell—high contamination
Borrow Pit SB 2	-54	0.9	-2.0	0.05	Up-gradient of cell—high contamination
Borrow Pit SB 3	-79	0.2	-5.7	0.08	Up-gradient of cell—high contamination
River	-91	0.3	-12.6	0.01	San Juan River
DM-7	-95	0.2	-11.2	0.09	Up-gradient well next to cell
425	-84	1.1	-10.4	0.11	Seep from Mancos Shale
426	-96	1.5	-12.7	0.08	Seep from Mancos Shale
600	-88	0.8	-10.9	0.05	Escarpment monitoring well
602	-80	0.3	-8.4	0.05	Monitoring well next to the cell
611	-92	1.4	-12.2	0.14	Escarpment monitoring well
613	-77	0.4	-10.5	0.07	Floodplain monitoring well
616	-89	2.1	-11.6	0.24	Floodplain monitoring well
648	-105	1.2	-14.2	0.22	Deep artesian well
730	-54	0.5	-7.3	0.01	Monitoring well up-gradient of cell
817	-78	0.1	-9.0	0.21	Monitoring well down-gradient
818	-83	1.5	-8.5	0.21	Extraction well in main plume area
855	-104	1.9	-13.3	0.09	Floodplain monitoring well in clean area
1004	-93	2.0	-11.3	0.18	Escarpment monitoring well
1007	-74	0.6	-8.3	0.07	Escarpment monitoring well
1011	-86	0.6	-10.9	0.11	Escarpment monitoring well
1070	-80	0.0	-8.4	0.02	Extraction well in main plume area
1071	-60	0.4	-7.0	0.03	Extraction well in main plume area
1078	-79	1.0	-9.1	0.18	Far down-gradient extraction well
1087	-77	0.6	-9.3	0.10	Bob Lee Wash extraction drain sump
1087	-74	1.8	-9.1	0.27	Bob Lee Wash extraction drain sump
1088	-69	0.2	-7.9	0.20	Many Devils Wash extraction drain sump
1089	-91	1.4	-12.2	0.16	Floodplain extraction well
1091	-78	0.9	-7.8	0.20	Extraction well in main plume area
1092	-87	1.5	-9.0	0.14	Extraction well in main plume area
1093	-70	1.3	-7.3	0.18	Extraction well in main plume area
1095	-81	1.4	-8.8	0.21	Extraction well in main plume area
1100	-85	0.5	-10.6	0.03	Unknown
1104	-90	0.9	-11.6	0.17	Floodplain extraction well
1109	-85	0.3	-11.4		Extraction trench
1130	-92	0.5	-12.5	0.04	San Juan River monitoring well
1133	-82	1.4	-10.3	0.24	Monitor well next to 1109
Cell Center	-69	0.3	-9.5	0.07	
Cell NE Corner	-72	0.9	-8.7	0.03	
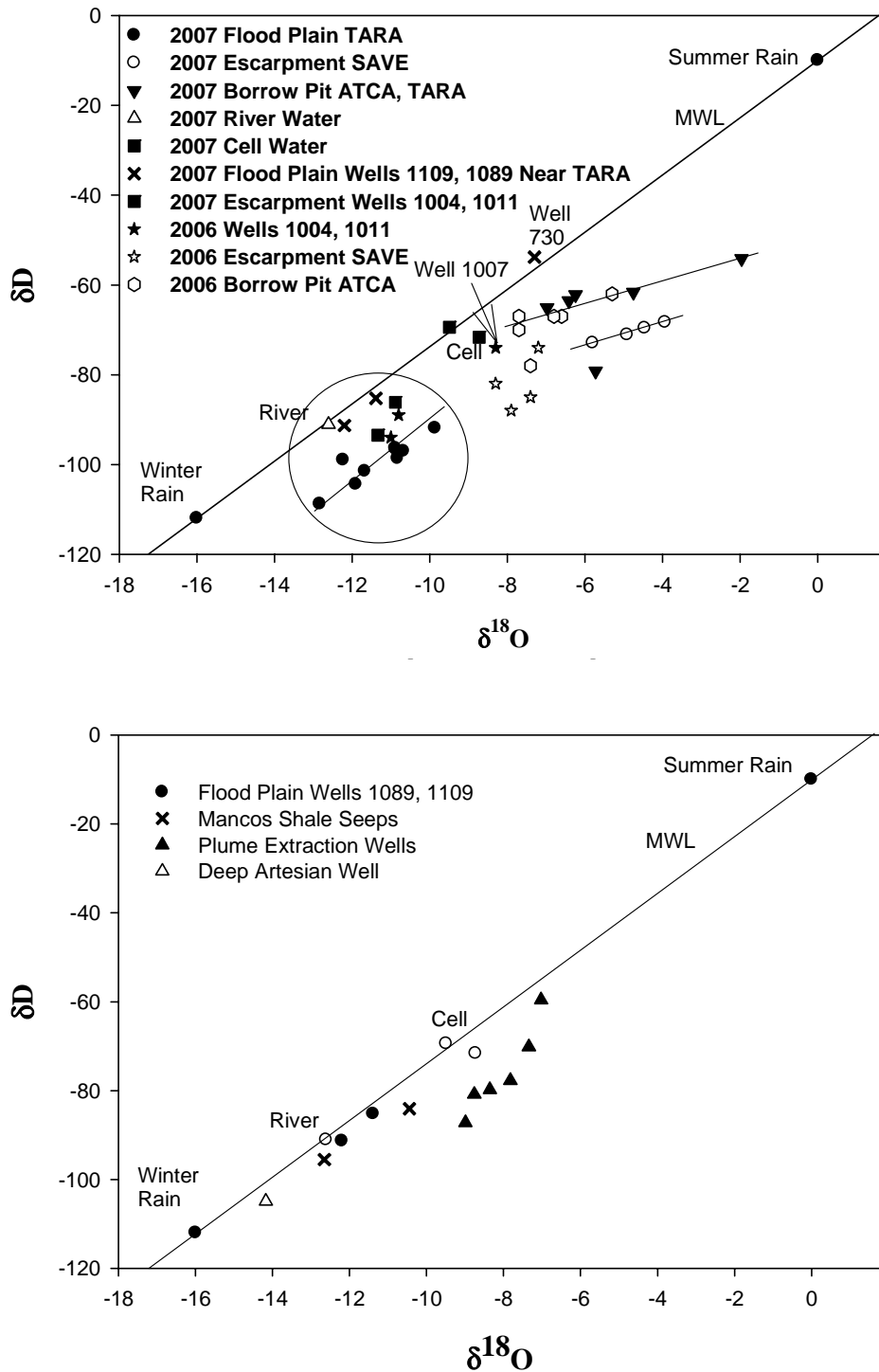
Figure 3–4. Top: plant isotope signatures compared to selected water sources. Bottom: additional water sources.

Isotope signatures for water from floodplain wells 1089 and 1109, near the TARA plants sampled on the floodplain, were similar to river water, indicating that these wells are intercepting the floodplain aquifer recharged by the river. TARA plants collected near the these wells plotted along a line parallel to, but below, the river and well signatures, indicating that these plants are

rooted into and using aquifer water for ET. The downward shift of the line is due to the preferential uptake of water molecules richer in hydrogen than deuterium, a characteristic of salt-tolerant plants, such as TARA, that filter water through cells in their root endodermis to remove salts prior to loading them into the xylem vessels (Ellsworth and Williams 2007). This process selects water molecules rich in hydrogen compared to deuterium, but it does not discriminate between oxygen isotopes.

Terrace wells 1004 and 1011 plotted to the right of the river value, which indicates that the water originated from the river but had undergone some evaporation. Results were similar in 2006 and 2007. SAVE plants from the escarpment did not plot close to the terrace wells. SAVE plant water plotted along an evaporation line that could be extrapolated back to water from the alluvial aquifer. A possible interpretation of these data is that the SAVE plants are extracting water from the alluvial aquifer that rises by capillary action up into the escarpment. These plants would extract water from the phreatic zone at the top of the capillary fringe, which would be more enriched in heavy isotopes (more evaporated) than bulk water from escarpment wells 1004 and 1011. The evaporation line for SAVE plants shifted to the right from 2006 to 2007, indicating that the SAVE plants may be accessing different layers of water sources within the terrace as their roots extend further into the terrace each year.

Escarpment well 1007, at the northeast corner of the cell, had a different isotope signature than wells 1004 and 1011. This well had a signature that plotted close to water from the tailings (disposal cell probe ports), indicating possible leakage of water from the disposal cell to the floodplain at this point along the Terrace.

ATCA and TARA plants from the Borrow Pit area generally plotted along a common evaporation line, indicating that they are likely using locally recharged rainwater to support growth. Some of the plants had anomalous signatures, indicating that there are likely different rain events contributing to vadose zone water or a combination of shallow groundwater and rainwater in the borrow pit area, accessed by ATCA and TARA plants. However, no well samples were available to match with these plant signatures. Well 730, which was considered a possible source of water for these plants, plotted along the MWL above the plant values.

Figure 3–4 (bottom panel) plots some of the other well samples. Deep artesian water and Mancos Shale seeps plotted along the MWL near river water, indicating that their origins were either the river or recharge from local (mainly winter) rain events. The plume extraction wells plotted as a cluster to the right of cell water samples, indicating that they might have originated originally from leakage from the cell and undergone some evaporation over time. These interpretations are tentative, and they should be regarded as hypotheses needing further testing at this point.

4.0 References

Bonham, C.D., 1989. *Measurements for Terrestrial Vegetation* (New York: John Wiley and Sons).

Coplen, T., A. Herczeg, and C. Barnes, 2000. "Isotope engineering using stable isotopes of the water molecule to solve practical problems," in P.G. Cook and A.L. Herczeg (eds.), *Environmental Tracers in Subsurface Hydrology* (Norwell, MA: Kluwer Academic Publishers), 79–10.

Cottam, Grant and J.T. Curtis, 1956. "The use of distance measures in phytosociologal sampling," *Ecology*, 37: 451–460.

DOE (U.S. Department of Energy), 2002. *Phytoremediation of Nitrogen Contamination in Subpile Soils and in the Alluvial Aquifer at the Monument Valley, Arizona, Uranium Mill Tailings Site*, GJO-2002-312-TAR, U.S. Department of Energy, Grand Junction, Colorado.

DOE (U.S. Department of Energy), 2004a. *Environmental Assessment of Ground Water Compliance at the Monument Valley, Arizona, Uranium Mill Tailings Site*, Draft, DOE/EA-1313, U.S. Department of Energy, Office of Legacy Management, Grand Junction, Colorado.

DOE (U.S. Department of Energy), 2004b. *Phytoremediation of the Nitrogen-Contaminated Subpile Soil at the Former Uranium Mill Tailings Site in Monument Valley, Arizona: 2004 Status Report*, DOE-LM/GJ768-2004 (ESL-RPT-2004-07), Environmental Sciences Laboratory, U.S. Department of Energy, Grand Junction, Colorado.

DOE (U.S. Department of Energy), 2004c. *Monument Valley Ground Water Remediation: Pilot Study Work Plan,* DOE-LM/GJ757-2004, Office of Legacy Management, U.S. Department of Energy, Grand Junction, Colorado.

DOE (U.S. Department of Energy), 2006. *Soil and Ground Water Phytoremediation Pilot Studies at Monument Valley, Arizona: 2005 Status Report,* DOE-LM/1254-2006, Office of Legacy Management, U.S. Department of Energy, Grand Junction, Colorado.

DOE (U.S. Department of Energy), 2007. *Natural and Enhanced Attenuation of Soil and Ground Water at Monument Valley, Arizona, and Shiprock, New Mexico: 2006 Status Report,* DOE–LM/1428, Office of Legacy Management, U.S. Department of Energy, Grand Junction, Colorado.

Ellsworth, P. and D. Williams, 2007. "Hydrogen isotope fractionation during water uptake by woody xerophytes," *Plant and Soil*, 291: 93–107.

Jordan, F., W.J. Waugh, E.P. Glenn L. Sam, T Thompson, and T.L. Thompson, 2008. "Natural bioremediation of a nitrate-contaminated soil-and-aquifer system in a desert environment," *Journal of Arid Environments*, 72(5): 748–763.

Lin, G., S. Phillips, and J. Ehleringer, 1996. "Monsoonal precipitation responses of shrubs in a cold desert community on the Colorado Plateau," *Oecologia*, 106: 8–17.

Lindsay, W.L., 1979. *Chemical Equilibria in Soils* (Wiley-Interscience).

Waugh, W.J., 2002. *Distance (Plotless) Methods for Estimating Shrub Density on the Monticello ACAP Lysimeter*, U.S. Department of Energy Grand Junction Office, Grand Junction, Colorado.

End of current text

Appendix A

Vegetation Density and Evapotranspiration in a Heavily Grazed Phreatophytic Shrub Community in a Nitrate-Contaminated Desert Watershed: Implications for the Local Water Balance

This page intentionally left blank

Title: Scaling sap flux measurements of grazed and ungrazed shrub communities with fine and coarse-resolution remote sensing

Authors: Edward P. Glenn[a]*, Kiyomi Morino[b], Kamel Didan[c], Fiona Jordan[a], Kenneth Carrol[c], Pamela L. Nagler[d], Kevin Hultine[e], Linda Sheader[f], and Jody Waugh[f]

[a]Environmental Research Laboratory of the University of Arizona, 2601 East Airport Drive, Tucson, AZ 85706 USA

[b]Tree Ring Laboratory, 105 West Stadium, University of Arizona, Tucson, AZ 85721 USA

[c]Department of Soil, Water and Environmental Science, Room 429 Shantz Bldg., University of Arizona, Tucson, AZ 85721 USA

[d]U.S. Geological Survey, 125 Biological Sciences East, University of Arizona, Tucson, AZ 85721 USA

[e]Department of Biology, University of Utah, Salt Lake City, UT 84112 USA

*Corresponding author: eglenn@ag.arizona.edu; Phone 1 520 626 2664; Fax 1 520 573 0852

Abstract

We measured transpiration by black greasewood (*Sarcobatus ermiculatus*) (SAVE) and fourwing saltbush (*Atriplex canescens*) (ATCA) over a nitrate-contaminated aquifer in Monument Valley, Arizona, on the Colorado Plateau. Heat-balance sap flow sensors were used to measure transpiration by shrubs in 2006 and 2007 and results were scaled to larger landscape units and longer time scales using leaf area index, fractional vegetation cover, meteorological data, and the Enhanced Vegetation Index from MODIS sensors on the Terra satellite. Transpiration was high on a leaf-area basis (2.95 – 6.72 kg m^{-2} d^{-1}) and was controlled by vapor pressure deficit (D) in the atmosphere. SAVE tended to have higher transpiration rates than ATCA and had a steeper response to D, but both exhibited midday depression of leaf conductance. Over most of the site, fractional vegetation cover (f_c) and area-wide leaf area index (LAI), were low (0.10 and 0.37, respectively), due to heavy grazing by cattle and sheep. However, a portion of the plume that had been protected from grazing for ten years had f_c = 0.75, LAI = 2.88. Transpiration rates on a ground area basis varied with LAI, with mid-summer daily values ranging from 1.44 mm d^{-1} (LAI = 0.36) to 13.1 mm d^{-1} (LAI = 2.88 mm) over the site, corresponding to projected annual values of 159 mm yr^{-1} to 1447 mm yr^{-1}. Controlling grazing could theoretically slow or halt the movement of the contamination plume by allowing the shrub community to extract more water than is recharged in the aquifer.

Keywords: *Atriplex*, *Sarcobatus*, nitrate contamination, transpiration, ground water depletion

1. Introduction

1.1 Evapotranspiration by desert phreatophyte shrub communities

Vegetation plays a key role in determining rates of discharge and recharge of aquifers in arid and semiarid rangelands (Wilcox and Thurow, 2006). Removal of vegetation, as through over-grazing, can result in increased runoff and recharge whereas an intact vegetation community generally consumes nearly all of the annual precipitation (Huxman et al., 2005). The zone of active water uptake by plants can extend deep into desert soils; phreatophytic shrubs and trees can extract water from alluvial aquifers tens of meters from the soil surface, and can be the major biological component of the water cycle in shrub ecosystems (Nichols, 2000; Groeneveld et al., 2007). Determining the rate of ground water discharge by phreatophytes is important in assessing local and regional water budgets, as the area occupied by non-riparian phreatophytes is very large (tens of millions of ha) in the western U.S. (Shreve, 1942). Across much of the Colorado Plateau and Great Basin Province of the western U.S., phreatophyte communities are the principal or only source of ground water discharge (Nichols, 1994, 2000). Phreatophytes can also influence the rate of migration of contaminants in aquifers through their effects on ground water movement (Jordan et al., 2008). However, only a few studies have attempted to quantify rates of phreatophyte transpiration over wide areas (Nichols, 1993, 1994; Steinwand et al., 2001, 2006; Cooper et al., 2006; Groeneveld et al., 2007; Groeneveld and Baugh, 2007), and different methods have yielded different results (discussed in Nichols, 1994; Cooper et al., 2006).

1.2 Methods to estimate phreatophyte transpiration

Early estimates of phreatophyte water consumption depended on indirect approaches, such growing phreatophytes in concrete tanks to measure water consumption, then extrapolating the results to natural stands of plants. Nichols (1994) used a Bowen ratio micrometeorological method to estimate total evapotranspiration (ET), including plant water consumption and bare soil evaporation, in natural stands of phreatophytes in the Great Basin Province, and concluded that the earlier estimates were prone to large errors. Steinwand et al. (2001) used porometry to measure stomatal conductance of individual leaves of two phreatophyte shrubs in Owens Valley, California, then developed crop coefficients to scale transpiration over wide areas based on fractional vegetation cover (f_c) and leaf area index (LAI). However, that approach required enclosing the leaves in a leaf-chamber, and the results may not be representative of natural conductance rates. Furthermore, their use of crop coefficients was criticized as inappropriate for desert plants because it assumes unstressed conditions, which might not apply to desert plants (Mata-Gonzalez et al., 2005).

More recently, Bowen ratio (Cooper et al., 2006) and eddy covariance (Groeneveld et al., 2007; Steinwand et al., 2006) moisture flux towers have been used to measure ET of phreatophyte communities. Flux towers unobtrusively measure ET over areas of several thousand m^2 of uniform vegetation cover, and the measurements can be scaled to larger areas by remote sensing methods. Flux towers measure both bare soil

evaporation and plant transpiration, so the plant contribution to ET is not directly measured.

Reported rates of transpiration or ET in non-riparian, arid-zone phreatophyte communities vary widely, from as low as 20 mm yr^{-1} to greater than 600 mm yr^{-1} depending on vegetation type and site characteristics (Groeneveld et al., 2007; Cooper et al., 2006; Steinwand et al., 2006). Transpiration rates are influenced by precipitation (Lin et al., 1996), soil type (Hultine et al., 2006), depth to ground water (Nichols, 1994), fluctuations in ground water level (Naumberg et al., 2005), and land use practices such as grazing pressure (McKeon et al., 2006) and pumping of ground water for human use (Cooper et al., 2006). The percentage of transpired water derived from ground water also varies widely; in the Owens Valley study, ground water accounted for 20-30% of ET from shrubs but 60-80% of ET from high cover meadows with ground water 1-3 m beneath the surface (Steinwand et al., 2006). More site-specific information on phreatophyte water consumption is needed for the common phreatophyte associations in the western U.S. Remote sensing methods for estimating phreatophyte water use over wide areas are also needed.

1.3 Purpose of the present study

This study measured wide-area transpiration in a phreatophyte community growing over a nitrate-contaminated alluvial aquifer at a former uranium mill site in the Great Basin Desert of the U.S. The two main shrubs growing over the contamination plume are black greasewood (*Sarcobatus vermiculatus* hereafter referred to as SAVE) and fourwing saltbush (*Atriplex canescens*, hereafter referred to as ATCA). Black greasewood – saltbush plant associations are widely distributed in the western U.S., dominating many intermountain basins that support alluvial aquifers within 10 m of the surface (Shreve, 1942; Anderson, 2004). The saltbush component can be fourwing saltbush, as in the present study, shadscale (*A. confertifolia*, hereafter referred to as ATCO), quailbush (*A. lentiformis*), or less widely distributed saltbush species.

Analyses of oxygen, hydrogen and nitrogen isotopes in water samples from soils, the aquifer, and plant stems showed that these shrubs are extracting water and nitrate from the contamination plume, at depths of 6-12 m below the soil surface (McKeon et al., 2005, 2006; Jordan et al., 2008). The site is heavily grazed by sheep and cattle, and previous studies also showed that when shrubs were fenced to prevent grazing, they increased 2-3 fold in biomass over just four years (McKeon et al., 2006). Therefore, reduction of grazing would allow greater shrub cover, and therefore more transpiration, minimizing the recharge of ground water and thereby reducing the migration of the plume. However, rates of transpiration were not estimated, and it was unknown what actual impact the shrub community has on the local water balance.

In the present study, we used sap flow sensors to estimate transpiration by each shrub type and remote sensing methods to scale the results over larger landscape units and over multiple years (2000-2007) for grazed and ungrazed areas over the plume. We compared transpiration rates to precipitation and to estimates of aquifer recharge. We

found that these plants have high rates of transpiration on a leaf area and canopy area basis, and they discharge large volumes of groundwater even when heavily grazed. The results and methods are relevant to other shrub communities in the western U.S.

2. Materials and Methods

2.1 Site description

The Monument Valley Uranium Mill Tailings Remediation (UMTRA) site is located on Navajo Nation land in Northern Arizona, approximately 24 km southeast of Mexican Hat, Utah in a high desert (1540 m elevation), dune-and-swale environment on the Colorado Plateau (U. S. Department of Energy, 1999). Site characteristics and previous research are reported in McKeon et al. (2005, 2006), Jordan et al. (2008), and in on-line documents from the United States Department of Energy (1999, 2000, 2004, 2006). Annual precipitation is approximately 110 mm**Error! Hyperlink reference not valid.**, arriving as summer monsoon rains and winter snow and rain. Figure 1 shows the areas of interest at the site covered in the present study. Phreatophyte shrubs growing over the plume consists primarily of ATCA and SAVE shrubs, with some ATCO shrubs, but annual plants and non-phreatophytic perennials augment the flora (United States Department of Energy, 1999; McKeon et al., 2006). The source area, site of the former milling activities, has been fenced since 1997. However, outside the fence the phreatophyte community is heavily grazed, as elsewhere on the Navajo Nation (McFadden and McAuliffe, 1997; Savage, 1991).

2.2 Research objectives

Our objectives were: 1) to determine rates of leaf-level transpiration (E_L) by representative plants inside and outside animal exclosures (fenced areas) using sap flow sensors; 2) to scale E_L to larger landscape units using plant leaf area determined by leaf harvesting and f_c determined on high-resolution Quickbird satellite images; and 4), to scale plot-level measurements over seasons and years for areas of interest over the contamination plume using moderate resolution MODIS satellite imagery and ground meteorological data. Terminology and units can differ among ET studies; here we follow Ewers and Oren (2000) for sap flux, transpiration and stomatal conductance terminology and units, and Monteith and Unsworth (1990) for other units. In this paper we also distinguished between leaf area index (LAI) defined as m^2 of leaf area per m^2 of ground area, including both plant canopies and areas of bare soil; and plant leaf area index (LAPS) defined as m^2 of leaf area per m^2 of plant horizontal surface (Groeneveld and Warren, 1992).

2.3 Sap flow measurements

The procedures have been described in detail in Grime and Sinclair (1999), Kjelgaard et al., 1997; and Nagler et al. (2003, 2007). We used home-made sensors described in Scott et al. (2006), which were validated by measurements of ET by flux towers in that study. In the heat balance method, a branch containing leaves is wrapped

by a heating wire and a constant source of low-grade heat is applied to the branch through an electric heating wire (Kjelgaard et al., 1997). Thermocouples embedded in the branch measure temperatures upstream and downstream from the heat source, and a thermopile outside the heating wire in the surrounding layer of insulation measures heat lost radially from the stem. A heat balance equation is then solved to calculate heat transported by convection in the transpiration stream, and the results are expressed in terms of grams of water transported per hour.

The sap flow measurements were made inside and outside two, 50 m x 50 m, livestock exclosures at the site (see Figure 1 for locations), which were erected in 2006 for long-term monitoring of grazing effects. ATCA and SAVE are co-dominants at the South Exclosure while ATCA alone dominated the North Exclosure (see Table 1). Data were collected from September 8 to September 18, 2006, and July 9 to August 15, 2007. In 2006 sap flows sensors were attached to 8-10 individual ATCA and SAVE plants inside and outside each exclosure. In 2007 8-10 SAVE plants inside and outside the South Exclosure were gauged, and 8-10 ATCA plants inside and outside the North Exclosure were gauged (18 plants per species each year).

Not all sensors produced reliable data throughout the study periods. Some sensors were lost due to rodents chewing the electric cables connecting the sensors to the data logger and voltage regulator. Others were lost to grazing damage by cattle, or to heat damage to the stem from the heating wire. Some sensors produced aberrant diurnal patterns of temperature response, such as higher temperature readings at the thermocouple below the heating wire compared to above the wire during the daytime (the opposite is expected because the heating wire should raise the temperature of water in the transpiration stream). This is attributed to solar heating of the plant stem below the sensor. We screened the sensor data to eliminate sensors that did not survive the entire measurement period or that produced aberrant temperature patterns. We also employed a filtering program that eliminated spikes in the sap flow traces. The final data set consisted of sap flux per branch (J) in g H_2O h^{-1} reported at half-hour intervals. Of the 36 sensors deployed each year, 16 produced complete data sets in 2006 and 20 produced data in 2007.

2.4 Determining species composition and fractional cover inside and outside exclosure plots

Ground surveys using a line-intercept method were conducted in November, 2007, to compare vegetation inside and outside of exclosure plots. For inside measurements, 20 randomly placed, 5 m transects were established in each plot and cover classes were determined at 10 cm intervals along the transects (n = 1000 observations per plot). Cover classes include bare soil, plant litter, or vegetation, determined to species level. The same procedure was used to score outside vegetation, within a 50 m x 50 m area adjacent to the east side of each exclosure plot.

2.5 Scaling sap flux measurements

Sap flux per branch was scaled to a unit leaf area basis as:

$$E_L = J/A_L \qquad\qquad (1)$$

where A_L is leaf area per branch in m^2. On a daily time step E_L is reported in units of kg H_2O m^{-2} leaf d^{-1}, and on an hourly time step in units of mmol H_2O m^{-2} sec^{-1} for comparison with leaf conductance values (Ewers and Oren, 2000). At the end of the measurement period, all branches with gauges were harvested and returned to the laboratory in paper bags. Plant material was dried in a solar drier, then all leaves on the branch were collected by hand-sorting leaves from stems and twigs. Dry mass of leaves were converted to m^2 of leaf area by determining the specific leaf area (SLA) of subsamples of leaves. Each year, SLA was determined during the period of sap flux measurements by collecting a sample of several hundred fresh leaves from 10 plants of each species (five inside and five outside exclosures)(Nagler et al., 2004, 2007). The area of a leaf sample was quantified by placing them on graph paper and counting the area covered by leaves, then the sample was then dried to determine m^2 of leaf area per g dry weight of leaves. Leaf area in m^2 g^{-1} was 0.00636 (SE = 0.000135) for fourwing saltbush and 0.00670 (SE = 0.000738) for black greasewood pooled over years and treatments (P > 0.05).

E_L was converted to E on a ground-area basis (E_G) as:

$$E_G = E_L \text{ x LAI} \qquad\qquad\qquad (2)$$

with:

$$LAI = LAPS \text{ x } f_c \qquad\qquad\qquad (3)$$

where f_c is fractional cover of shrubs over the ground (see **Section 2.5**) and LAPS is the plant leaf area index (Groeneveld and Warren, 1992). E_G is reported in volumetric units of mm d^{-1}, which are equivalent to units of kg H_2O m^{-2} ground area d^{-1}, with 1 mm of H_2O equal to 1 kg m^{-2} H_2O. LAPS was determined by a leaf harvesting method (Nagler et al., 2004) for each plant canopy that received sap flow sensors (total of 36 ATCA and 36 SAVE plants). In 2006, a 0.25 m^2 (0.5 m x 0.5 m) frame was held horizontal to the ground over a randomly selected portion of the plant canopy, and all leaves within the frame were harvested and dried to determine g leaves m^{-2} of plant canopy area projected on the ground. The procedure was the same in 2007 except that a 0.0625 m^2 (0.25 m x 0.25 m) frame was used. We then calculated LAPS of a canopy by multiplying by SLA, determined as described above. Since LAPS and SLA can change over the year, we determined these parameters during the periods of sap flux measurements.

2.5 Determining f_c and standing biomass from Quickbird images

Fractional cover was determined on Quickbird images (Digital Globe, Inc., Longmont, CO) acquired on October 20, 2006, and July 12, 2007. The images were sharpened, panchromatic (natural color) images with 0.3 m resolution, and individual shrubs could be resolved on the images. Images were imported into ERDAS Imagine software (Leica Geosystems, Inc., Atlanta, GA) and processed in an unsupervised classification program in which pixels were partitioned into four classes, one of which corresponded to shrubs on the site. However, the shrub class also included shadows cast by the shrubs. We corrected for shadows by measuring the dimensions of individual canopies of ten ATCA and ten SAVE plants on the ground in 2007, then comparing the ground estimates of canopy area to those calculated for the same shrubs from the classified 2007 Quickbird image (Figure 2A). A linear equation was fit to the data for individual shrubs. However, as f_c increases, the effect of shadows cast on bare soil decreases, since shadows are an edge effect on clumped vegetation. To correct for shadows, the linear projection of fractional cover ($f_{clinear}$) in Figure 2A was multiplied by a correction factor (C):

$$C = 0.83 + 0.17 \text{ x } f_{clinear} \tag{4}$$

with

$$f_c = f_{clinear} \text{ x } C \tag{5}$$

As $f_{clinear}$ approaches 0, C approaches 0.83, the slope of the linear equation through the origin in Figure 2A, but as $f_{clinear}$ approaches 1.0, C approaches 1.0, because shadows will be cast within a full canopy. We tested the relationship between f_c estimated by Quickbird and ground estimates of f_c over wider areas within the site where individual canopy dimensions were measured (see **Results**).

Standing dry biomass was estimated from canopy area projected on the ground from a sample of 20 ATCA plants of varying sizes, for which canopy area and dry biomass were both determined (Figure 2B)(McKeon et al., 2005).

2.8 MODIS estimates of E_G and LAI

One of the goals of the research was to project how vegetation density and E_G change in response to factors such as rainfall, revegetation efforts, and grazing intensity over time. Satellite imagery can be used for this task, as phreatophyte ET is highly correlated with vegetation indices such as NDVI acquired during summer (Groeneveld and Baugh, 2007; Groeneveld et al., 2007). We used a method based on imagery from the MODIS sensor system on the Terra satellite to estimate foliage density and E_G over the site (Nagler et al., 2005). We used the Enhanced Vegetation Index (EVI) product, which estimates foliage density with a pixel resolution of 250 m (Huete et al., 2002, 2008). The data are pre-processed to correct for view angle and atmospheric effects, and only cloud-

free images are selected for each 16 day reporting period. EVI is calculated from the Blue, Red and Near Infrared bands as:

$$EVI = 2.5 \times (\delta NIR - \delta Red)/(1 + \delta NIR + (6 \times \delta Red - 7.5 \times \delta Blue) \quad (6)$$

where the coefficient "1" accounts for canopy background scattering and the Blue and Red and coefficients, 6 and 7.5, minimize residual aerosol variations. The EVI is one of the two VIs available from the MODIS sensors and it is widely used in phenological, productivity and evapotranspiration (ET) studies (e.g., Waring et al., 2006; Huete et al., 2002, 2008).

We calculated ET from EVI and maximum daily air temperature (T_a) using a modification of the algorithm developed by Nagler et al. (2005). This algorithm was developed by correlating EVI and T_a with ET measured over multiple years at nine moisture flux tower sites in western riparian corridors, and was further tested against sap flow results in a cottonwood planting (Nagler et al., 2007). We first converted EVI to scaled EVI (EVI*) which stretches the values between 0 (minimum EVI) and 1 (maximum EVI):

$$EVI^* = 1 - (EVI_{max} - EVI)/(EVI_{max} - EVI_{min}) \quad (7)$$

We used 0.542 and 0.091 for EVI_{max} and EVI_{min}, respectively. These values are those from the data set used to develop the predictive equation for ET in Nagler et al. (2005) and represent full vegetation cover and bare soil, respectively:

We then used EVI* and T_a values to calculate ET:

$$E_G \ (kg \ m^{-2} \ d^{-1}) = 11.5 \times (1 - \exp^{(-1.63 EVI^*)}) \times 0.883/(1 + \exp^{-(Ta - 27.9)/2.57}) \quad (8)$$

The expression containing EVI* is based on the formula for light extinction through a canopy (Monteith and Unsworth, 1990). The temperature term is in the form of a sigmoidal curve, where there is a minimum temperature due to the physiological status of the plants; a middle, exponential portion of the curve which fits the vapor pressure deficit:temperature response in the Penman-Moneith equation (Allen et al., 1998); and an upper limit, where physiological limitations to E also apply (Hultine et al., 2007). Hence, air temperature is a scalar from 0 to 1.0 that accounts for both atmospheric water demand and the physiological limitations on E, at the low and high end of the temperature scale (Nagler et al., 2005).

Equation (8) is identical to the one derived in Nagler et al. (2005) except that the original algorithm had a constant term representing minimum (bare soil) ET, which was 1.07 mm day^{-1} in the original study of riparian phreatophyte vegetation (Nagler et al., 2005). It was required because none of the tower-based values of ET reached zero even in winter or when EVI* approached 0, due to bare soil evaporation. However, in this study the sap flow sensors measured plant transpiration only, and bare soil evaporation is very low due to lack of surface moisture and scant rainfall, so we did not include the constant term in Equation (8).

We estimated LAI from EVI* by calibrating EVI* to f_c values determined on the 2007 Quickbird image. A mask was prepared for the area covered by each MODIS pixels that fell within the site (Figure 1), and the masks were overlain on the Quickbird image. Then f_c was determined for the area covered by each pixel and multiplied by 4.15 (the weighted mean LAPS) over the site determined by leaf harvesting of ATCA and SAVE) to give LAI of each pixel. EVI* values for each pixel were calculated as the mean value of July-August, 2007, EVI* values, concurrent with sap flux measurments. A regression equation through the origin gave an expression for LAI:

$$LAI = 3.21 \text{ x } EVI* \tag{9}$$

with $r^2 = 0.77$ (n = 55, P < 0.001).

2.9 Other methods and data sources

Daily meteorological data for 2007 were obtained as the mean values from three, on-site automated micrometeorological stations (Vista Engineering, Inc., Grand Junction, CO) operated by the U.S. Department of Energy (U.S. Department of Energy, 2006). The data was reported in hourly increments and included solar radiation (R_s, kW m^{-2}), air temperature (T, ^{o}C), the partial pressure of water vapor in the air (kPa), wind speed (m s^{-1}) and precipitation (mm). Vapor pressure deficit (D) was determined by subtracting vapor pressure measured at the micrometeorological stations from vapor pressure at saturation as a function of air temperature. Daily values of precipitation and maximum daily air temperature (T_{max}) from 2000-2007 were obtained from the NOAA station at Monument Valley, AZ, approximately 30 km from the site.

Leaf conductance estimated from sap flux measurements (G_S) was calculated as in Phillips and Oren (1998) from E_L, D and a conductance coefficient (K_G) based on atmospheric pressure:

$$G_S = (K_G \text{ x } E_L)/D \tag{10}.$$

K_G combines the density of air, the latent heat of vaporization, the specific heat of air at constant pressure, and the psychrometric constant into a single term corrected for temperature, based on a series of regression analyses (Phillips and Oren, 1998):

$$K_G \text{ (kPa)} = 115.8 + 0.4226T \tag{11}.$$

K_G ranged from 125-130 kPa in our study. Equation (10) is an approximation of G_S that applies when transpiration is strongly coupled to atmospheric conditions, and it assumes that D in the bulk air above the canopy is the driving force for E_L and that leaves are at the same temperature as the bulk air over the canopy (Ewers and Oren, 2000). These are appropriate assumptions for small-leaved shrubs with relatively open canopies and a constant supply of water as in the present study (Ewers and Oren, 2000). The term, E_L/D, is the ratio of stand water flux to vapor pressure deficit, and is an indicator of the

degree of stomatal opening at a given value of D (Monteith and Unsworth, 1990; Phillips and Oren, 1998; Ewers and Oren, 2000).

Statistical analyses included Analyses of Variance (ANOVA), Analysis of Co-variance (ANCOVA), and linear and non-linear regression carried out using Systat (Systat Software, Inc., Chicago, IL).

3. Results

3.1 Plant cover inside and outside the exclosure sites

Based on the ground survey, f_c by ATCA, SAVE and ATCO was 0.273 inside the South Exclosure plot and 0.065 in the adjacent control area outside the plot in November, 2007 (Table 1). However, inspection of the October, 2006 Quickbird image (the year the exclosure fence was erected) showed that this reflects pre-existing plant cover differences and was not due to fencing the site. Phreatophyte shrub cover was 0.106 and 0.089 inside and outside the North Exclsoure, and ATCA was the only phreatophyte species present. At both sites, annual forbs increased total plant cover by approximately 0.10, as this survey was taken at the end of the summer monsoon season when summer annuals were most abundant. By contrast, non-phreatophyte shrubs had f_c of 0.031 or lower. ATCA and SAVE plants ranged in height from 1-2 m inside and outside exclosures, whereas ATCO were < 0.5 m.

3.2 LAPS and E_L by sap flow sensors and correlation with meteorological variables

LAPS and mean daily E_L values were subjected to a 3-Way ANOVA in which Year (2006 or 2007), Plant Type (ATCA or SAVE), and Grazing Treatment (In or Out of exclosures) were the categorical variables. E_L and LAPS were lower in 2006 than 2007, but Plant Type and Grazing Treatment were not significant (P > 0.05)(Table 1). LAPS was high in both years, averaging 2.96 and 3.85 in 2006 and 2007 across species and treatments, respectively. LAPS in 2006 was determined late in the season when plants contained fruits, which lowered LAPS.   Although Plant Type was not significant in the ANOVA, E_L of SAVE tended to be higher ATCA across years and treatments (P = 0.057 by Tukey's test across treatments)(Figure 3).

On a daily time step, E_L of ATCA and SAVE were strongly correlated with D calculated over daylight hours (0700-1800 hrs), and less strongly correlated with T_{max} and total daily R_s (Figure 3, Table 3). Wind speed averaged 1.66 m s^{-1} (SE = 0.10) over the study and was only weakly correlated with E_L or other meteorological variables. As expected, T_{max} and D were strongly autocorrelated as were SAVE and ATCA E_L. ATCA and SAVE E_L were analyzed by ANCOVA against D; both species responded positively to D (P < 0.001), and SAVE had a steeper linear response to D than ATCA (P = 0.013). The relationship between E_L and D was best described by an exponential decay function (Figure 4).

On an hourly time step, E_L of SAVE and ATCA both closely tracked the daily radiation curve, whereas T and D peaked latter in the day (Figure 5, Table 4). However, G_S peaked at about 1000 hrs for both species and declined gradually for the remainder of the daylight period, then dropped sharply at sunset. G_S was moderately correlated with R_s (r = 0.62 and 0.50 for ATCA and SAVE, respectively, P < 0.01) but not with other meteorological variables.

Because the MODIS remote sensing method for E_G uses T_{max} as the only environmental variable and combines E across species due to the low resolution of the images, we tested the strength of this relationship, using a sigmoidal response of E_L to T_{max} for 2006 and 2007 sap flux data (Figure 6). Although the MODIS model of necessity is an oversimplification of the factors controlling E_L, a sigmoidal relationship between T_{max} and combined SAVE and ATCA E_L had a r^2 of 0.76, providing a reasonable approximation of E_L over a seasonal cycle.

3.3 Vegetation cover, LAI, standing biomass and E_G over the site

Table 5 gives f_c, LAI, standing biomass, and E_G for areas of interest at the site in 2007. Cover was generally low over most of the site (ca. 0.10) but was very high (0.75) inside a portion of the site that has been fenced since 1997 (Area 1). This area also had very high projected biomass, LAI, and E_G. Estimates of f_c in exclosure plots by Quickbird were reasonably close to those determined by ground survey (Table 5). Figure 7 shows LAI values projected from MODIS EVI* for selected areas from 2000 – 2007. LAI declined slightly from 2000 to 2003, then increased up to 2007, except for 2006, when LAI values were low. The trends generally fit informal observations we made of grazing pressure at the site, which was high from 2000 to 2003, and declined somewhat in subsequent years. Grazing pressure is not constant, because livestock are moved over the range from year to year to exploit fresh browse. Although the MODIS pixel encompassing Area 1 only covered part of the area and also included adjacent land outside the fence (see Figure 1), MODIS LAI showed a clear increasing trend for this pixel over time due to grazing exclusion. Figure 8 shows Area 1 before and after fencing, going from nearly bare in 1997 to 0.75 cover in 2007.

Estimates of E_G over the whole site by MODIS were in agreement with sap flux estimates in 2006 and 2007 (Figure 9). From 2000 – 2007, E_G by MODIS showed a gradually increasing trend over the site and ranged from 73 – 159 mm yr^{-1} (Table 6). Although E_G was approximately equal to site precipitation over all years, there was no significant relationship (P > 0.05) between E_G and precipitation on either on a 16-day or yearly time step, indicating that water from the aquifer was the main source of water for shrubs at this site.

4. Discussion

4.1 Meteorological controls on E_L

Although the diurnal curve of E_L closely tracked Rs, stomatal opening as indicated G_S actually peaked early in the day then decreased. Midday depression of G_S and photosynthesis is common in plants growing in bright, low humidity environments (Xu and Shen, 2005), and has been noted before for *Atriplex* spp. (das Neves et al., 2008) and SAVE (Donovan et al., 2003). Midday depression of photosynthesis is a complex phenomenon that is controlled by both internal (e.g. metabolic) and external (meteorological) factors (Xu and Shen, 2005). In the present research, peak G_S occurred well before D, T or R_s reached their daily peaks. E_L continued to increase into early afternoon even after G_S peaked due to increasing atmospheric water demand even though stomata presumably were partially closed.

On a daily time step, E_L was closely correlated with D, showing a high degree of coupling between ET and atmospheric water demand (the advective term in the Penman-Monteith equation)(Monteith and Unsworth, 1990). Similar to other studies (e.g., Hultine et al., 2007), the response of E_L to D followed an exponential decay function, and SAVE responded more steeply to D and tended to have higher EL than ATCA. SAVE is a deciduous shrub that develops new leaves in spring and maximizes growth through the summer, whereas ATCA is evergreen and spreads growth and water uptake over a longer annual cycle than SAVE. Similar to the present results, Steinwand et al. (2001) reported a one-third higher rate of transpiration as a function of LAI for SAVE compared to *A. lentiformis* in Owens Valley, California, U.S.

4.2 Comparison to other studies

Table 8 compares the present results with other studies in which SAVE was a dominant or co-dominant shrub in western U.S. phreatophyte communities. In general, range of values among studies overlap for E_L, G_S, LAI, f_c and standing biomass. The range of values are wide, as expected, due to the different biological, edaphic and climatic factors affecting plant growth both within and among sites. Although rates of E_G tend to be moderate (1.5-3.0 mm d^{-1}) due to low f_c, and LAI, under favorable conditions phreatophyte communities can extract 5-7 mm d^{-1} of water from the aquifer, rates that approach potential ET rates for a grass reference crop (Allen et al., 1998). The Monument Valley plants were remarkable for their high LAPS values (ca. 4.0) compared to other sites, where LAPS ranged from < 0.5 to 2.7. This was due to their greater height (1-2 m) compared to other locations, where plant heights were generally 0.3-1 m (e.g**.,** Driese and Reiners, 1997).

Early studies (e.g. Nichols, 1994) emphasized depth to water table as a controlling factor in phreatophyte E_G. However, Cooper et al. (2006) and Steinwand et al. (2006) found that the relationship between E_G and depth to water was only moderately strong, and it can be mitigated by other factors such as soil type affecting hydraulic conductivity (e.g., Hultine et al., 2006). Depth to water was greater at Monument Valley (> 6 m) than

in the other studies in Table 8 (1-3 m), but we still recorded high rates of E_L and high LAPS. The aquifer at Monument Valley is in sand that supports high hydraulic conductivity (United States Department of Energy, 1999), leading to high rates of water extraction by the shrub community.

4.3 Quickbird and MODIS satellite images to project f_c, LAI and E_G over large areas

Desert phreatophyte communities lend themselves to remote sensing analyses for several reasons. Shrubs tend to grow in relatively sparse stands in which f_c can be estimated by high-resolution satellite imagery, as by Quickbird images in the present study. When LAI is under 4.0, plant communities exhibit a linear response of E_G to LAI (Kelliher et al., 1995; Granier et al., 1999), hence LAI estimated by a vegetation index can be calibrated to estimate seasonal E_G for phreatophyte communities (Groeneveld et al., 2007). In our study, E_G was linear with LAIs ranging from 0.32 to 1.32 over the four stations where sap flow was measured ($r^2 = 0.99$, $P < 0.01$). Furthermore, arid-zone phreatophytes derive most of their water from the aquifer and the surface soil is normally dry, so transpiration dominates ET (Scott et al., 2006), producing a high correlation between vegetation indices and ET (Groeneveld et al., 2007, Nagler et al., 2005).

In the present study, we used a simple empirical relationship between EVI, T_{max} and ET measured at flux towers for riparian phreatophytes to scale E_G. A more desirable approach would be to use underlying ecophysiological principles to account for E at different levels of organization (Waring, 1993). The Penman-Monteith equation provides a complete model for ET (Allen et al., 1998). An impediment to applying the Penman-Monteith equation is uncertainty about the roughness lengths for sparse shrub communities, which determine turbulent transfer coefficients. Driese and Reiners (1997) found roughness lengths for a sparse shrub community in Wyoming ranging from 0.01 to 0.07 m, lower than used in models, and with no strong relationship to either shrub height or density that could support scaling by remote sensing. However, vegetation in our study tended to be taller than at their site, and the average wind speed and high local turbulence associated with low LAI values and bare soil should create low aerodynamic resistance. The low correlation between E_L and windspeed suggests that atmospheric resistance is not a limiting factor for E_L at our site. Hence, at our site the components of the Penman-Monteith equation that exercised the greatest control on E_L were bulk atmospheric water demand (D), and apparent partial stomatal closure during midday (G_S).

Steinwand et al. (2001) and Groeneveld et al. (2007) successfully used the Penman-Monteith equation to project phreatophyte E_G based on crop coefficients relating phreatophyte E_G to potential ET by a grass reference crop. Although Mata-Gonzalez et al. (2005) criticized this approach as inappropriate for desert vegetation, Groeneveld et al. (2007) showed that the ratio of actual ET measured at flux towers to potential ET of a reference crop was highly correlated with satellite NDVI values over three different phreatophyte communities and could form the basis of a remote sensing method for phreatophyte ET.

Our simplified method for projecting E_G by MODIS EVI produced reasonable agreement with sap flux results at two sample intervals, but a more rigorous test against long-term flux tower measurements of ET would be desirable. Although D exercised the most important control on E_L at daily time steps, T_{max} could be used as a proxy for D due to their autocorrelation. T_{max} can be obtained from thermal bands on satellite images (Glenn et al., 2007), or from the vast array of weather reporting stations in the U.S. and the world.

4.3 Wide area E_G estimates and effects of grazing control

E_G was low over the whole site due to low overall plant cover (ca. 0.10), similar to the plant cover in North Exclosure. However, some areas, such as the South Exclosure plot over the hot spot of the plume, had high plant cover (0.34) and high projected E_G compared to the whole site. Protecting vegetation from grazing did not increase rates of E_L, and over the two years that the exclosures have been in place, plant cover has not yet significantly increased. However, over longer time periods, grazing control had a marked effect on vegetation cover (McKeon et al., 2006). The area inside the site fence that had been protected from grazing for ten years developed 0.75 plant cover compared to just 0.15 for plants just over the fence line, and had a projected midsummer E_G of 13 mm d^{-1}. However, this rate was projected from sap flux measurements made in sparser stands, and it is likely that self-shading reduced the actual E_G achieved in this dense stand. Furthermore, we do not now if the increase in cover achieved over this small portion of the site can be projected over the whole site. At the UMTRA site in Tuba City, AZ, exclusion of livestock for ten years resulted in an increase in cover from 0.11 to 0.24 (Lash et al., 1999), and similar results were reported along a fence line contrast at the Monument Valley National Monument close to the present site (Brotherson et al., 1983). Hence, over the sparse-cover area of the plume, an approximate doubling of shrub cover and ET is a realistic estimate of what can be achieved by control of grazing.

At present, E_G is approximately equal to precipitation over the plume, presumably controlling local recharge, but the volume of the plume has been increasing at a rate of 50,000 m^3 yr^{-1}, providing an estimate of the rate of recharge from other water sources (Jordan et al., 2008). Over 130 ha, this volume is equivalent to a water depth of 38 mm yr^{-1} (24% of the 2007 transpiration rate). Hence, an increase in E_G by this amount should arrest the movement of the plume, and further E_G increases would be expected to shrink the volume of the plume. The present study shows that these goals are well within the capacity of the phreatophyte community if it were protected from grazing. The water balance at present is tipped slightly in favor of recharge, but could, in theory, be tipped towards discharge even if only part of the plume area was protected from grazing.

4.4 Wider relevance of the findings

Like arid and semiarid rangelands throughout the subtropics (Dregne, 1986), the Navajoan Desert has been extensively altered by over grazing, starting in the 1830s and continuing to the present (McFadden and McAuliffe, 1997; Savage, 1991). Some studies

have concluded that the vegetation changes have resulted in hydrological and geomorphological changes in the landscape over the past 200 years (reviewed in Graf, 1987), but other studies have emphasized the role of climate shifts in producing these changes (e.g., McFadden and McAuliffe, 1997). The present study and previous work at this site show that even small shifts in vegetation cover can potentially impact the site water balance, tipping the balance from extraction to recharge depending on the status of the vegetation.

The nitrate in the alluvial aquifer in this study was of human origin, but southwestern U.S. soils and aquifers can have naturally high levels of nitrates as well (Walvoord et al., 2003). Land use practices such as conversion of grasslands to shrublands, or reduction in overall plant cover, could mobilize these stored nitrates to enter aquifers and drainages where they can conceivably present an environmental hazard to wildlife and humans. Phreatophyte shrub communities can play an important role in controlling the mobility of nitrates in the environment.

References

Allen, R., Pereira, L., Rais, D., Smith, M. 1998. *Crop evapotranspiration – Guidelines for computing crop water requirements – FAO irrigation and drainage paper 56*. Food and Agriculture Organization of the United Nations, Rome.

Anderson, M.   2004. Sarcobatus vermiculatus. In: *Fire Effects Information System*, [Online]. U.S. Department of Agriculture, Forest Service, Rocky Mountain Research Station, Fire Sciences Laboratory (Producer). Available: http://www.fs.fed.us/database/feis/.

Brotherson, J., Rushforth, S., Johansen, J. 1983. Effects of long-term grazing on cryptogam crust cover in Navajo National Monument, Arizona. *Journal of Range Management* **36**, 579-581.

Cooper, D., Sanderson, J., Stannard, D., Groeneveld, D. 2006. Effects of long-term water table drawdown on evapotranspiration and vegetation in an arid region phreatophyte community. *Journal of Hydrology* **325**, 21-34.

das Neves, J., Ferreira, L., Vaz, M., Gazarini, L. 2008. Gas exchange in the salt marsh species *Atriplex portulacoides* L. and Limoniastrum monopetalum L. in southern Portugal. *Acta Physiologiae Plantarum* **30**, 91-97.

Donovan, L., Richards, J., Linton, M. 2003. Magnitude and mechanisms of disequilibrium between predawn plant and soil water potentials. *Ecology* **84**, 463-470.

Dregne, H. E. 1986. Desertification of arid lands. In *Physics of desertification,* ed. F. El-Baz and M. H. A. Hassan. Dordrecht, The Netherlands: Martinus, Nijhoff.

Driese, K., Reiners, W. 1997. Aerodynamic roughness parameters for semi-arid natural shrub communities of Wyoming, USA. *Agricultural and Forest Meteorology* **88**, 1-14.

Ewers, B., Oren, R. 2000. Analyses of assumptions and errors in the calculation of stomatal conductance from sap flux measurements. *Tree Physiology* **20**, 579-589.

Glenn, E., Huete, A., Nagler, P., Hirschboeck, K., Brown, P. 2007. Integrating remote sensing and ground methods to estimate evapotranspiration. *Critical Reviews in Plant Sciences* **26**, 139-168.

Graf, F. 1987. Geomorphological research in the Colorado Plateau. In: Graf, W. (ed.), *Geomorphic systems of North America: The decade of North American geography*, Geological Society of America, Centennial Special Issue, Volume 2, pp. 259-265.

Granier, A., Breda, N., Biron, P., Villete, S. 1999. A lumped water balance model to evaluate duration and intensity of drought constraints in forest stands. *Ecological Modelling* **116**, 269-283.

Grime, V., Sinclair, F. 1999. Sources of error in stem heat balance sap flow measurements. *Agricultural and Forest Meteorology* **94**, 103-121.

Groeneveld, D., Baugh, W. 2007. Correcting satellite data to detect vegetation signal for eco-hydrologic analyses. *Journal of Hydrology* **344**, 135-145.

Groeneveld, D., Baugh, W., Sanderson, S., Cooper, D. 2007. Annual groundwater evapotranspiration mapped from single satellite scenes. *Journal of Hydrology* **344**, 146-155.

Groeveveld, D., Warren, D. 1992. Total transpiration from land areas estimated from hand-held porometer measurements. In: D. Wilson, R. Reginato and K. Hollett (eds.), *Evapotranspiration Measurements of Native Vegetation, Owens Valley, California, June 1986*. U.S. Geological Survey Water-Resources Investigations Report 91-4159, Sacrament, CA, pp. 49-59.

Huete, A., Didan, K., van Leeuwen, W., Miura, T., Glenn, E. 2008. MODIS vegetation indices. In: *Land Remote Sensing and Global Environmental Change: NASA's Earth Observing System and the Science of ASTER and MODIS* (in press).

Huete, A., Didan, K., Miura, T., Rodriquez, E., Gao, X., Ferreira, L. 2002. Overview of the radiometric and biophysical performance of the MODIS vegetation indices. *Remote Sensing of Environment* **83**, 195-213.

Hultine, K., Bush, S., West, A., Ehleringer, J. 2007. Effect of gender on sap-flux-scaled transpiration in a dominant riparian tree species: Box elder (Acer negundo). *Journal of Geophysical Research* **112**, G03S06, doi:10.1029/2006JG00232.

Hultine, K., Koepke, D., Pockman, W., Fravolini, A., Sperry, J., Williams, D. 2006. Influence of soil texture on hydraulic properties and water relations of a dominant warm-desert phreatophyte. *Tree Physiology* **26**, 313-323.

Huxman, T., Wilcox, B., Breshears, D., Scott, R., Snyder, K., Small, E., Hultine, K., Pockman, W., Jackson, R. 2005. Ecohydrological implications of woody plant encroachment. *Ecology* **86**, 308-319.

Jordan, F., Waugh, J., Glenn, E., Sam, L., Tompson, T., Tompson, T.L. 2008. Natural bioremediation of a nitrate-contaminated soil-and-aquifer system in a desert environment. *Journal of Arid Environments* (in press).

Kelliher, F., Leuning, M., Raupauch, R., Schultze, E. 1995. Maximum conductances for evaporation from global vegetation types. *Agricultural and Forest Meteorology* **73**, 1-16.

Kjelgaard, J., Stockle, C., Black, R., Campbell, G. 1997. Measuring sap flow with the heat balance approach using constant and variable heat inputs. *Agricultural and Forest Meteorology* **85**, 239-250.

Lash, D., Glenn, E., Waugh, J., Baumgartner, D. 1999. Effects of grazing exclusion and reseeding on a former uranium mill site in the Great Basin desert, Arizona. *Arid Soil Research and Rehabilitation* **13**, 253-264.

Lin, G., Phillips, S., Ehleringer, J. 1996. Monsoonal precipitation responses of shrubs in a cold desert community on the Colorado Plateau. *Oecologia* **106**, 8-17.

Mata-Gonzalez, R., McClendon, T. Martin, D. 2005. The inappropriate use of transpiration coefficients (Kc) to estimate evapotranspiration in arid ecosystems: A review. *Arid Land Research and Management* **19**, 285-295.

McFadden, L., McAuliffe, J. 1997. Lithologically influenced geomorphic responses to Holocene climatic changes in the Southern Colorado Plateau, Arizona: A soil-geomorphic perspective. *Geomorphology* **19**, 303-332.

McKeon, C., Glenn, E., Waugh, W., Eastoe, C., Jordan, F., Nelson, S. 2006. Growth and water and nitrate uptake patterns of grazed and ungrazed desert shrubs growing over a nitrate contamination plume. *Journal of Arid Environments* **64**, 1-21.

McKeon, C., Jordan, F., Glenn, E., Waugh, W., Nelson, S. 2005. Rapid nitrate loss from a contaminated desert soil. *Journal of Arid Environments* **61**, 119-136.

Monteith, J., Unsworth, M. 1990. Principles *of Environmental Physics, 2nd. Edition.* Edward Arnold, London.

Nagler, P., Glenn, E., Thompson, T. 2003. Comparison of transpiration rates among saltcedar, cottonwood and willow trees by sap flow and canopy temperature methods. *Agricultural and Forest Meteorology* **116**, 73-89.

Nagler, P., Glenn, E., Thompson, T., Huete, A. 2004. Leaf area index and Normalized Difference Vegetation Index as predictors of canopy characteristics and light interception by riparian species on the Lower Colorado River. *Agricultural and Forest Meteorology* **116**, 103-112.

Nagler, P., A. Jetton, J. Fleming, K. Didan, E. Glenn, J. Erker, K. Morino, J. Milliken, Gloss, S. 2007. Evapotranspiration in a cottonwood (Populus fremontii) restoration plantation estimated by sap flow and remote sensing methods. *Agricultural and Forest Meteorology* **144**, 95-110.

Nagler, P., R. Scott, C. Westenburg, J. Cleverly, E. Glenn, Huete, A. 2005. Evapotranspiration on western U.S. rivers estimated using the Enhanced Vegetation Index from MODIS and data from eddy covariance and Bowen ratio flux towers. *Remote Sensing of Environment* **97**, 337-351.

Naumberg, E., Mata-gonzalez, R., Hunter, R., Mclendon, T., Martin, D. 2005. Phreatophytic vegetation and groundwater fluctuations: A review of current research and application of ecosystem response modeling with an emphasis on Great Basin vegetation. *Environmental Management* **35**, 727-740.

Nichols, W. 1993. Estimating discharge of shallow groundwater by transpiration by greasewood in the northern Great Basin. *Water Resources Research* **29**, 2771-2778.

Nichols, W. 1994. Groundwater discharge by phreatophyte shrubs in the Great Basin as related to depth to groundwater. *Water Resources Research* **30**, 3265-3274.

Nichols, W. 2000. Regional ground-water evapotranspiration and ground-water budgets, Great Basin, Nevada. *U.S. Geological Survey Professional Paper 1628*, 82 pp.

Phillips, N., Oren, R. 1998. A comparison of daily representations of canopy conductance based on two conditional time-averaging methods and the dependence of daily conductance on environmental factors. *Annales des Sciences Forestieres* **55**, 217-235.

Romo, J., Haferkamp, M. 1989. Water relations of Artemisia tridentate ssp. Wyomingensis and Sarcobatus vermiculaus in the steppe of southeastern Oregon. *American Midland Naturalist* **121**, 155-164.

Savage, M. 1991. Structural dynamics of a southwestern pine forest under chronic human influence. *Annals of the Association of American Geographers* **81**, 271-289.

Scott R., Huxman, T., Cable, W., Emmerich, W. 2006. Partitioning of evapotranspiration and its relation to carbon dioxide exchange in a Chihuahuan Desert shrubland. *Hydrological Processes* 20 , 3227-3243.

Shreve, F. 1942. The desert vegetation of North America. *Botanical Review* **7**, 195-246.

Sperry, J., Hacke, U. 2002. Desert shrub water relations with respect to soil characteristics and plant functional types. *Functional Ecology* 16, 367-378.

Steinwand, A., Harrington, R., Groeneveld, D. 2001. Transpiration coefficients for three Great Basin shrubs. *Journal of Arid Environments* **49**, 555-567.

Steinwand, A., Harrington, R., Or, D. 2006. Water balance for Great Basin phreatophytes derived from eddy covariance, soil water, and water table measurements. *Journal of Hydrology* **329**, 595-605.

United States Department of Energy. 1999. *Final Site Observational Work Plan for the UMTRA Project Site at Monument Valley, Arizona, Volume I*, MAC-GWMON 1.1. U.S. United States Department of Energy Department of Energy, Grand Junction Office, Grand Junction, CO.

United States Department of Energy. 2000. *Evaluation of Active Remediation Alternatives for the Monument Valley, Arizona, UMTRA Project Site*. MAC-GWMON 10.6, US Department of Energy, Grand Junction Office, Grand Junction, CO.

United States Department of Energy. 2004. *Monument Valley Ground Water Remediation: Pilot Study Work Plan*. DOE-LM/GJ757-2004, Office of Legacy Management, U.S. Department of Energy, Grand Junction, CO.

United States Department of Energy. 2006. *Soil and Ground Water Phytoremediation Pilot Studies at Monument Valley, Arizona: 2005 Status Report*. DOE-LM/1254-2006, Office of Legacy Management, U.S. Department of Energy, Grand Junction, CO.

Walvoord, M., Phillips, F., Stonestrom, D., Evans, R., Hartsough, P., Newman, B., Striegl, R. 2003. A reservoir of nitrate beneath desert soils. *Science* **302**, 1021-1024.

Waring, R. 1993. How ecophysiologists can help scale from leaves to landscapes. In: J. Ehleringer and C. Field (eds.), *Scaling Physiological Processes: Leaf to Globe*, Academic Press, Inc., San Diego, CA, pp. 159-166.

Waring, R., Milner, K., Jolly, W., Phillips, L., McWethy, D. 2006. Assesment of site index and forest growth capacity across Pacific and Inland Norwest USA with a MODIS satellite-derived vegetation index. *Forest Ecology and Management* **228**, 285-291.

Wilcox, B., and Thurow, T. 2006. Emerging issues in rangeland ecohydrology: vegetation change and the water cycle. *Rangeland Ecology and Management* **59**, 220-224.

Xu, D., Shen, Y. 2005. External and internal factors responsible for midday depression of photosynthesis. In: M. Pessarakli (ed.), *Handbook of Photosynthesis, Second Edition*, Taylor & Francis, Boca Raton, pp. 297-298.

Table 1. Fractional cover of plants, litter, and bare soil inside and outside livestock exclosure plots where sap flow measurements were made at the Monument Valley UMTRA site, November, 2007.

Cover Type	SOUTH Inside	NORTH Inside	SOUTH Outside	NORTH Outside
Phreatophyte shrubs				
Atriplex canescens	0.163	0.106	0.016	0.089
Atriplex confertifolia	0.006	-	0.008	-
Sarcobatus vermiculatus	0.104	-	0.041	-
Total phreatophyte shrubs	0.273	0.106	0.065	0.089
Non-phreatophyte shrubs				
Ephedra torreyana	-	0.013	-	-
Ephedra viridis	-	0.002	-	-
Gutierrezia sarothrae	0.003	-	0.009	-
Poliomintha incana	-	0.007	-	0.004
Vanclevea stylosa	-	0.003	-	0.021
Yucca angustifolia	-	-	-	0.006
Total non-phreatophyte shrubs	0.003	0.025	0.009	0.031
Forbs				
Ambrosia acanthicarpa	-	0.009	-	-
Chamaesyce maculate	-	0.005	-	-
Descurainia sophia	0.016	0.034	0.028	0.022
Machaeranthera **sp.**	-	0.001	-	-
Mentzelia multiflora	0.1	0.2	0.1	0.2
Salsola tragus	0.092	0.036	0.066	0.057
Suaeda torreyana	-	-	0.023	-
Total forbs	0.109	0.087	0.118	0.081
Plant litter	0.156	0.152	0.121	0.128
Bare ground	0.459	0.631	0.687	0.670
Total vegetative cover	**0.385**	**0.217**	**0.192**	**0.202**

Table 2. Summary of plant leaf area index (LAPS) and leaf-level transpiration (E_L) at the Monument Valley UMTRA site, 2006 – 2007, showing means and standard errors in parentheses. ATCA = *Atriplex canescens* (fourwing saltbush); SAVE = *Sarcobatus vermiculatus* (black greasewood).

	LAPS 2006	LAPS 2007	E_L 2006 (kg m^{-2} d^{-1})	E_L 2007 (kg m^{-2} d^{-1})
ATCA				
In	2.96 (0.45)	3.78 (0.68)	1.66 (0.04)	2.95 (0.34)
Out	3.19 (0.36)	4.47 (0.46)	2.81 (0.09)	4.38 (1.26)
SAVE				
In	3.71 (0.50)	3.98 (0.45)	3.06 (0.52)	6.72 (1.65)
Out	2.05 (0.20)	4.45 (0.57)	3.07 (0.95)	4.42 (1.25)

Table 3 . Analysis of Variance (ANOVA) of plant leaf area index (LAPS) and leaf-level transpiration (E_L) at the Monument Valley UMTRA site, 2006-2007. Mean daily sensor values over each measurement period were subjected to a three-way ANOVA in which Year (2006 or 2007), Plant (*Atriplex canescens* or *Sarcobatus vermiculatus*), and In or Out of the exclosure fences were categorical variables. None of the interaction terms were significant at $P < 0.05$.

	LAI			E_L		
	F	**P**	**df**	**F**	**P**	**df**
Year	6.58	0.013	55	5.88	0.024	22
Plant	1.20	0.279	55	2.85	0.105	22
In/Out	1.30	0.259	55	0.01	0.929	22

Table 4. Correlation coefficients between hourly leaf-level transpiration rates of *Atriplex canescens* (ATCA) and *Sarcobatus vermiculatus* (SAVE) plants and meteorological variables at the Monument Valley UMTRA site, July 8-August 15, 2007. Asterisks denote significant correlations at $P < 0.05$ (*), $P < 0.01$ (**) or $P < 0.001$(***).

	ATCA	SAVE	D	Temp	Rad	Wind
ATCA	1.00	0.99***	0.749***	0.56**	0.94***	-0.145
SAVE		1.00	0.67***	0.45*	0.91***	-0.160
D			1.00	0.96***	0.84***	-0.103
Temp				1.00	0.68***	-0.183
Rad					1.00	-0.106
Wind						1.00

Table 5. Correlation coefficients between hourly leaf-level transpiration rates of *Atriplex canescens* (ATCA) and *Sarcobatus vermiculatus* (SAVE) plants and meteorological variables at the Monument Valley UMTRA site, July 8-August 15, 2007. Asterisks denote significant correlations at $P < 0.05$ (*), $P < 0.01$ (**) or $P < 0.001$ (***).

	ATCA	SAVE	D	Tmax	Rad
ATCA	1.00	0.76***	0.78***	0.62***	0.40*
SAVE		1.00	0.77***	0.65***	0.47**
D			1.00	0.92***	0.59*
Tmax				1.00	0.65**
Rad					1.00

Table 6. Site shrub fractional cover, LAI, biomass, and projected transpiration rates (E_G) over selected areas of the Monument Valley UMTRA site from July 8 to August 15, 2007. Cover was determined by Quickbird imagery and LAI by cover times leaf area of individual plants. E_G was calculated from sap flux estimates for SAVE and ATCA projected over each area of interest, using values of ATCA for ATCO. The proportion of ATCA, SAVE and ATCO in each area was from ground surveys reported in McKeon et al. (2006) or from the present study (areas in Table 1). Biomass was determined by an allometric relationship between cover and dry weight of shrubs. For the North and South Exclosure Plots, fractional cover determined by ground surveys is also given in parenthesis. Sites correspond to areas of interest illustrated in Figure 1.

Site	Area (ha)	Fractional Cover	LAI	Biomass (kg ha^{-1})	Shrubs Ratio (ATCA:SAVE:ATCO)			E_G (mm d^{-1})
1	1.15	0.749	2.88	10,411	1	0.9	0.00	13.1
2	1.57	0.152	0.58	2113	1	8.6	0.80	2.90
3	21.45	0.136	0.52	1890	1	1.2	0.12	2.40
4	182.4	0.094	0.36	1302	1	0.00	0.10	1.42
SE IN	0.26	0.344 (0.273)	1.32 (1.05)	4782	1	0.64	0.04	5.72
SE OUT	0.26	0.101 (0.065)	0.39 (0.25)	1404	1	2.56	0.5	1.84
NE IN	0.26	0.095 (0.106)	0.37 (0.41)	1315	1	0.00	0.00	1.44
NE OUT	0.26	0.082 (0.089)	0.32 (0.34)	1140	1	0.00	0.00	1.84
Whole Site	**318**	**0.0964**	**0.37**	**1340**	**1**	**0.20**	**0.10**	**1.54**

Table 7. Annual precipitation and pheatophyte transpiration (E_G) at the Monument Valley UMTRA site, 2000 – 2007. E_G was estimated by the MODIS EVI – T_a method.

Year	Precipitation (mm yr^{-1})	E_G (mm yr^{-1})
2000	109	123
2001	117	96
2002	140	73
2003	60	125
2004	74	89
2005	172	163
2006	89	103
2007	117	159
Mean (SE)*	110 (12.7)	116 (11.4)

*Means not significantly different at $P = 0.05$ by Paired t-Test.

Table 8. Comparison of the present results with other studies in which *Sarcobatus vermicultatus* was a dominant or co-dominant species in western U.S. phreatophyte communties. Values are the range across phreatophyte shrub species at each site. E_L and G_S are peak diurnal values in mmol m^{-2} s^{-1}; E_G are mean daily values in mm d^{-1}; and standing dry biomass is in kg ha^{-1}.

Study	E_L	G_S	E_G	LAI	LAPS	f_c	Biomass	Location
This study	5.0-7.8	215-395	1.4-5.7	0.33-1.54	3.98-4.47	0.082-0.344	1140-4782	Monument Valley, Arizona
Sperry and Hacke (2002)	-	-	-	-	-	-	-	Skull Valley, Utah
Driese and Reiners (1997)	-	-	-	0.02-0.06	0.27-0.46	0.076-0.349	317-7706	Great Divide Basin, Wyoming
Romo and Haferkamp (1989)	1.7-5.6	89-178	0.86-2.88	-	-	-	-	Southeast Oregon
Groeneveld and Warren (1992)	3.4-10.2	169-335	1.48-7.20	0.57-0.70	0.99-2.70	0.292-0.337	-	Owens Valley, California
Cooper et al. (2006)	-	-	0.9-2.2	-	-	-	-	San Luis Valley, Colorado

Figure Captions

Figure 1. Satellite images used in determining ET and fractional cover, and areas of interest at the Monument Valley UMTRA site. Top – location of MODIS pixels superimposed on a 2007, panchromatic Quickbird image, showing the extent of the contamination plume in black and the fenced source area in red. Bottom - Quickbird image classified to show shrubs cover as black pixels. Areas of interest in the study were: (Site 1) an area of volunteer plants (mainly *Atriplex canescens*)(ATCA) inside the site fence; (Site 2) a portion of the natural plant stand (mixed A. canescens and *Sarcobatus vermiculatus*)(SAVE) just outside the site fence to compare with (Site 1); (Site 3) the full extent of the naturally dense plant stand over the hot spot area of the contamination plume north of the fenced area; (Site 4) a large area of sparse cover (mainly ATCA) over the whole plume; (Site 5) the South Exclosure plot (mixed ATCA and SAVE); (Site 6) the North Exclusion plot (mainly ATCA); (Site 7) an irrigated planting (only partly shown).

Figure 2. Relationships between shrub cover determined on a classified Quickbird image and ground measurement (A), and between canopy area projected on the ground and dry biomass (B) for shrubs at the Monument Valley UMTRA site.

Figure 3. (A) Mean daily values of transpiration (E_L) for ATCA (closed circles) and SAVE in (DOY 251-261) and 2007 (DOY 189-227) at the Monument Valley UMTRA site. Bars show standard errors of means. (B) Mean daily values of vapor pressure deficit (D)(closed circles), maximum daily temperature (T_{max})(open circles), and daily radiation (Rad)(closed triangles). Only temperature data was available in 2006.

Figure 4. Relationship between vapor pressure deficit (D) and mean daily values of transpiration (E_L) of ATCA (closed circles) and SAVE (open circles) at the Monument Valley UMTRA site. D was determined for daylight hours (5 am to 8 pm).

Figure 5. (A) Daily time course of vapor pressure deficit (D)(open circles), air temperature (T)(closed circles) and radiation (open squares) during the period of sap flux data collection at the Monument Valley UMTRA site from July 9 to August 15, 2007. (B) Daily time course of transpiration (E_L) of *Atriplex canescens* (ATCA)(closed circles) and *Sarcobatus vermiculatus*)SAVE)(open circles). (C) Daily time course of leaf conductance (G_S) of ATCA (closed circles) and SAVE (open circles). Error bars are standard errors of hourly measurements.

Figure 6. Relationship between pooled mean daily transpiration rates (E_L) of *Atriplex canescens* and *Sacrobatus vermiculatus* and maximum daily air temperature at the Monument Valley UMTRA site during sap flux measurement periods in 2006 and 2007.

Figure 7. Leaf area index (LAI) values estimated by the Enhanced Vegetation Index from MODIS satellite sensors for selected area at the Monument Valley UMTRA site from 2000 – 2007, showing 16-day composite values of LAI over time. See Figure 1 for pixel locations.

Figure 8. Contrast between shrub density in 1997 and 2007 at the Monument Valley UMTRA site. The line shows the location of the fence enclosing the former mill site. (A) shows the growth of volunteer plants inside the fence and B shows an irrigated planting over a portion of the source area of contamination at the site.

Figure 9. Evapotranspiration at the Monument Valley UMTRA site estimated by the MODIS EVI – T_a method (open circles), by sap flow measurements (large closed circles with standard error bars), and by the relationship between sap flow results and daily maximum temperature projected over the sap flow measurement period in 2006 – 2007 (small closed circles).
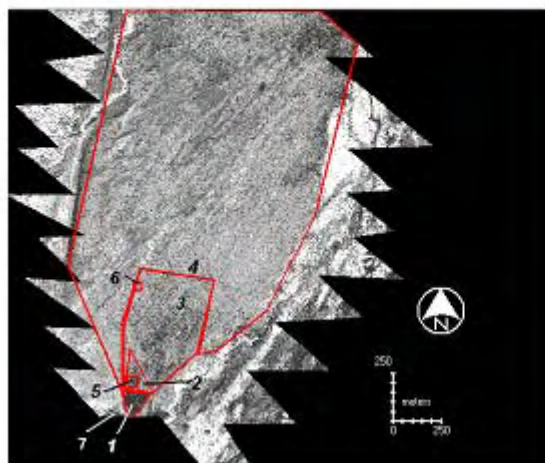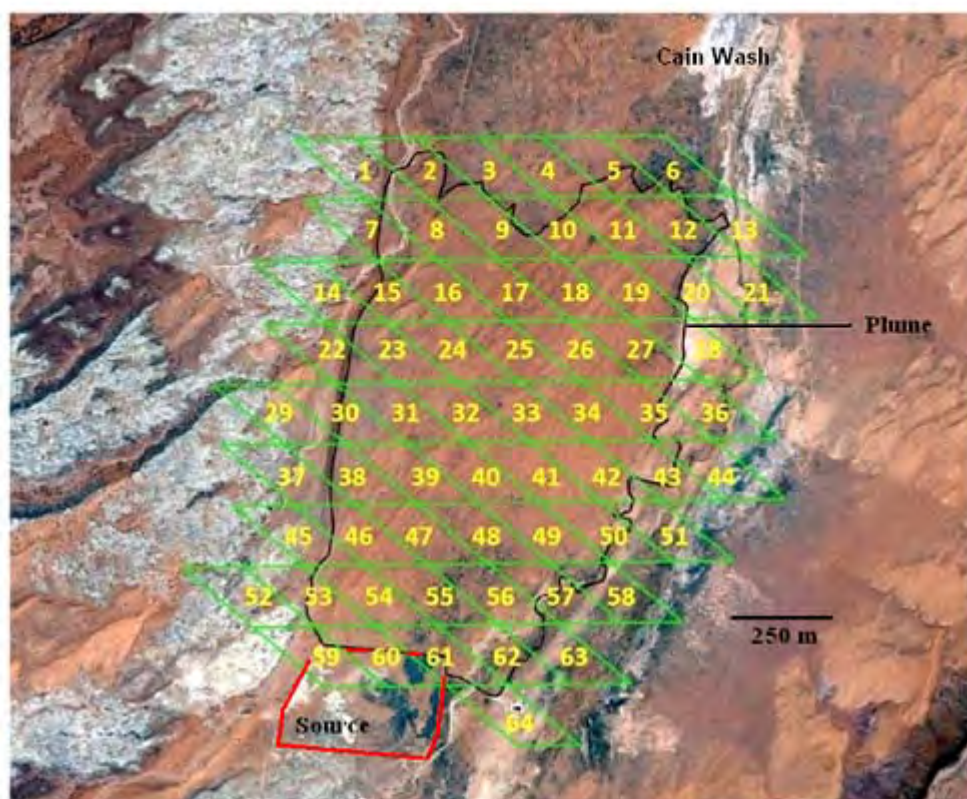
Figure 1

Figure 2.

Figure 3.

$y = 3.71(1-e^{-0.623x})$
$r^2 = 0.58$

$y = 4.46(1-e^{-0.623x})$
$r^2 = 0.60$

E_L (kg m^{-2} d^{-1})

D (kPa)
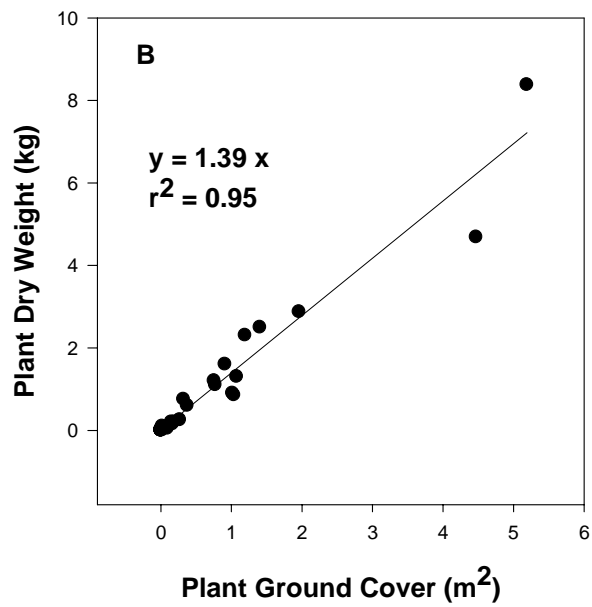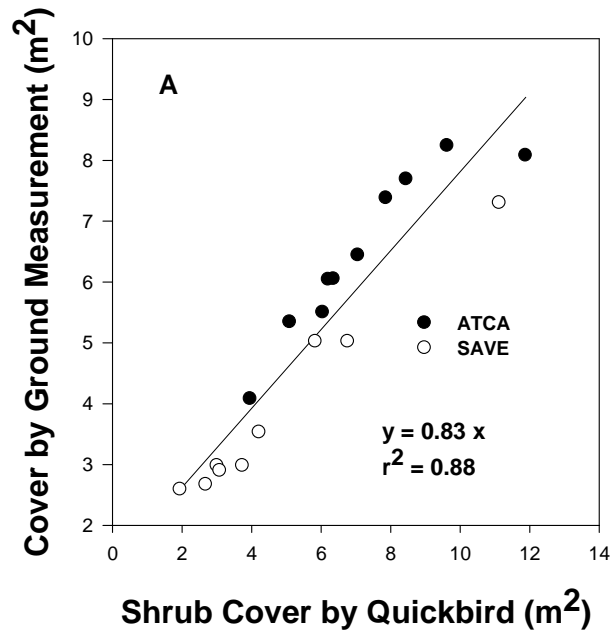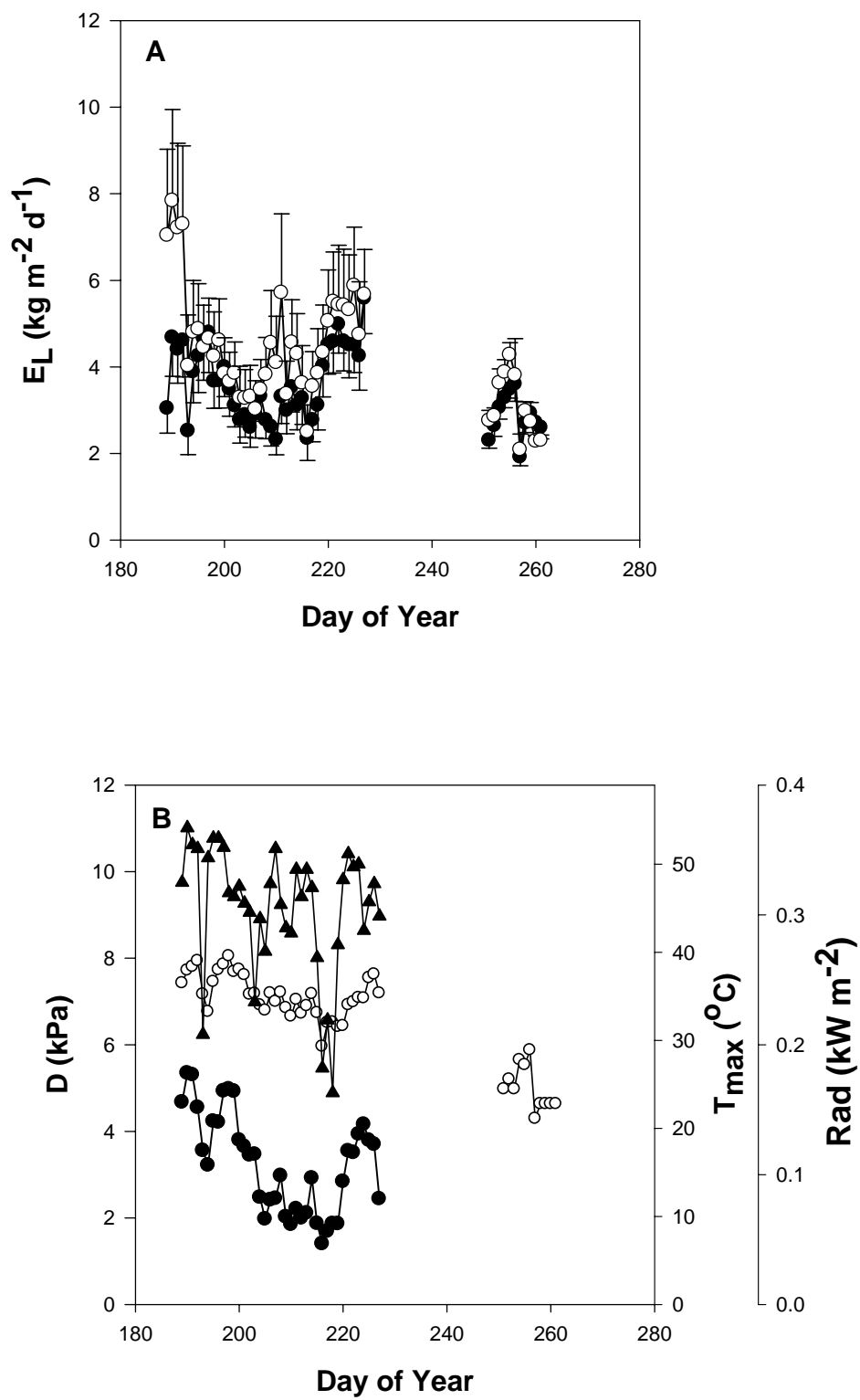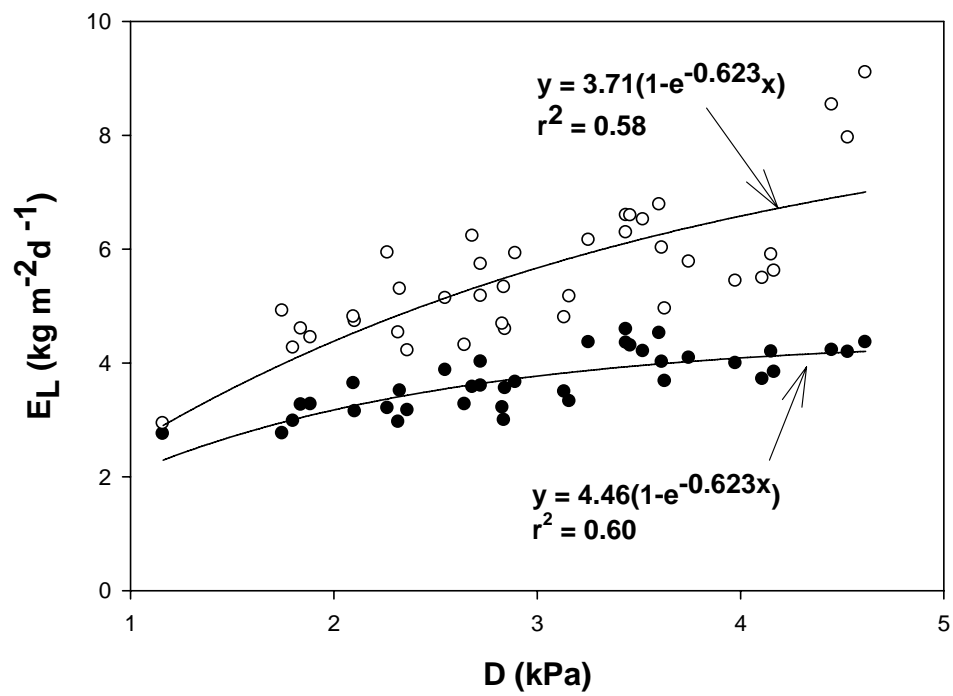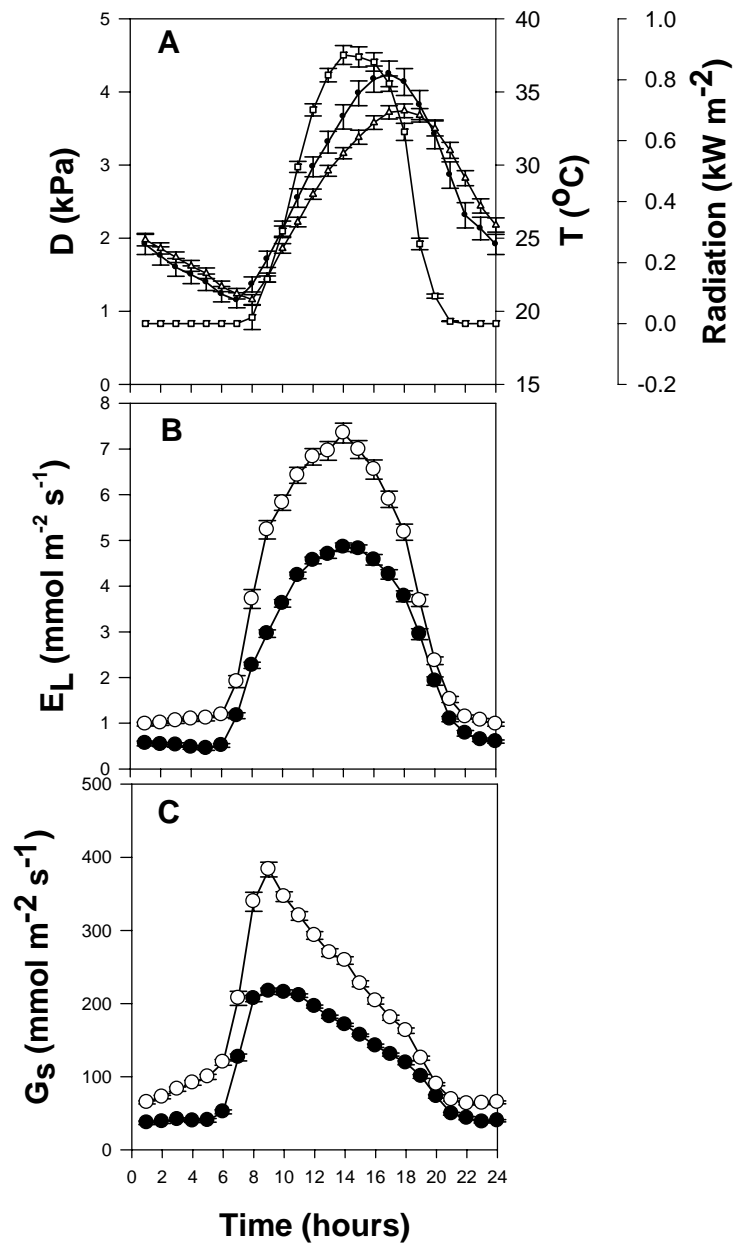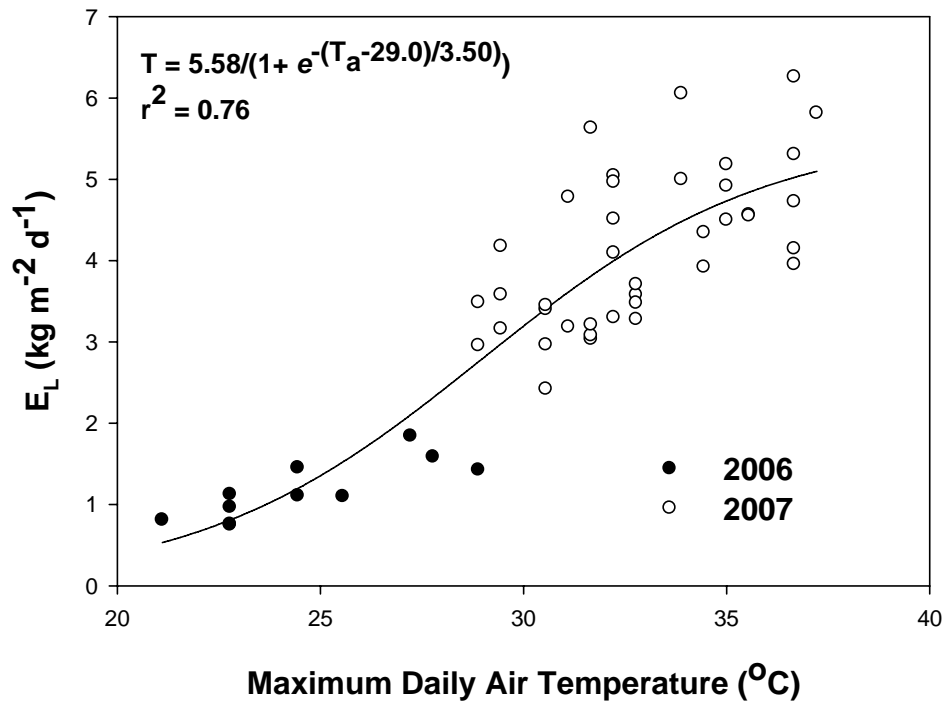
Figure 4.

Figure 5.

Figure 6.
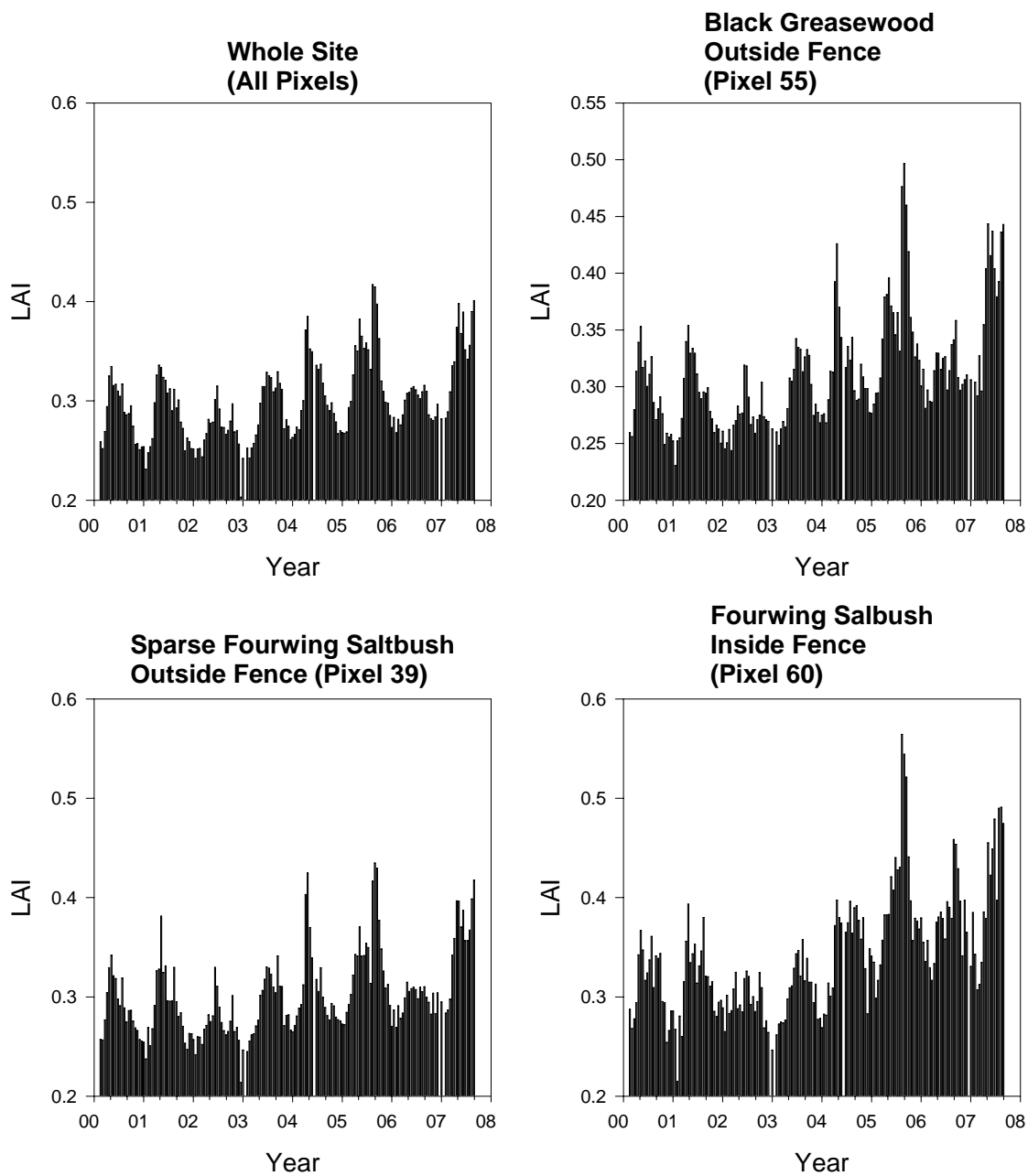
Figure 7.
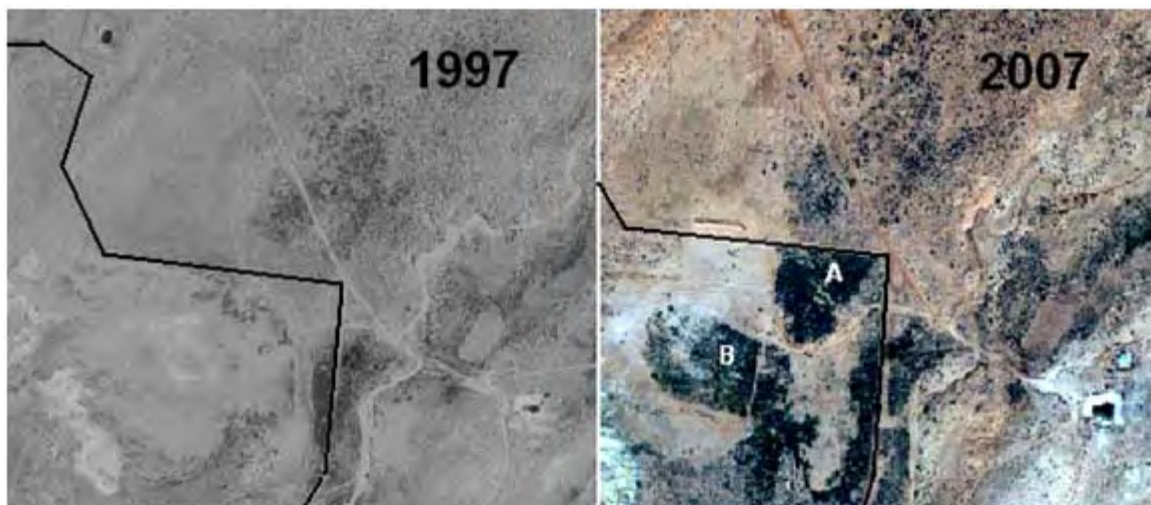
Figure 8.
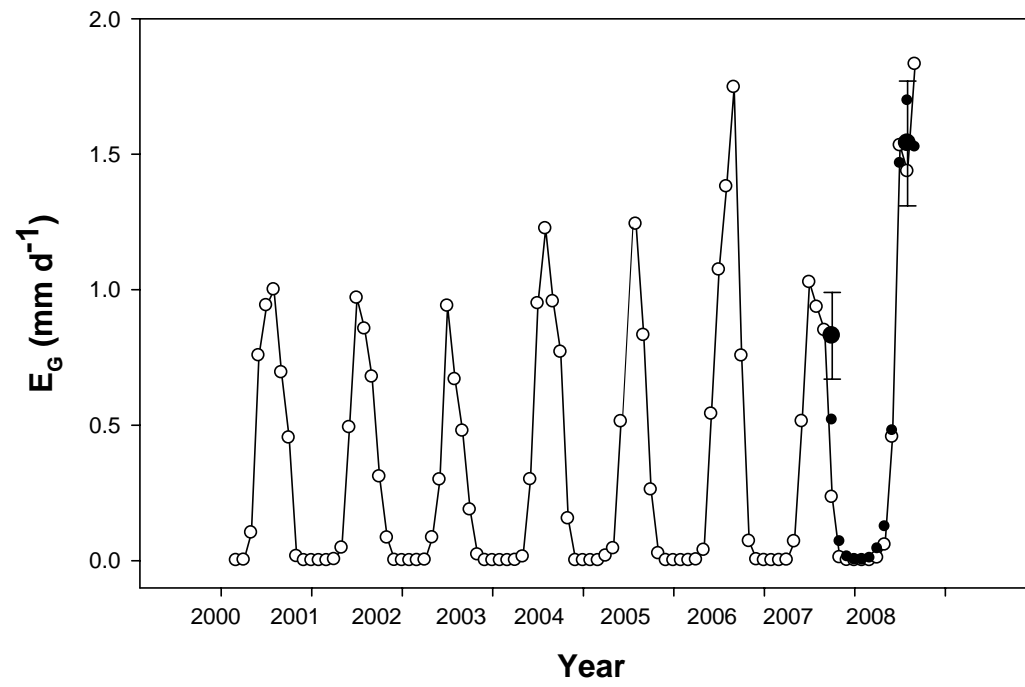
Figure 9.

Appendix B

**Characterizing Natural Attenuation of the Nitrate Plume at the
Uranium Mill Tailings Site in Monument Valley, Arizona**

This page intentionally left blank

CHARACTERIZING NATURAL ATTENUATION OF THE NITRATE PLUME AT THE URANIUM MILL TAILING SITE IN MONUMENT VALLEY, ARIZONA

Prepared for:

U.S. DEPARTMENT OF ENERGY
Grand Junction Office
Grand Junction, Colorado

Prepared by:

K.C. Carroll, F.L. Jordan, M.L. Brusseau, and E.P. Glenn
THE SOIL, WATER, AND ENVIRONMENTAL
SCIENCE DEPARTMENT
University of Arizona
Tucson, Arizona

January 30, 2008

This page intentionally left blank

TABLE OF CONTENTS

TABLES

Table 1. Natural, ethanol- and methanol-enhanced denitrification first-order rate coefficients obtained from laboratory microcosm concentration data.

Table 2. Natural, ethanol- and methanol-enhanced denitrification first-order rate coefficients obtained from laboratory microcosm ^{15}N isotopic enrichment data.

Table 3. Natural attenuation first-order rate coefficients obtained from field concentration data.

Table 4. Natural denitrification first-order rate coefficient obtained from field ^{15}N isotopic enrichment data.

Table 5. Natural denitrification first-order rate coefficients obtained from MT3DMS model calibration, and rate coefficient used for ethanol enhanced denitrification prediction.

1

FIGURES

SUMMARY

Groundwater in the alluvial aquifer at the Monument Valley site is contaminated by ammonium and nitrate. There is evidence that natural attenuation is occurring at the site, but the feasibility of using natural attenuation as a remediation strategy remains uncertain. The purpose of this investigation was to characterize the occurrence and rate of natural attenuation at the site. Spatial and temporal nitrate concentration data collected from a transect of monitoring wells located along the plume centerline was used for the evaluation. Denitrification rate coefficients were estimated from microcosm experiments, nitrogen isotopic fractionation analysis, and solute transport modeling. Overall, the rate coefficients were comparable for each of the methods. The model was used to predict the time required for natural attenuation (i.e. plume concentrations decreased to the 10 mg/L regulatory standard), which was predicted to occur by approximately 160 years after the start time of the simulation. Additionally, the microcosm rate coefficient for ethanol-enhanced denitrification (which was increased by two orders of magnitude) was used to predict the reduction in cleanup time, which was about 110 years earlier than the prediction for non-enhanced natural attenuation.

1. INTRODUCTION

The Monument Valley site is a former uranium mining site located in northern Arizona (DOE, 1999). Uranium was mined at the site from 1943 to 1968, and seepage through mill tailings stockpiles into a shallow alluvial aquifer resulted in a groundwater contamination plume that is the focus of this and other remediation investigations. Surface remediation activities conducted from 1992 through 1994 under the UMTRA Program have removed all of the tailings material from the site (DOE, 1999; Sam, 2006). Ammonium and nitrate concentrations in groundwater have since begun to decrease, which suggests that monitored natural attenuation may be a viable remediation strategy for the site. Additionally, the Environmental Research Lab (ERL) conducted a phytoremediation pilot study to remove nitrate from the soil in the former tailings area. The project resulted in reduced nitrate concentrations, and monitoring since then suggests that denitrification is responsible for nitrate transformation at the site (Jordan et al., In Press). However, groundwater at the Monument Valley site continues to exceed the 10 mg/L standard.

This report presents the results of a study to characterize the occurrence and rate of natural attenuation of the nitrate groundwater contaminant plume at the Monument Valley site. Natural attenuation is the combined effect of several naturally occurring processes, such as biodegradation, dispersion, and sorption, that decrease the concentrations of chemicals in the subsurface (e.g. Wiedemeier et al., 1999; Newell et al., 2002; Beyer et al., 2007). There are three types of rates that can be characterized with respect to natural attenuation, local composite rates, field-scale composite rates, and biodegradation-specific rates. Local composite attenuation rates incorporate all processes contributing to attenuation of the target contaminant at a specific location. The associated rate coefficients are estimated by analyzing concentration versus time data, for a selected location, which may be used to evaluate the remediation time at a monitoring well or compliance point. The composite field-scale rate coefficients are estimated by analyzing concentration versus distance data. These are typically measured with distance away from a source area along the major axis of the contaminant plume, and describe the effect of natural

3

attenuation processes occurring in the direction of average movement of the contaminant at a specific time. The biodegradation rates are the rates at which the contaminant is attenuated by microbial mediated transformation processes.

The characterization of these naturally occurring processes that impact concentrations is required for the use of natural attenuation as a remediation strategy and the design of more aggressive remediation activities. Denitrification is a multi-step process through which nitrate is reduced to atmospheric nitrogen (Kendall and McDonnell, 1998), and it is commonly the most significant attenuation process for nitrate in groundwater. The overall objective of the current investigation was to characterize the occurrence and rate of natural attenuation in the groundwater nitrate plume.

2. DATA COLLECTION METHODS

2.1 Groundwater Sampling and Analysis

Groundwater samples were obtained from monitoring wells screened in the alluvial aquifer extending approximately 6,400 ft (2 km) from the source area (or former tailings area). Prior to sample collection, wells were purged with a micro-purge pumping unit (for approximately 3 well-bore volumes). Two liters of water were collected from each well and placed in sterile Nalgene bottles. All samples were stored on ice in a cooler or at 4^oC until analyzed. For the present investigation, a series of wells located along the centerline of the nitrate plume, coincident with the mean hydraulic gradient, were evaluated including 606, 771, 655, 765, 653, 648, and 650 at distances of 300, 1,010, 1,020, 1,750, 2,715, 2,717, 6,374 ft from the source area, respectively. This series of wells will be called transect A-A' throughout this report. Well 762 was not considered for transect A-A' due to its shallow screened interval, which raised concern about its representativeness for the evaluation of plume attenuation.

2.2 Nitrate Isotopic Analysis

Samples were analyzed for nitrate (NO_3) as nitrogen and ammonium (NH_4), which coincided with the semiannual site-wide monitoring. Stable isotopes for nitrogen (^{14}N and ^{15}N) were also analyzed from subsamples in the following manner. Fifty ml of groundwater from each sample were added to a 500 ml flask containing 0.4 g MgO, which was placed on a hotplate for 4 hours at 45^oC to remove NH_4 (Mulvaney and Khan, 1999). A subsample was analyzed to ensure complete liberation of NH_4 prior to evaporating the samples at room temperature in acid washed, oven-dried crucibles. Nitrogen content of the solid crystalline residue was measured on a continuous-flow gas-ratio mass spectrometer (Finnigan Delta PlusXL) at the Geosciences Department, University of Arizona. Samples were combusted using an elemental analyzer (Costech) coupled to the mass spectrometer. Standardization is based on acetanilide for elemental concentration, and IAEA-N-1 and IAEA-N-2 for ^{15}N; precision is better than $\pm$ 0.2 ‰ (or per mil). These analyses differentiated between isotopes of nitrogen and quantified total NO_3 -N per liter of water.

3. DATA ANALYSIS METHODS

3.1 Microcosm and Stable Isotope Analysis

Microcosm assays were conducted using sediment samples collected from within the plume region to obtain direct evidence of Denitrification, and to estimate denitrification rate coefficients. The results of the experiments were analyzed by two methods, characterization of nitrate loss and N_2O production, and characterization of changes in nitrogen stable isotopes. Core samples were obtained in 2005 by augering into the saturated zone of the alluvial aquifer, 10-11 m below the land surface. Quantifying denitrification requires that a significant depletion of initial N_2O in the sample occurs, so that a change in ^{15}N can be detected, which is often accomplished by adding a substrate to enhance denitrification (Blackmer and Bremner, 1977). Replicate slurries were made using 10 g of sediment and 1 mg NO_3-N supplemented with or without 7.5 mg carbon as ethanol or methanol. N_2O production and NO_3 depletion was assayed in 250 ml microcosms containing 10% acetylene in the headspace to prevent the conversion of N_2O to N_2. Vials were sampled at 0, 4, 12, 20, and 43 days after initiation for N_2O. Residual NO_3 in the microcosms was also measured. Each treatment initially contained 10 replicate flasks and two flasks were sacrificed for NO_3 and ^{15}N measurements at each time. First-order rate coefficients (k) for denitrification were derived from the laboratory microcosms as the slope of the natural log of the residual NO_3 concentrations.

Biological denitrification leads to an enrichment of the heavy isotope, ^{15}N, because denitrification favors the more abundant light isotope, ^{14}N. The nitrogen isotopic composition of water is typically reported as $\delta^{15}N$ in units of ‰, where $\delta^{15}N$ is the difference between the ^{15}N /^{14}N ratio of a sample to atmospheric N_2, as 0 ‰ (e.g. Kendall and Aravena, 1999):

$$\delta^{15}N \ (‰) = [(R_{sample}/R_{standard})-1] \times 1000$$

where Rsample is the isotopic ratio measured in a sample and Rstandard is the ratio of the atmospheric standard. Biological enrichment of ^{15}N in each of the samples was quantified by a simplified form of the Rayleigh equation (e.g. Kendall and McDonnell, 1998; Kendall and Aravena, 1999; Lund et al., 2000):

$$\varepsilon = (\delta S_{(t)} - \delta S_o)/[\ln(C_t/C_o)]$$

where $\delta S_{(t)}$ is the δ value of the sample at time (t), δS_o is the δ value in the sample at time 0, ε is the enrichment factor, C_t is the NO_3 concentration at time (t) and C_o is the initial NO_3 concentration. The enrichment factor can be used to estimate the extent of biological denitrification occurring in a groundwater system compared to other processes that might reduce NO_3 levels (Morrill et al., 2005).

5

First-order rate coefficients for denitrification were calculated from the nitrogen stable isotopic enrichment data. The rate coefficients (k) were calculated as (e.g. Morrill et al., 2005):

$$\varepsilon = b/1000$$
$$b = (\alpha - 1)$$
$$k = \ln\,[\delta S_{(t)}/(1000 + 1)/\delta S_o/(1000 + 1)]/[(1 - \alpha)t]$$

where the $\delta^{15}N$ results of the plume and microcosm samples were plotted against the natural log of the relative NO_3 concentration to obtain the enrichment factor (ε), which were used to calculate α and k.

3.2 Temporal and Spatial Analysis of Field Data

The Monument Valley site has groundwater concentration data extending back into the 1980s. The historical data up to the 2007 sampling event were plotted against time and distance from the source area. Exponential regression analyses were used to characterize natural attenuation and estimate first-order rate coefficients. For this study, we assume that natural attenuation and biological decay are both first-order decay processes with different rates. This simplified approach is often employed, especially for field applications (Wiedemeier et al., 1999; Newell et al., 2002; Beyer et al., 2007).

3.2.1 Temporal Data

The local composite decay rate describes the change in concentration with time at one location. The log of concentrations from samples collected through time at a monitoring location can be plotted versus time. Then least squares regression can be used to determine the exponential equation that best describes the data. This exponential equation is:

$$C(t) = Co\,e^{-kt}$$

were C is the concentration at time t, Co is the initial concentration, and k is the rate coefficient. The estimation of the time required to cleanup the chemical at this location can be estimated by taking the natural log of the ratio of the target and the original concentrations and then dividing by the rate coefficient. This local decay first-order rate coefficient may be especially useful in locations of maximum concentration for estimating rates of source decay.

3.2.2 Spatial Data

The composite natural attenuation first-order rate describes the changes in concentration with versus distance (measured at a point in time). The composite decay rate coefficient is generally measured with distance away from a source area along the major axis of the plume, and it describes the effect of natural attenuation processes occurring in the direction of average movement of the NO_3 at a specific time. The log of concentrations from samples collected at the same time through distance along the plume can be plotted versus distance. Then least squares

regression can be used to determine the exponential equation that best describes the data. This exponential equation is:

$$C(x) = Co \ e^{-(kx/v)}$$

where C is the concentration at distance x, v is the velocity of the contaminant transported in groundwater, and k is the rate coefficient. The distance away from the source that the concentration decreases to the cleanup level can be estimated by taking the natural log of the ratio of the target and the source concentrations and then dividing by the ratio of the rate coefficient and the groundwater velocity. A comparison of the composite rate coefficient at different times can be useful for indicating if a plume is changing in size.

3.2.3   Stable Isotope Data

Isotopic evidence for denitrification may be observed in the field if enough transformation has occurred to result in a measurable fractionation of ^{15}N. Over time, NO_3 from the source area has been transported down-gradient in the aquifer. If denitrification has occurred in the plume, NO_3 at the leading edge of the plume should be more enriched in ^{15}N than residual NO_3 in the source area. The rate of denitrification in the plume can therefore be estimated by measuring ^{15}N enrichment in samples taken from the plume at increasing distances from the source area. This method has been previously applied to carbon isotope evaluation of chlorinated solvent dechlorination (Morrill et al., 2005). Subsamples of groundwater samples collected at several monitoring wells were analyzed for nitrogen stable isotopes ^{15}N and ^{14}N using the previously discussed methods.

3.3 Numerical Modeling Analysis

Numerical modeling was used to quantify solute transport and attenuation processes including the denitrification rate for the nitrate plume at the Monument Valley site. The model was calibrated to observed concentration distributions, and it was also used to predict the time required to complete remediation with and without injection of ethanol as a carbon substrate to enhance microbial activity.

3.3.1   Conceptual Model

The DOE's previous site characterization described the site geology, hydrogeology, and contamination distribution (DOE, 1999). The NH_4 and NO_3 contamination at the Monument Valley site occurs in the shallow, unconsolidated alluvial aquifer, which overlies the Shinarump and De Chelly consolidated sedimentary units. The groundwater levels in the alluvial aquifer range from approximately 4,830 ft amsl near the source area to 4,774 ft amsl at the distal monitoring well (650), which results in an average hydraulic gradient of 0.01 across the entire site. There is negligible groundwater pumping, and the groundwater levels have remained relatively constant over the monitoring period. Hydraulic testing suggests that the alluvial aquifer is relatively homogeneous with geometric mean hydraulic conductivities ranging from 16 to 25 ft/day (DOE, 1999).

7

The alluvial aquifer at the Monument Valley site contains elevated concentrations of NH_4 and NO_3 (DOE, 1999). The historic mining operations used NH_4 in the uranium extraction process. Presumably, the NO_3 groundwater concentration distribution was generated by the decay of NH_4 through nitrification, which occurs in oxidizing environments. However, the tailings material was removed between 1992 and 1994, which coincided with the timing of a decrease in the dissolved oxygen concentrations in the alluvial aquifer. The decreases in oxygen were the likely cause of NO_3 decay to atmospheric nitrogen through denitrification, which requires reducing, or low oxygen, conditions. *Pseudomonas denitrificans* mediates denitrification at dissolved oxygen concentrations of less than approximately 0.5 mg/L (Hubner, 1986). Although the tailings materials were removed by 1994, the alluvial aquifer still contains NH_4 that may be continually decaying to NO_3, which would constitute a source for the NO_3 contamination. Previous investigations suggest that NO_3 undergoes negligible adsorption to the alluvial aquifer material (Sam, 2006). Thus, the primary natural attenuating processes that impact NO_3 concentrations may include diffusion, dispersion, and denitrification.

3.3.2 Groundwater Flow and Transport Modeling

A one dimensional (1D) steady state groundwater flow model was developed and calibrated to provide the pore water velocity for the solute transport model. The commonly used numerical model MODFLOW (Harbaugh and McDonald, 1996) was used for the groundwater flow simulation. The model mesh consisted of 64 cells that were each 100 ft long, which extended from the source area to beyond well 650 along the A-A' transect. Constant head boundary conditions were used for the first (4,830 ft amsl) and last cell (4,774 ft amsl). The results of the groundwater flow modeling were used with the same model domain for simulating transport of NO_3 along the A-A' transect. The commonly used numerical model MT3DMS (Zheng and Wang, 1999) was used for the solute transport simulations. The NO_3 concentration distribution observed from the monitoring well data in 1993 was used for the initial condition. Initial simulations indicated that the model required a source boundary condition in the first cell to facilitate transient calibration to the monitoring well concentration data. Therefore, the source decay rate (-0.02 yr^{-1}) was estimated from the observed NH_4 concentration verus time data using exponential regression.

Analysis and parameter estimation modeling of NO_3 transport without denitrification in a laboratory column (Sam, 2006) packed with material from the alluvial aquifer near well 606 was used to quantify adsorption and dispersion properties with automated parameter estimation using CFITIM (van Genuchten. 1980). The estimated NO_3 retardation (R = 1.2) was used for the adsorption modeling assuming a linear isotherm, and the estimated column-scale dispersivity was used for the field- scale dispersion calculations after upscaling. Figure 1 presents the laboratory column NO_3 transport data and comparison to the CFITIM analytical model simulation after estimation of dispersivity. The laboratory derived dispersivity (0.054 cm) was upscaled linearly from the experimental transport length (14.5 cm) to the field scale longitudinal dispersivity (23.8 ft) assuming a field transport length of 6,374 ft, and horizontal and vertical transverse dispersivities were assumed to be 1/10th the longitudinal dispersivity. The porosity was assumed to be 25 %, and the molecular diffusion coefficient (9.3×10^{-4} ft^2/day) was estimated from the molecular weight (Schwarzenbach et al., 1993).

3.3.3   Denitrification Rate Coefficient Estimation

The MT3DMS numerical model of NO_3 transport at the Monument Valley site was calibrated to the field concentrations by varying the denitrification first-order rate coefficient. The 1993 concentration distribution was used for the initial condition for the transient calibration, and the NO_3 concentration distribution along the A-A' transect with distance from the source was compared to the observed monitoring well concentrations from the years 1998, 2003, and 2007.

3.3.4   Natural Attenuation Prediction

Upon completion of the Monument Valley transient calibration, a predictive solute transport simulation was performed, which began with the calibration results for 2007 and progressed through time until the NO_3 concentrations reached the 10 mg/L standard at every location. Additionally, another predictive simulation was conducted to evaluate the effect of enhanced remediation using ethanol injection to stimulate denitrification. A first-order rate coefficient obtained from the ethanol amended laboratory microcosm experiment was used in the prediction for the first 3 cells (from the source to 300 ft; near well 606), and this prediction was also initiated with the 2007 calibration results and progressed through time until the NO_3 concentrations reached the regulatory standard.

4. RESULTS AND DISCUSSION

4.1 Laboratory Microcosm Experiment and Analysis

The results of the microcosm experiments are presented in Figures 2 and 3. Figure 2 presents the production of nitrous oxide over time, and Figure 3 exhibits the NO_3 decay kinetics. Natural NO_3 denitrification (without amendment) was minor compared to the decay observed with both ethanol and methanol amendments. These data, as well as the enrichment factor derived for a previous ethanol study, are presented in Table 1. The denitrification rate coefficients were 0.2 and 0.7 yr^{-1}, and the ethanol enhanced rate coefficients varied from 17 to 29 yr^{-1}, which represents an increase of approximately two orders of magnitude. Table 2 contains the rate coefficients for the laboratory microcosm ^{15}N enrichment. The denitrification rates estimated from isotopic fractionation were 0.34 yr^{-1} for the natural attenuation and 29.7 yr^{-1} for the ethanol enhanced decay.

4.2 Temporal and Spatial Analysis of Field Data

4.2.1   Temporal Data

The monitoring well concentrations along the A-A' transect were plotted versus time to evaluate the transient attenuation behavior. Figure 4 contains the dissolved oxygen transient concentrations, Figure 5 shows the NH_4 data, and Figure 6 presents the NO_3 concentration data. The oxygen content in the aquifer decreased from 1992 to 1994 to the range required to initiate denitrification (Hubner, 1986). NH_4 concentrations had a decreasing trend along the transect. The groundwater near the source area also had a decreasing trend for NO_3 concentrations, but groundwater at distances down-gradient from the source area had an increasing trend for NO_3

Appendix B.doc
January 30, 2008

concentrations (wells 653 and 650). Exponential regression analysis is also shown for the NH_4 and NO_3 plots. The local first-order rate coefficient estimated from well 606 data (-0.0174 yr^{-1}) represents rate of attenuation for NO_3 at that location (Table 3). However, the increasing concentration trends at the edge of the plume suggest that the plume is moving or expanding.

4.2.2 Spatial Data

The spatial behavior of the groundwater contamination plume was evaluated by plotting the transect NO_3 concentrations versus distance from the source area, which is approximately the center-line of the major axis of the plume. Figures 7 shows the dissolved oxygen concentration distributions at various years, and Figures 8 and 9 contain the NH_4 and NO_3 data at various years, respectively. The oxygen content has decreased over time, especially beyond approximately 2,000 ft away from the source area. Both NH_4 and NO_3 decrease with distance from the source, but the NO_3 extends further from the source. Exponential regression analysis is also shown for the NH_4 and NO_3 data. The composite rate coefficient was estimated for NO_3 from the regression exponent multiplied by the nitrate transport velocity. The rate coefficient was 0.36 yr^{-1} for the 1993 data and 0.35 yr^{-1} for the 2007 data (Table 3).

4.3 Stable Isotopic Fractionation Analysis

Figure 10 presents the monitoring well sample NO_3 isotopic fraction data as delta $(\delta)^{15}N$ versus ln C/C_o. The results of a linear regression analysis is also shown that was used to estimate the enrichment factor for denitrification in the alluvial aquifer. Figure 11 contains the plot of the regression analysis used to estimate the denitrification rate coefficient estimation based on the ^{15}N fractionation. Table 4 presents the field groundwater sample ^{15}N enrichment data, which resulted in a denitrification rate coefficient of 0.36 yr^{-1}. The natural denitrification rate coefficients were similar for laboratory and field-scale methods, which is atypical but of great utility for this study.

4.4 Numerical Modeling Analysis

The results of the MODFLOW groundwater flow model calibration are presented in Figure 12 along with the observed groundwater elevations from 2002 and 2007. Calibration of the model was accomplished by comparing simulated and measured groundwater elevation data for 2007. The calibration required using two zones of different conductivities. The conductivity values used for the two zones were the geometric mean values from previous hydraulic testing (DOE, 1999). The region from the source zone extending down-gradient 2,000 ft was 16.1 ft/day, and the zone from 2,000 ft to 6,400 ft was 24.9 ft/day.

MT3DMS was used to simulate the transport of NO_3 in the alluvial groundwater along the A-A' transect. The denitrification rate coefficient was modified to achieve a calibration from 1993 to 2007, and the results of the NO_3 solute transport model after calibration are shown in Figure 13. The optimal calibration was achieved by using two zones with different rates of denitrification, as was done with the zones of hydraulic conductivity. The first zone with a rate coefficient of 0.1 yr^{-1} was applied from the source area to approximately 2,000 ft down-gradient of the source area, and the second zone with a rate coefficient of 0.3 yr^{-1} extended from 2,000 ft to 6,400 ft

10

(Table 5). The zone locations were selected based observation of a change in redox conditions along the A-A' transect. The dissolved oxygen concentrations have been higher near the source zone with a shift to lower concentrations after approximately 2,000 ft from the source zone (Figures 4 and 7), and this decrease in oxygen is assumed to facilitate increased denitrification activity.

4.5 Comparison of Denitrification Rate Coefficient Data

Various methods were used in this investigation to estimate first-order rate coefficients for natural attenuation and denitrification. An interesting result is that the rate coefficients were comparable for all methods. This suggests that the denitrification, estimated with stable isotope analysis, is the dominant process controlling the nitrate attenuation. The isotopic method yielded similar rates for both laboratory and field denitrification. Also, the ethanol enhanced denitrification rates were similar for the concentration decay and isotopic fractionation evaluation of the microcosms. The similarity of the results helps to support the characterization of the nitrate attenuation processes at the site.

4.6 Model Predictions of Natural and Enhanced Attenuation

The calibrated MT3DMS nitrate transport model was then used for prediction of natural attenuation. Figure 14 presents the results of the prediction for natural attenuation conditions. This simulation was extended through time until the concentrations in the entire model domain reached the 10 mg/L standard, which occurred in approximately 160 years. Another prediction simulation was conducted using a denitrification rate coefficient of 29 yr^{-1} for the first 3 cells (source area), which was the value derived from the microcosm studies for ethanol enhanced denitrification (Figure 14). The enhanced denitrification prediction shows NO_3 concentrations lowered to the regulatory standard throughout the model domain approximately 50 years after the start time of the prediction, which is 110 years earlier than the natural attenuation prediction.

5. CONCLUSIONS AND RECOMMENDATIONS

5.1 Conclusions

This report has summarized efforts to characterize the natural attenuation of the NO_3 plume at the Monument Valley UMTRA site. Remediation of tailings at the site occurred prior to 1994. However, NH_4 and NO_3 remain in the groundwater system, and NO_3 concentrations measured at monitoring wells continues to exceed the regulatory limit. Natural attenuation of NO_3 has been observed at the site by the decreases in concentrations over space and time at the site. The feasibility of using natural attenuation for a remediation strategy for groundwater requires that attenuation occurs at a rate that will achieve cleanup within a reasonable time frame. The rates of composite attenuation were estimated from groundwater concentration data, which combine the effects of dispersion, diffusion, sorption, and denitrification. Dispersion and sorption were estimated from laboratory experiments, but had minor effects on NO_3 transport. The rate of microbial biodegradation through denitrification, which was the dominant attenuation process, was also quantified through a variety of methods including microcosm decay and isotopic fractionation, field-scale isotopic fractionation, and numerical modeling.

5.2 Recommendations

The results suggest that NO_3 located in the Monument Valley alluvial aquifer is naturally attenuating. However, the rate of natural attenuation is such that it may take more than one hundred years to complete cleanup. The model predictions of enhanced denitrification with the addition of ethanol as a substrate showed a substantial increase in the rate of NO_3 attenuation. This work suggests that the use of enhanced denitrification may significantly reduce the time required for attenuation of the NO_3 plume.

References:

Beyer, C., Chen, C., Gronewold, J., Koldity, O., and Bauer, S., 2007. Determination of First-Order Degradation Rate Constants from Monitoring Networks. Groundwater, V45, No. 6, 774-785.

Blackmer, A., Bremner, J., 1977. Nitrogen isotope discrimination in denitrification of nitrate in soils. Soil Biology and Biochemistry 9, 73-77.

Jordan, F., Waugh, J., Glenn, E.P., Sam, L., Thompson, T., and Thompson, T.L., In Press. Natural Bioremediation of a Nitrate-Contaminated Soil-and-Aquifer System in a Desert Environment, Journal of Arid Environments.

Harbaugh AW and McDonald MG, 1996. User's documentation for MODFLOW-96, an update to the U.S. Geological Survey modular finite-difference ground-water flow model, USGS Open-File Report 96-485

Hubner, H., 1986. Isotope effects of nitrogen in the soil and biosphere. In: P. Fritz & J.C. Fontes (Eds.) Handbook of Environmental Isotope Geochemistry, Vol 2b, The Terrestrial Environment, Elsevier, pp 361-425.

Kendall, C., Aravena, R., 1999. Nitrate isotopes in groundwater systems, in: P. Cook and A. Herczeg (Eds.), Environmental Tracers in Subsurface Hydrology. Kluwer Academic Publishers, Norwell, MA (1999), pp. 261-297

Kendall, C. and McDonnell, J.J. (Eds.), 1998. Isotope Tracers in Catchment Hydrology. Elsevier. New York, 839 pp.

Lund, L., Horne, J., Williams, A., 2000. Estimating denitrification in a large constructed wetland using stable nitrogen isotope ratios. Ecological Engineering 14, 67-76

Morrill, P. L. Lacrampe-Couloume, G. F., Slater, B.E., Sleep, E. A. Edwards, M. L. McMaster, D. W., Major, Sherwood-Lollar, B., 2005. Quantifying chlorinated ethane degradation during reductive dechlorination at Kelly AFB using stable carbon isotopes. J. Contam. Hydrol. 76: 279-293.

Appendix B.doc
January 30, 2008

Mulvaney, R., Khan, S., 1999. Use of diffusion to determine inorganic nitrogen in a complex organic matrix. Soil Science Society fo America Journal, 6, 240-246.

Newell, C.J., H.S. Rifai, J.T. Wilson, J.A. Connor, J.A. Aziz, and M.P. Suarez, 2002. Calculation and Use of First-Order Rate Constants for Monitored Natural Attenuation Studies. EPA Ground Water Issue Paper. EPA/540/S-02/500.

Sam, L.B., 2006. Simulated Natural attenuation and Enhanced Bioremediation of Nitrate-Contaminated Aquifer Materials in Monument Valley, Arizona, M.S. Thesis Department of Soil, Water, and Environmental Science, University of Arizona, 52 p.

Schwarzenback, R.P., Gschwend, P.M., and Imboden, D.M., 1993. Environmental Organic Chemistry. Wiley-Interscience, New York, 681pp.

U.S. Department of Energy Office of Legacy Management, 1999. Final Site Observational Work Plan for the UMTRA Project Site at the Monument Valley, Arizona. DOE Document:U0018101.

van Genuchten, M. Th., 1980. Determining Transport Parameters from Solute Displacement Experiments, Version 1.0. Research Report No. 118, U.S. Salinity Laboratory, USDA, ARS, Riverside, California.

Wiedemeier, T.H., H.S. Rifai, C.J. Newell, J.T. Wilson, 1999. Natural Attenuation of Fuels and Chlorinated Solvents in the Subsurface, John Wiley & Sons, Inc., New York, pp 617.

Zheng C and Wang PP, 1999. MT3DMS: A modular three-dimensional multispecies model for simulation of advection, dispersion and chemical reactions of contaminants in groundwater systems; Documentation and Users Guide, Contract Report SERDP-99-1, U.S. Army Engineer Research and Development Center, Vicksburg, MS.

Appendix B.doc

TABLES

Table 1. Natural, ethanol- and methanol-enhanced denitrification first-order rate coefficients obtained from laboratory microcosm concentration data.

First-order rate description	k (hr^{-1})	k (yr^{-1})	Half Life (yr)
2006-natural	2.00E-05	0.2	3.96
2007-natural	8.33E-05	0.7	0.95
2006-with ethanol	3.30E-03	28.9	0.02
2007-with ethanol	2.00E-03	17.5	0.04
2007-with methanol	1.95E-03	17.1	0.04

Table 2. Natural, ethanol- and methanol-enhanced denitrification first-order rate coefficients obtained from laboratory microcosm 15N isotopic enrichment data.

Substrate Description	E	$\Delta s(t)$[a]	$\delta s(o)$[b]	α	1- α	time (yr)	k (yr^{-1})	Half Life (yr)
natural	-0.91	0.3	-7	0.999	0.001	21.5	0.3407	2.03
methanol	-18.1	0.3	-7	0.982	0.018	0.12[#]	3.4541	0.20
ethanol	-9.45[c]	0.3	-7	0.991	0.009	0.03[#]	29.705	0.02

a: $\delta s(t)$ = average plume δ 15N

b: $\delta s(o)$ = most enriched plume δ 15N

c: enrichment value previously reported for ethanol (Jordan et al., 2007).

Table 3. Natural attenuation first-order rate coefficients obtained from field concentration data.

First-order rate description	Estimation Method	k (hr^{-1})	k (yr^{-1})	Half Life (yr)
Composite	1993 Data	4.167E-05	0.365	1.90
Composite	2007 Data	4.000E-05	0.350	1.98
Local	Data from Well 606	1.986E-06	0.017	39.84
Local	Data from Well 765	2.203E-06	0.019	35.91

14

Table 4. Natural denitrification first-order rate coefficient obtained from field 15N isotopic enrichment data.

Substrate Description	E	$\Delta s(t)^a$	$\delta s(o)^b$	α	1- α	time (yr)	k (yr^{-1})	Half Life (yr)
natural	-3.4	0.3	-22.9	0.997	0.003	21.5	0.3638	1.91

a: $\delta s(t)$ = average plume δ 15N

b: $\delta s(o)$ = most enriched plume δ 15N (most enriched δ 15N value from the subpile soil)

Table 5. Natural denitrification first-order rate coefficients obtained from MT3DMS model calibration, and rate coefficient used for ethanol enhanced denitrification prediction.

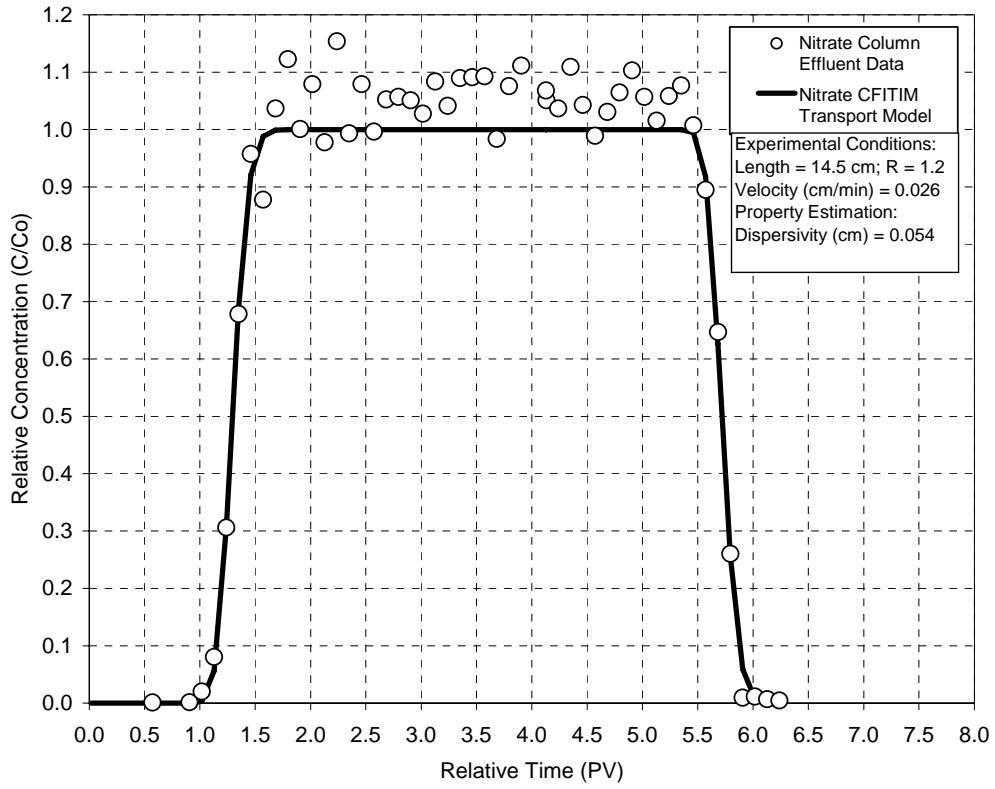| Substrate Description	Zone of Application Along Transect	k (hr^{-1})	k (yr^{-1})	Half Life (yr)
natural	Near source (0-2000 ft)	1.3E-05	0.1	6.33
natural	Away from source (2000-6400 ft)	3.3E-05	0.3	2.37
ethanol	Near source (0-300 ft)	3.3E-03	29	0.02

15

FIGURES

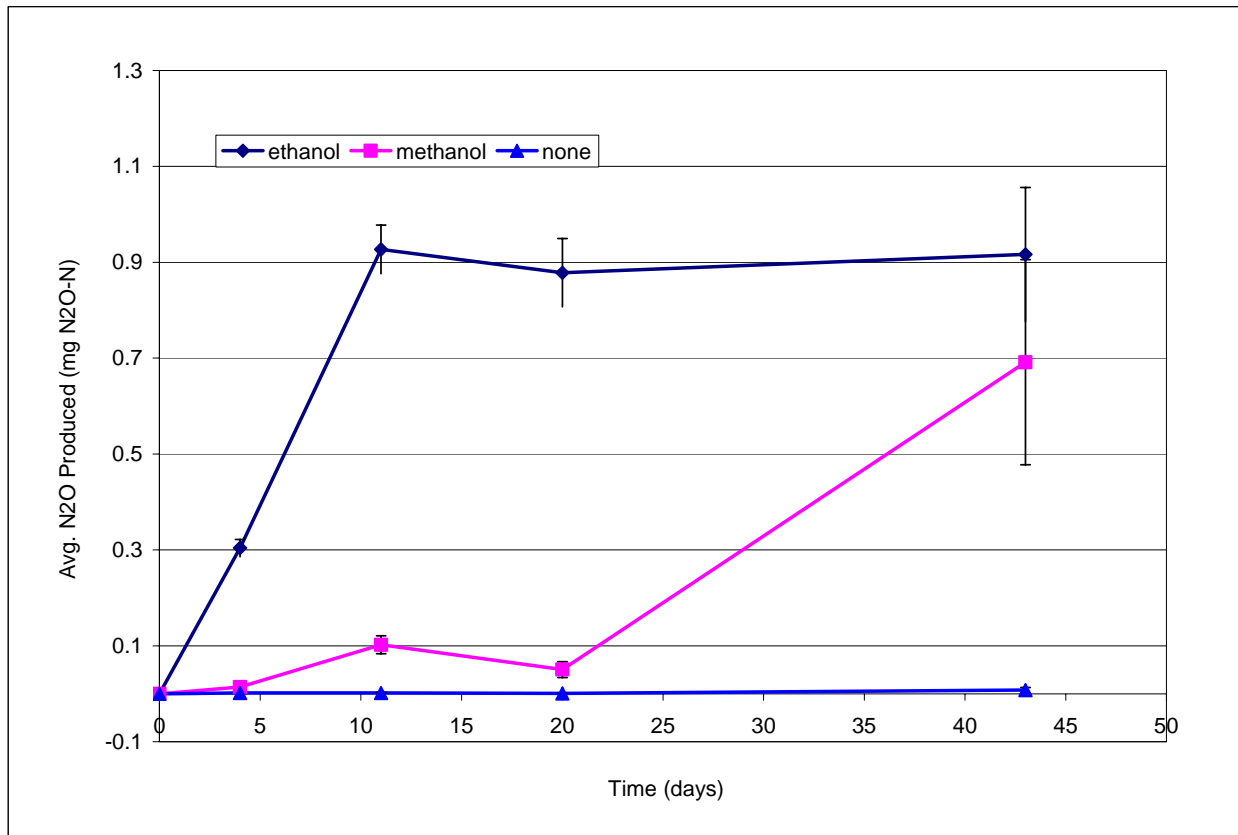Figure 1. Laboratory column transport and model simulation results.
Figure 2. Microcosm nitrous oxide production in soil slurries with or without methanol or ethanol amendment.
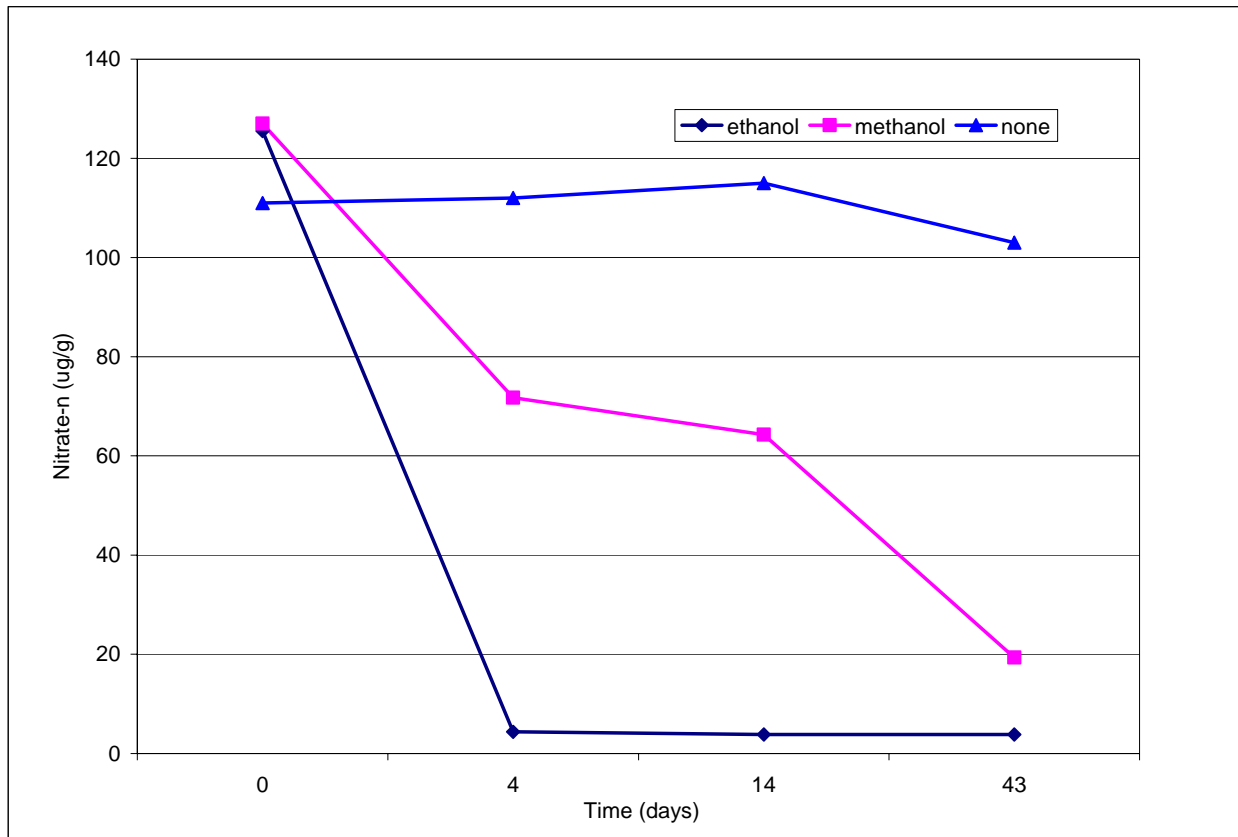Figure 3. Microcosm nitrate depletion in soil slurries with or without methanol or ethanol amendment.
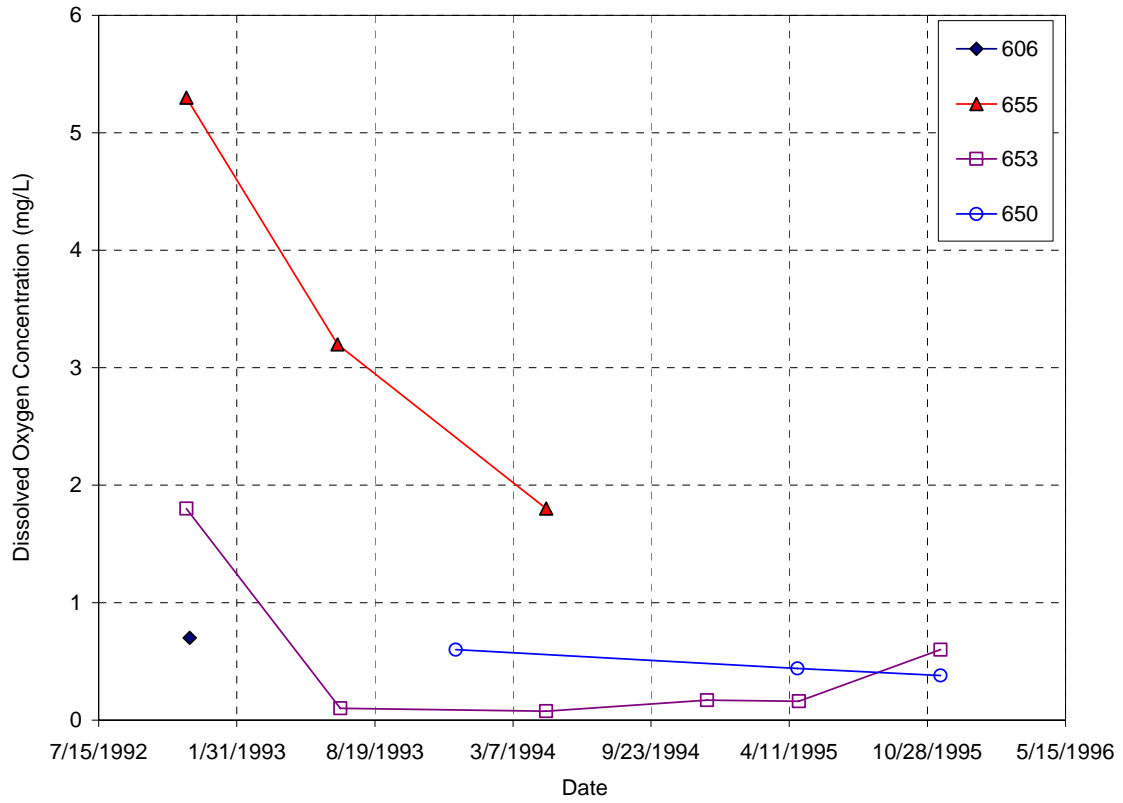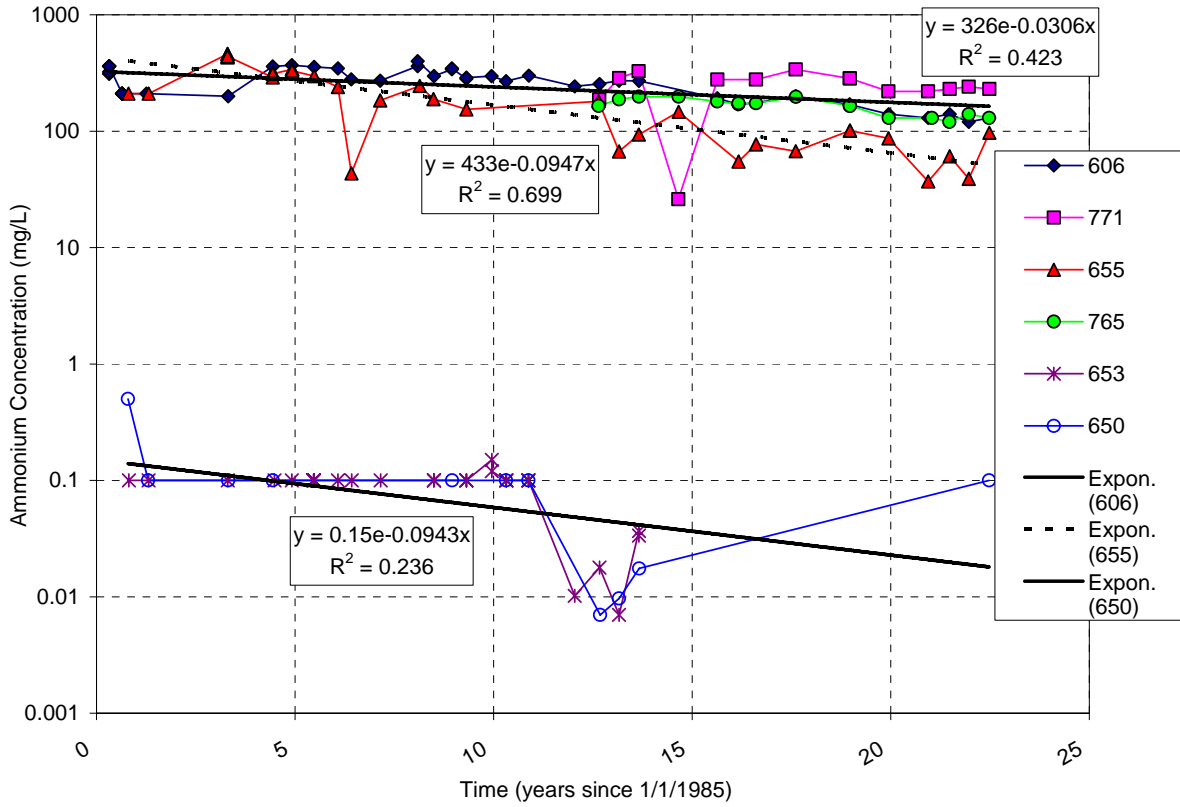Figure 4. Dissolved oxygen concentration as a function of time.
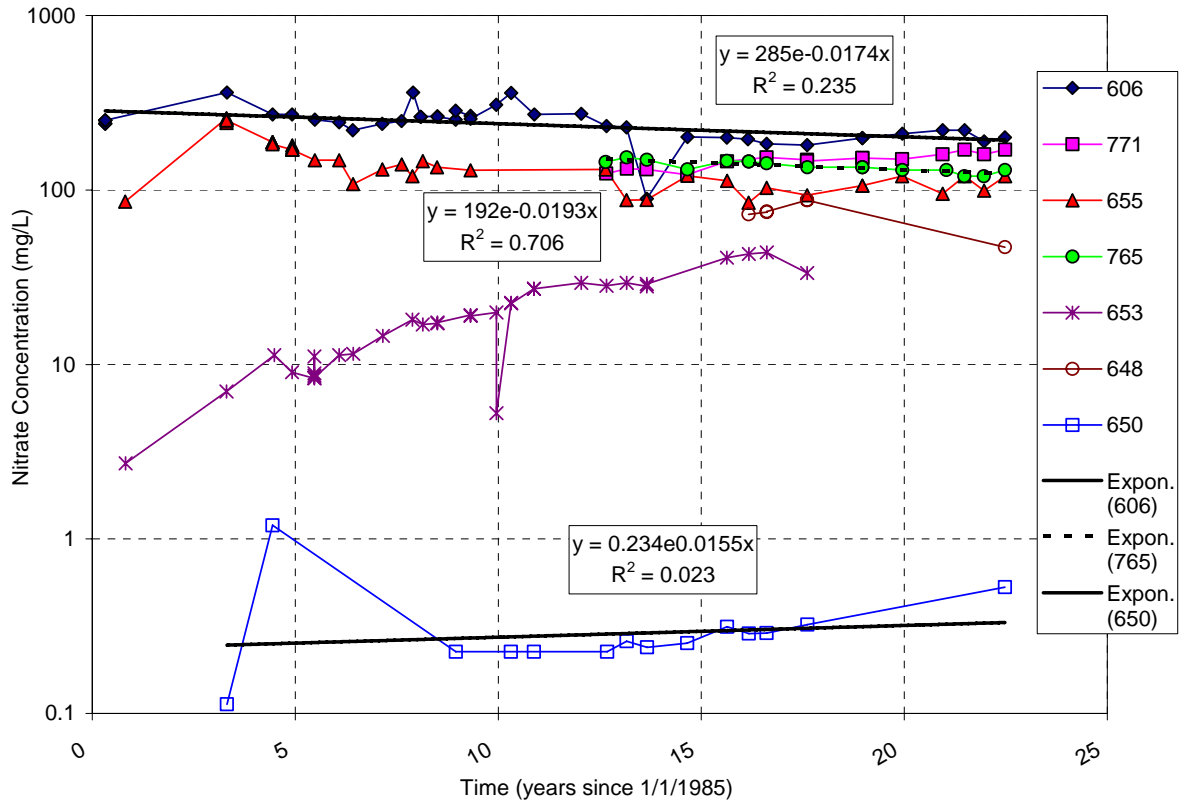Figure 5. Ammonium concentration as a function of time.
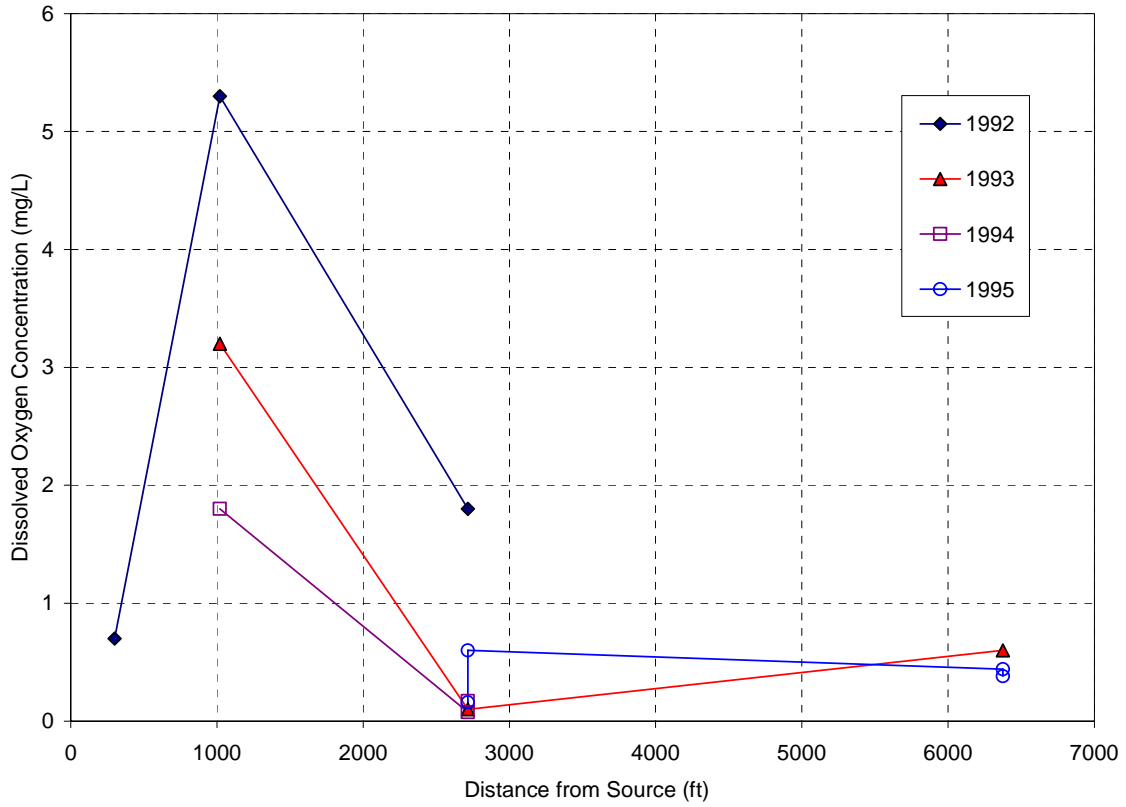Figure 6. Nitrate concentration as a function of time.
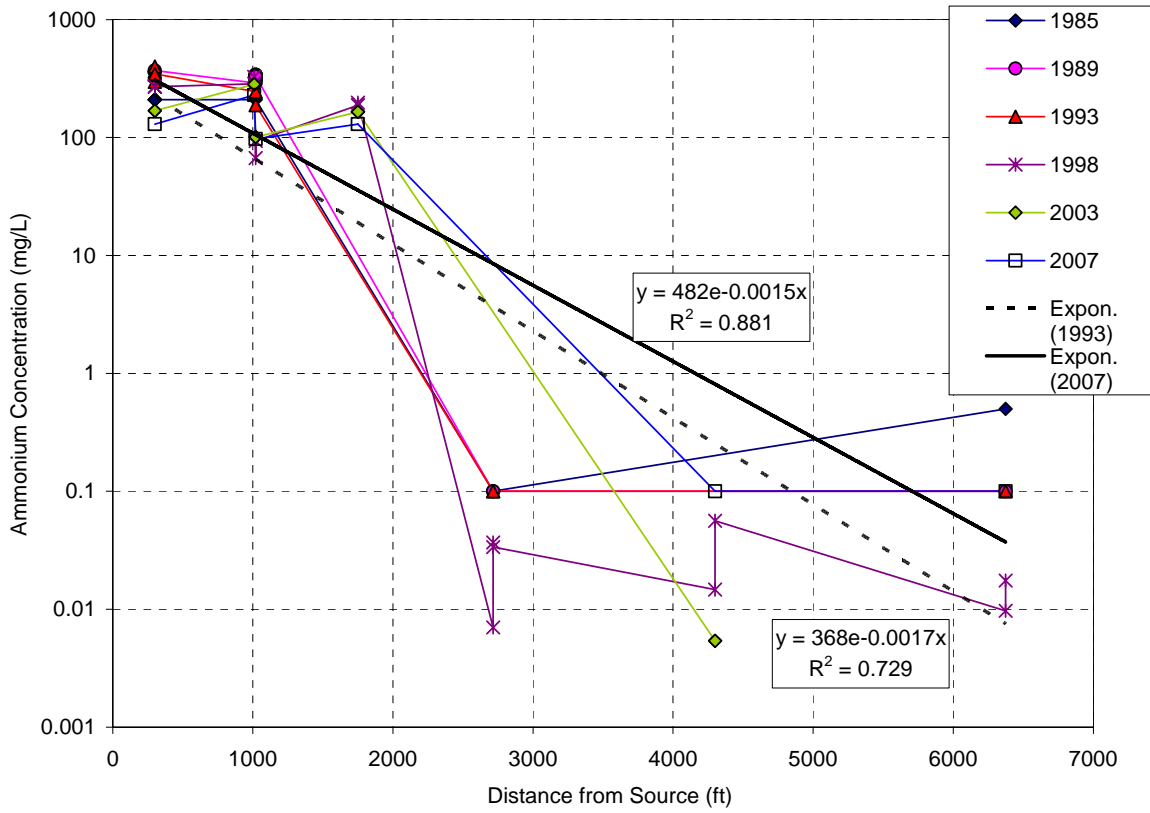Figure 7. Dissolved oxygen concentration as a function of distance along transect A-A'.
Figure 8. Ammonium concentration as a function of distance along transect A-A'.
Figure 9. Nitrate concentration as a function of distance along transect A-A'.
Figure 10. Nitrogen stable isotope enrichment evaluation along transect A-A'.
Figure 11. Nitrogen isotope stable fractionation regression used for rate coefficient estimation along transect A-A'.
Figure 12. Groundwater elevation data and MODFLOW calibration results.
Figure 13. MT3DMS transport model transient calibration to nitrate concentrations versus distance along transect A-A'.
Figure 14. MT3DMS transport model predictions of time required to complete cleanup of nitrate using the natural denitrification calibrated rate and the ethanol-enhanced denitrification rate coefficient.

Figure 1. Laboratory column transport and model simulation results.

Figure 2. Microcosm nitrous oxide production in soil slurries with or without methanol or ethanol amendment.

Figure 3. Microcosm nitrate depletion in soil slurries with or without methanol or ethanol amendment.

Figure 4. Dissolved oxygen concentration as a function of time.

Figure 5. Ammonium concentration as a function of time.

Figure 6. Nitrate concentration as a function of time.

Figure 7. Dissolved oxygen concentration as a function of distance along transect A-A'.

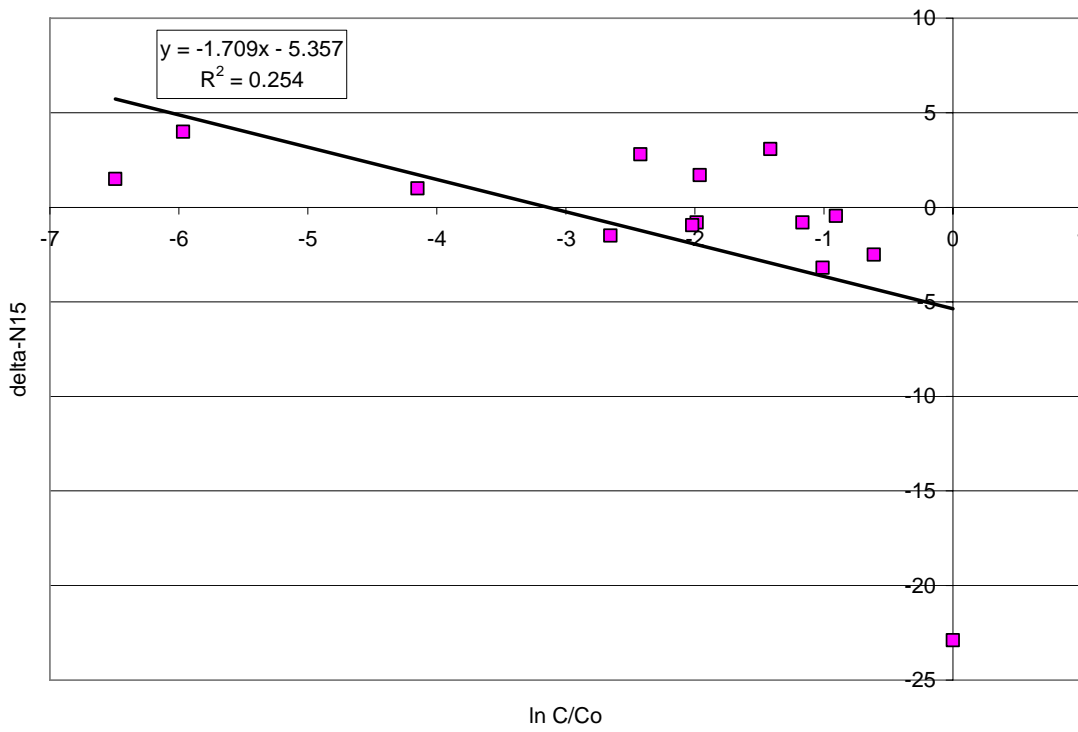Figure 8. Ammonium concentration as a function of distance along transect A-A'.

Appendix B.doc
January 30, 2008

Figure 9. Nitrate concentration as a function of distance along transect A-A'.

The chart legend contains:
- 1985
- 1993
- 1998
- 2001
- 2007
- Expon. (1993)
- Expon. (2007)

Equations shown on chart:

$$y = 427e^{-0.0008x}$$
$$R^2 = 0.762$$

$$y = 394e^{-0.0012x}$$
$$R^2 = 0.998$$

Axis labels:
- Y-axis: Nitrate Concentration (mg/L)
- X-axis: Distance from Source (ft)

Figure 10. Nitrogen stable isotope enrichment evaluation along transect A-A'.

Figure 11. Nitrogen isotope stable fractionation regression used for rate coefficient estimation along transect A-A'.
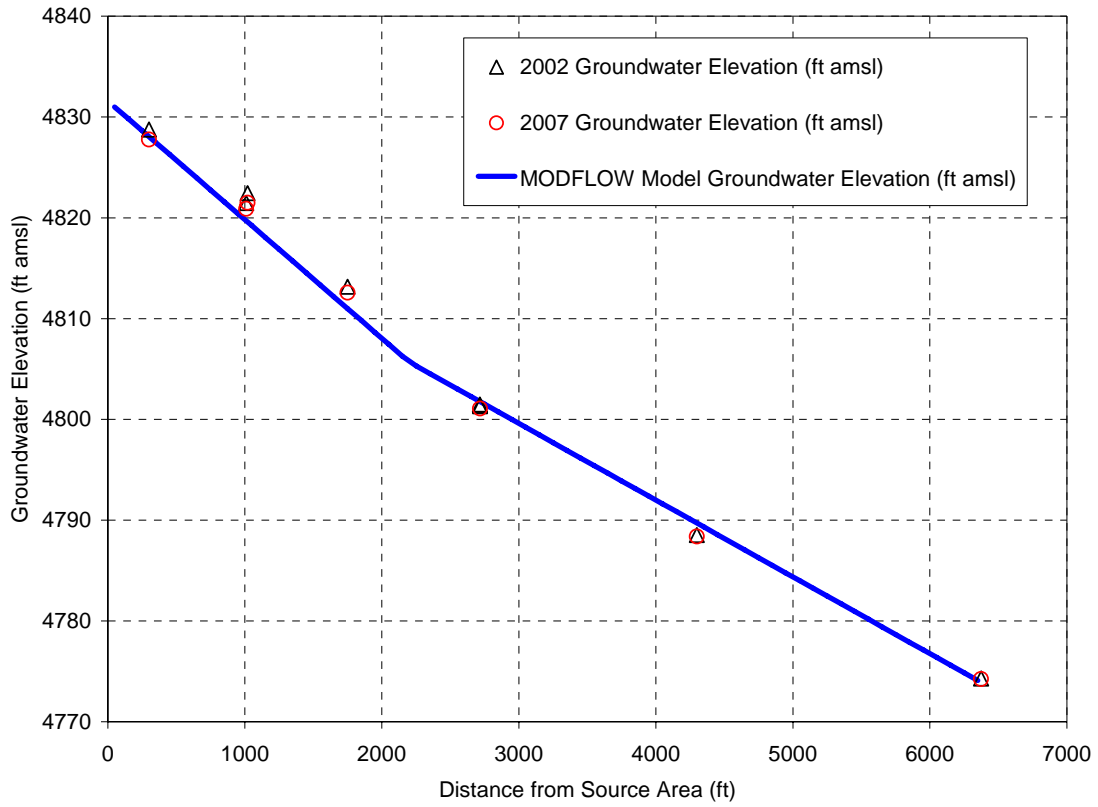
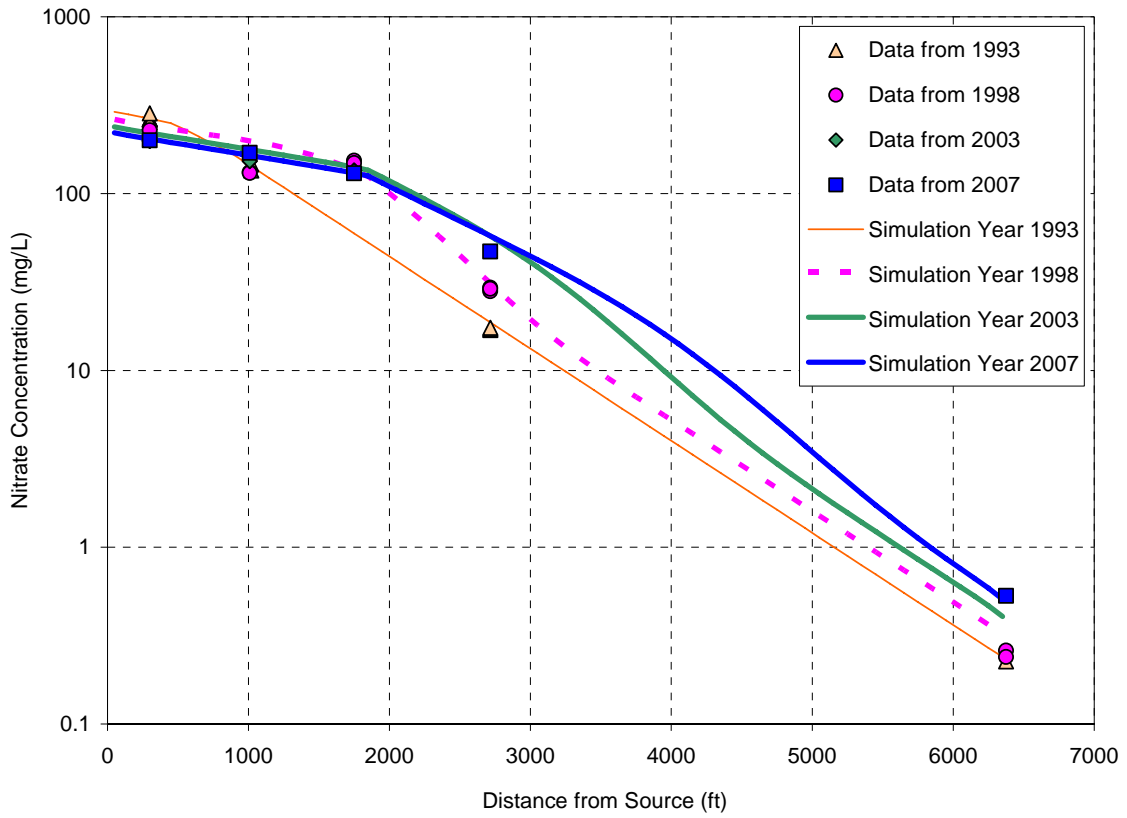Figure 12. Groundwater elevation data and MODFLOW calibration results.

Figure 13. MT3DMS transport model transient calibration to nitrate concentrations versus distance along transect A-A'.
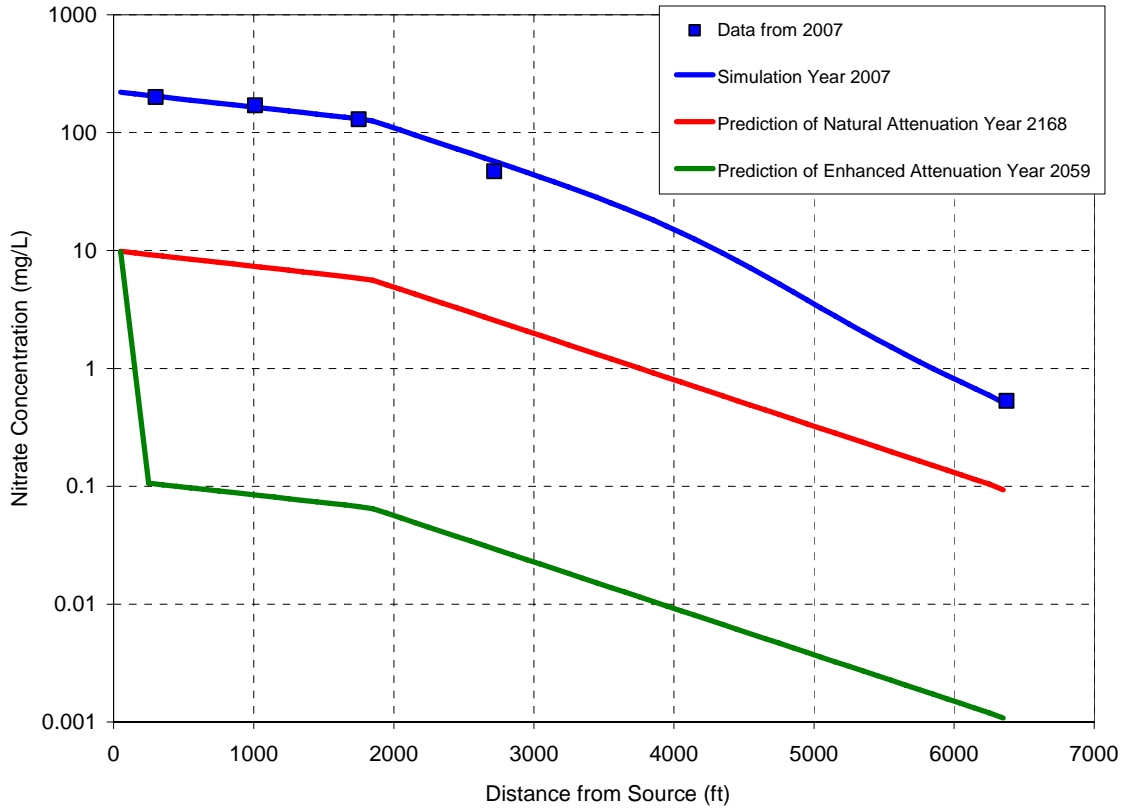
Figure 14. MT3DMS transport model predictions of time required to complete cleanup of nitrate using the natural denitrification calibrated rate and the ethanol-enhanced denitrification rate coefficient.

30